"When you can measure what you are speaking about, and express it in numbers, you know something about it; but when you cannot measure it, when you cannot express it in numbers, your knowledge is a meagre and unsatisfactory kind; it may be the beginning of knowledge, but you have scarcely, in your thoughts, advanced to the stage of science."

-Lord Kelvin

"Light, strong, cheap...

-Pick two."

-Keith Bontrager

NANOMETROLOGY AND MICROMETROLOGY IN BIOLOGICAL SYSTEMS

Brad Layton
Assistant Professor
Mechanical Engineering and Mechanics
Drexel University
Philadelphia, PA USA

NIST
November 29, 2005

OUTLINE

- WIEBULL STATISTICS IN SOFT TISSUE MECHANICS
- NANOMETROLOGY OF COLLAGEN
- NANOMETROLOGY OF MITOCHONDRIA
- ERROR REDUCTION IN NANOMANIPULATION
- BLOOD CELL SORTING
- NEURITE STRETCHING

OUTLINE

WIEBULL STATISTICS IN SOFT TISSUE MECHANICS

introduction: diabetic neuropathy

- type I diabetes:
  - lack of insulin
  - ~1 million Americans (5-10%)
- type II diabetes:
  - poor insulin utilization
  - ~14 million Americans
- prevalence: up to 50%
  - (increases with age)
  - diabetes is leading cause of neuropathy in developed world
- distal, symmetric progression
- clinical manifestation
  - reduced nerve conduction velocity
  - pain, numbness
  - increased injury and amputation risk

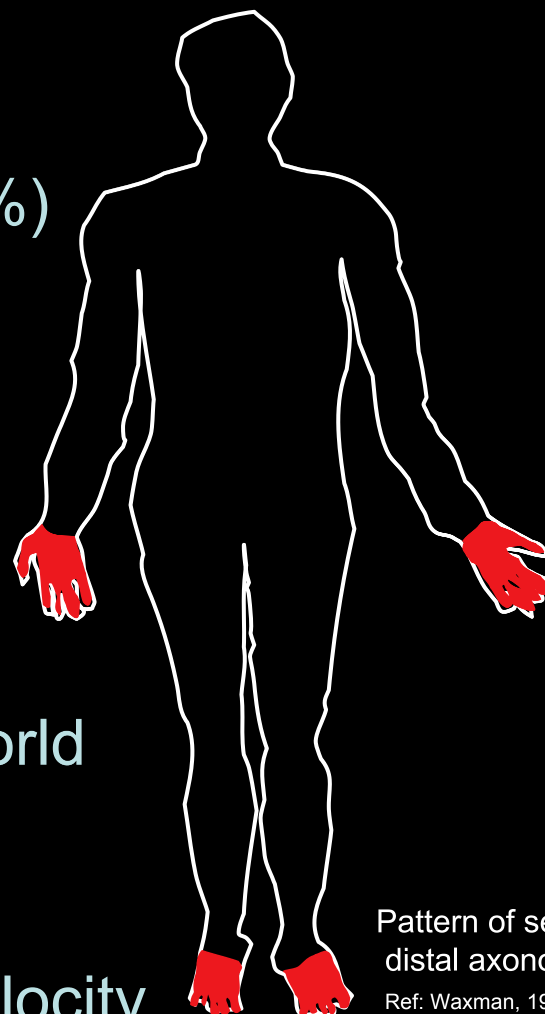

Pattern of sensory loss in distal axonopathy.
Ref: Waxman, 1995. The Axon. p 650

Kopelman and Hitman, 1998;O'Connor et al., 1998;Gavin et al., 1998;DCCT, 1995;Thomas and Tomlinson, 1993; Feldman et al., 2001

etiology?

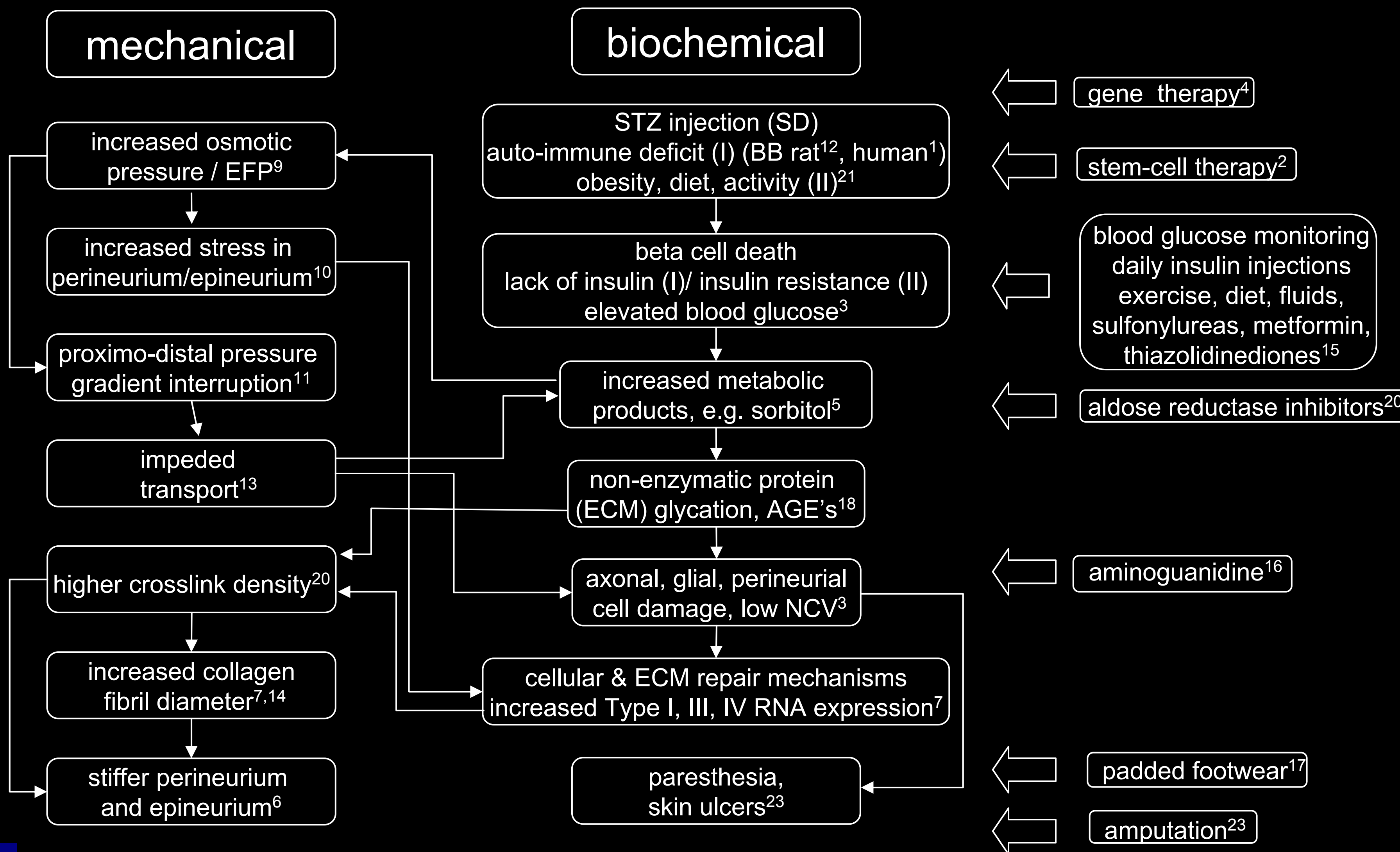

L:ayton, Sastry,Wang,Sullivan, Feldman, Komorwoski, Philbert JoB 2003

- molecular to tissue scale models of diabetic neuropathy

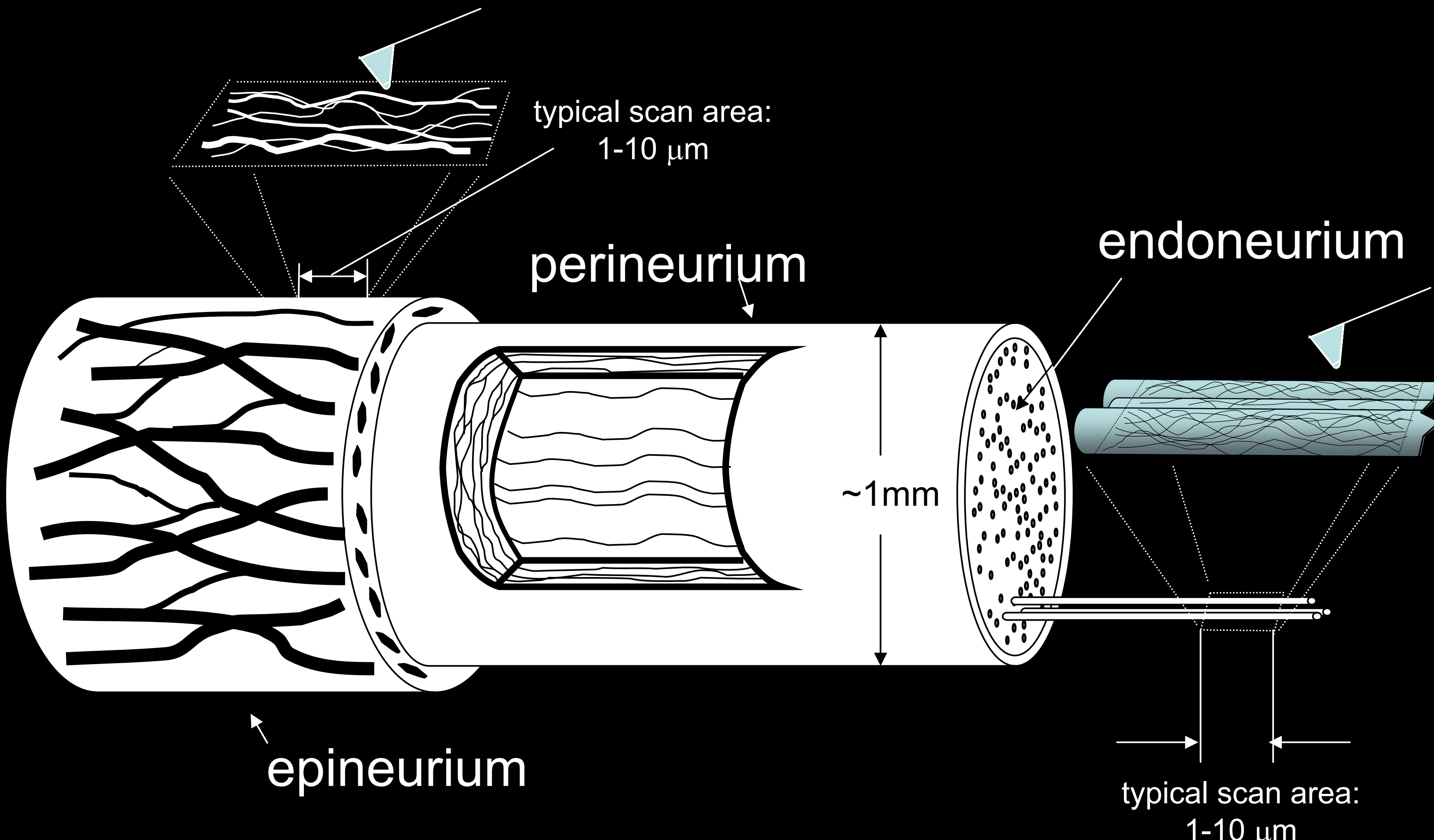

scale and pathology

at the scale of whole nerve tissue (~1mm), glucose enters the nerve primarily through transperineurial blood vessels, diffuses through the endothelial layers, of the capillaries and enters the endoneurial fluid, which contains abundant collagen.

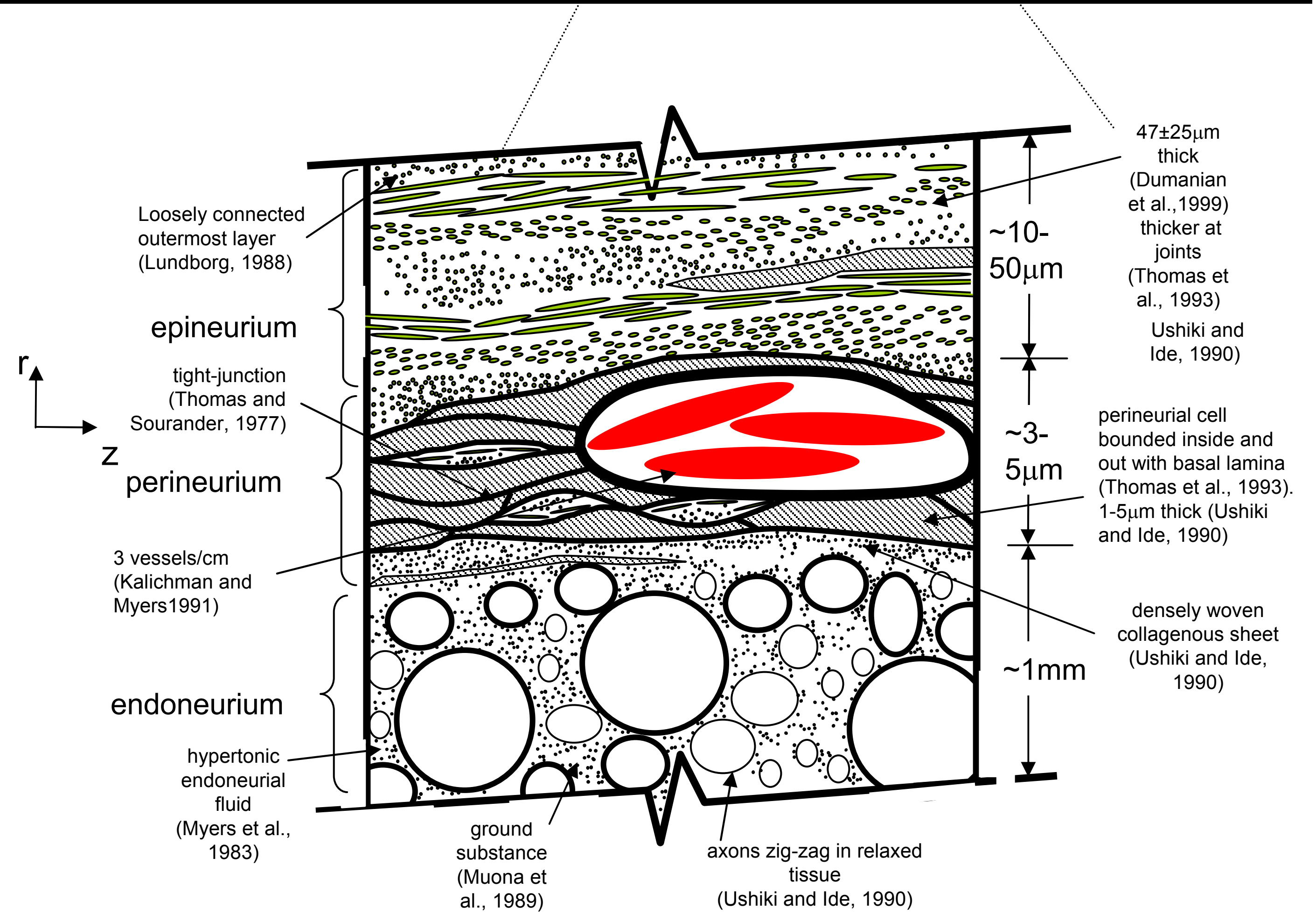

adapted from Ushiki and Ide, 1990, Fig 1[all values are for rat sciatic nerve unless otherwise noted]

- molecular to tissue scale models of diabetic neuropathy

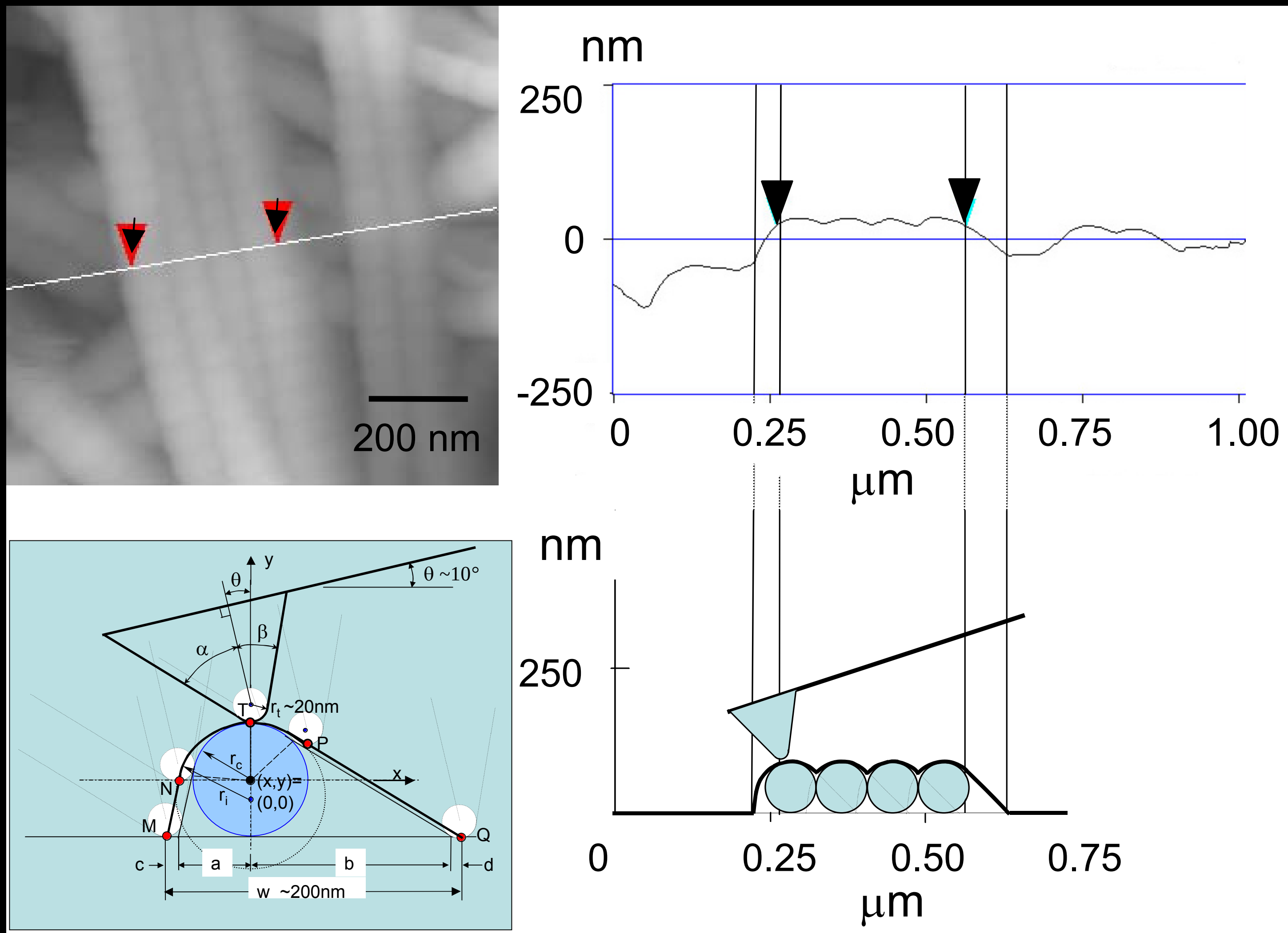

Wang, H., Layton, B.E., Sastry, A.M., 2003. Healthy and diabetic nerve collagens: an atomic force microscopy study on Sprague-Dawley and BioBreeding rats. Diabetes Metabolism Research and Reviews 19 (4) 288-298.

- molecular to tissue scale models of diabetic neuropathy

at the scale of collagen bundles (1-10um), glucose is relatively free to diffuse and bind among the hundreds of available collagen fibrils

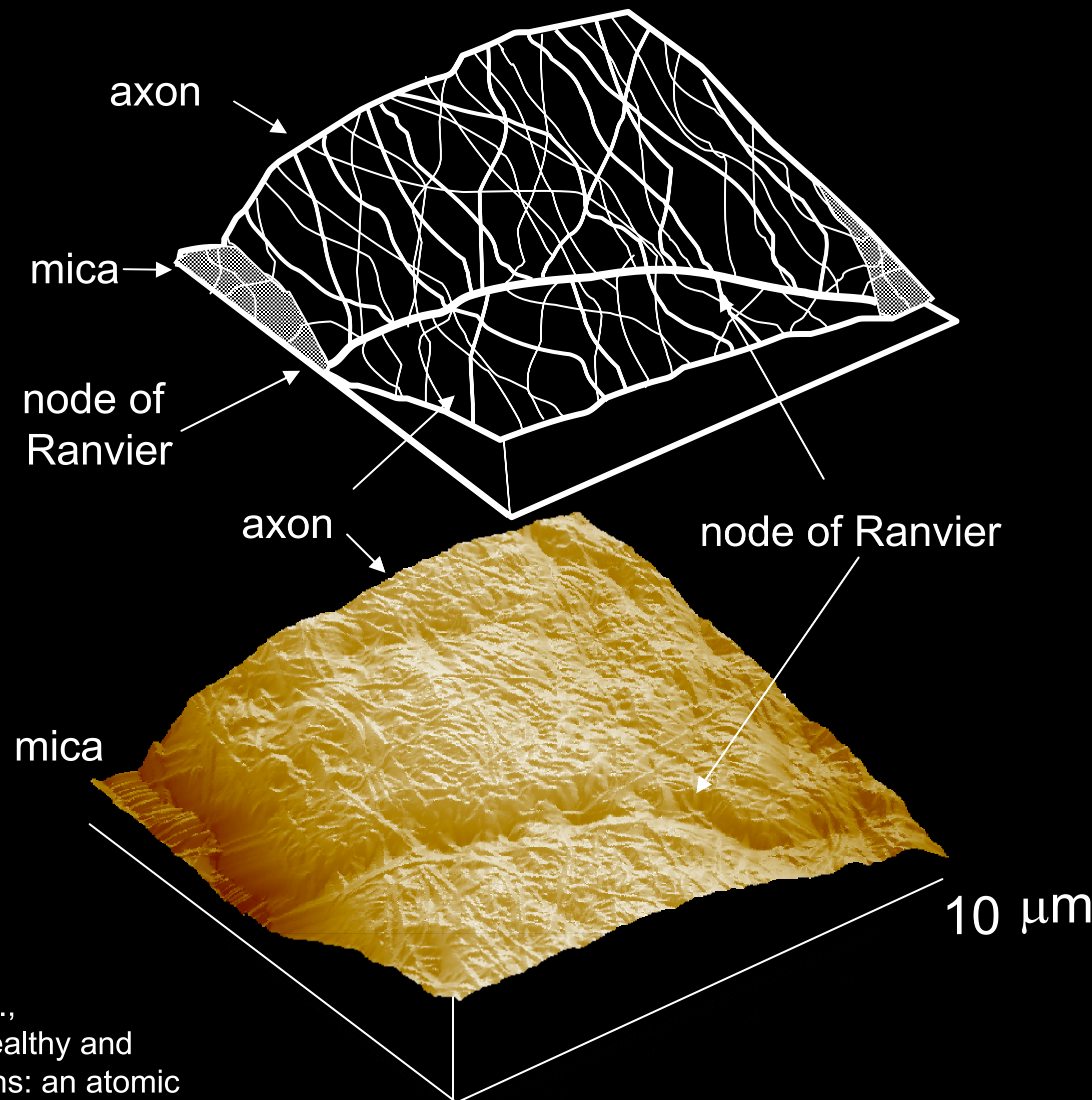

AFM image of collagen-ensheathed diabetic rat sciatic nerve axon

Wang, H., Layton, B.E., Sastry, A.M., 2003. Healthy and diabetic nerve collagens: an atomic force microscopy study on Sprague-Dawley and BioBreeding rats. Diabetes Metabolism Research and Reviews 19 (4) 288-298.

- molecular to tissue scale models of diabetic neuropathy

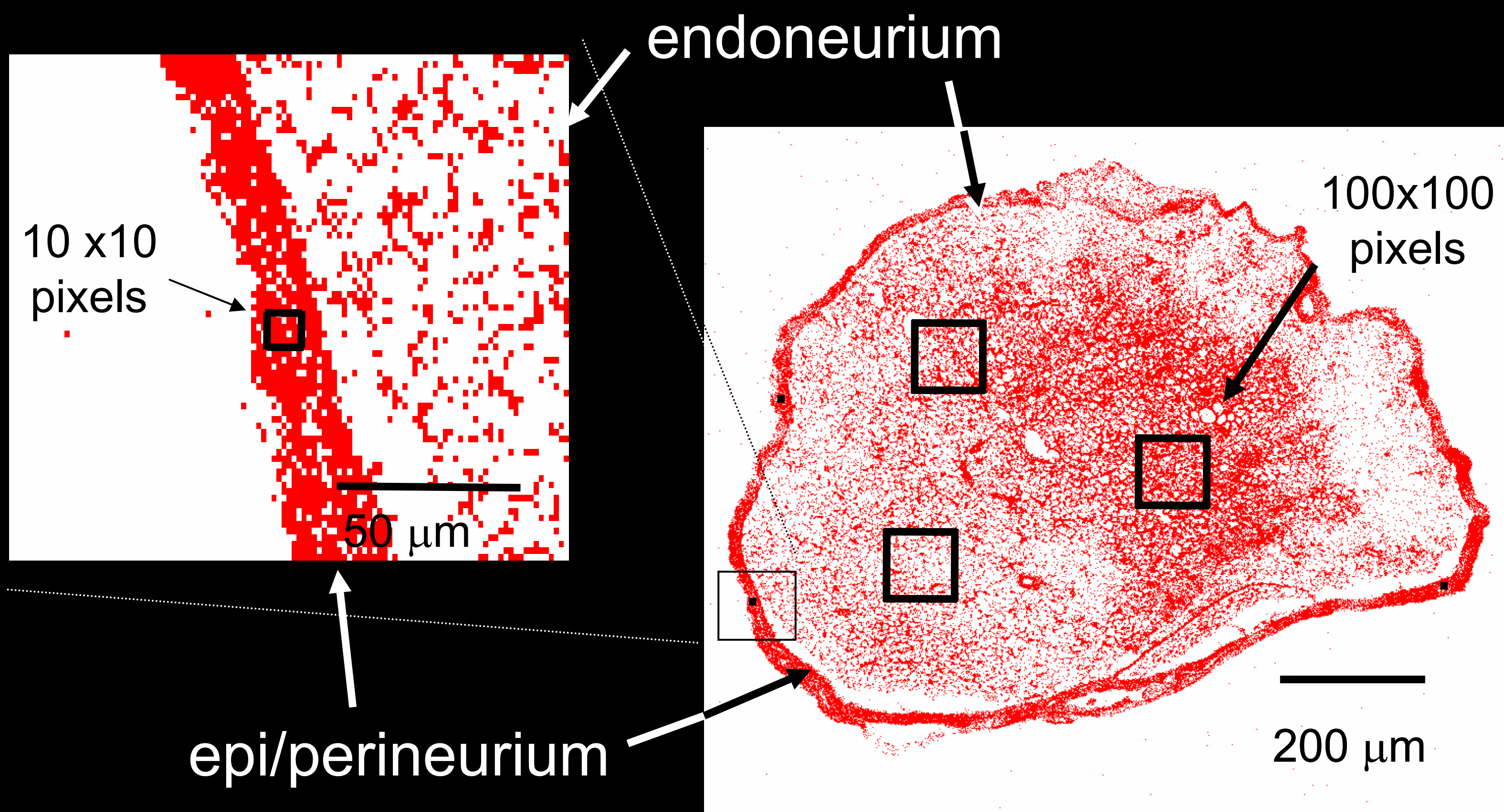

CI - type I collagen (fibrillar)
CIII - type III collagen (fibrillar)
CIV - type IV collagen (afibrillar)

Layton, B.E., Sastry, A.M., “A Mechanical Model for Collagen Fibril Load Sharing in the Peripheral Nerve of Diabetics and Non-Diabetics.” *to appear* ASME Biomechanical Engineering Journal

- collagen expression results

variable	controls	w. controls	diabetics	d - c	d - w	w - c
epi/perineurial Type I collagen	1.00 ± 0.54 (99)	1.43 ± 0.67 (63)	1.33 ± 1.05 (81)	0.021	0.486	<0.001
epi/perineurial Type III collagen	1.00 ± 0.40 (109)	1.28 ± 0.75 (61)	1.25 ± 0.91 (79)	0.031	0.856	0.013
epi/perineurial Type IV collagen	1.00 ± 0.42 (67)	1.55 ± 0.47 (40)	1.42 ± 0.53 (54)	<0.001	0.191	<0.001
endoneurial Type I collagen	1.00 ± 0.56 (33)	1.32 ± 0.67 (38)	0.96 ± 0.56 (54)	0.634	0.012	0.057
endoneurial Type III collagen	1.00 ± 0.57 (50)	1.47 ± 1.09 (43)	1.06 ± 0.63 (52)	0.736	0.039	0.022
endoneurial Type IV collagen	1.00 ± 0.67 (29)	2.06 ± 0.70 (27)	2.08 ± 1.30 (36)	<0.001	0.887	<0.001

Layton, B.E., Sastry, A.M., “A Mechanical Model for Collagen Fibril Load Sharing in the Peripheral Nerve of Diabetics and Non-Diabetics.” *to appear* ASME Biomechanical Engineering Journal

- molecular to tissue scale models of diabetic neuropathy

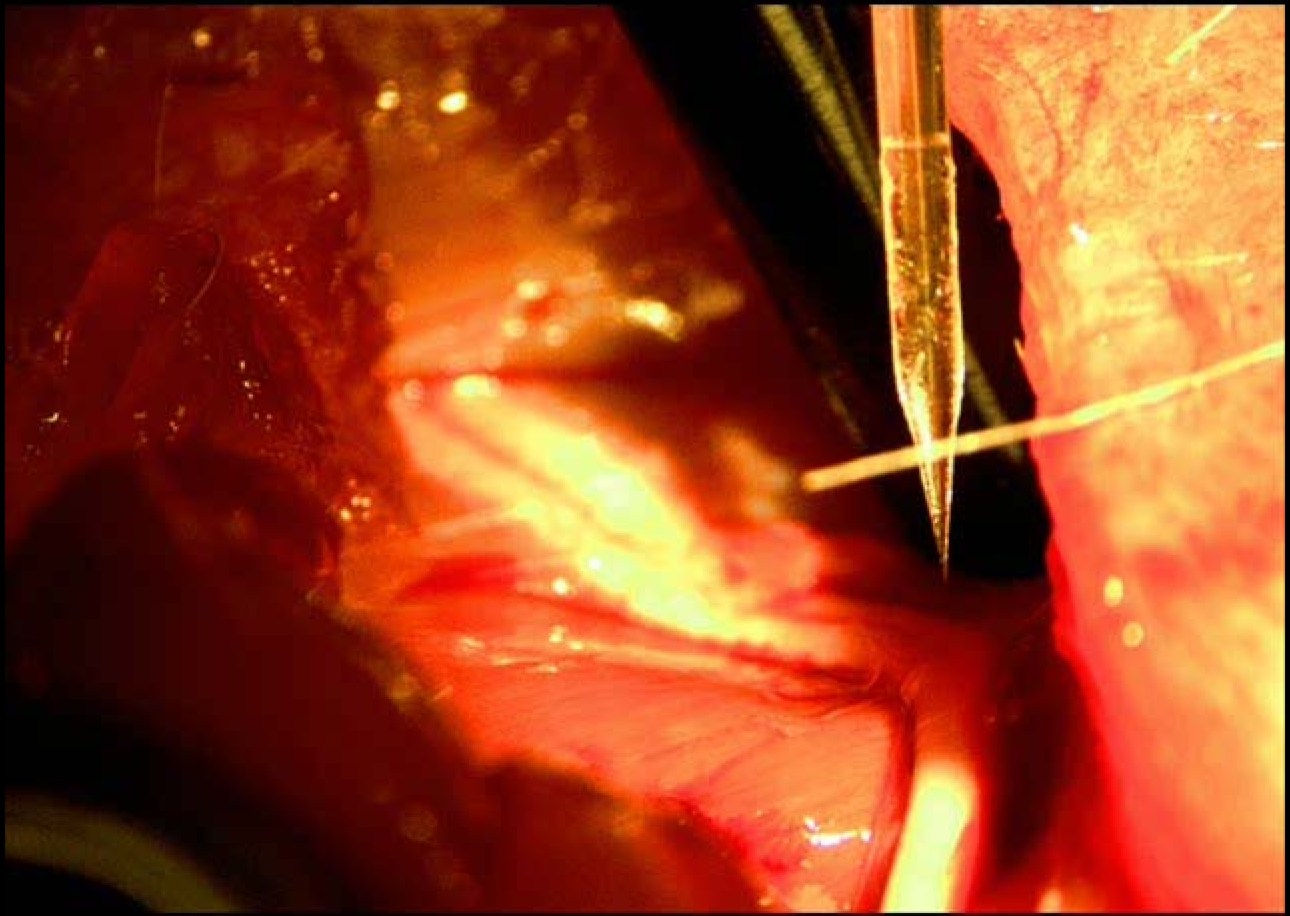

Layton, B.E., Sastry, A.M., "A Mechanical Model for Collagen Fibril Load Sharing in the Peripheral Nerve of Diabetics and Non-Diabetics." *to appear* ASME Biomechanical Engineering Journal

- molecular to tissue scale models of diabetic neuropathy

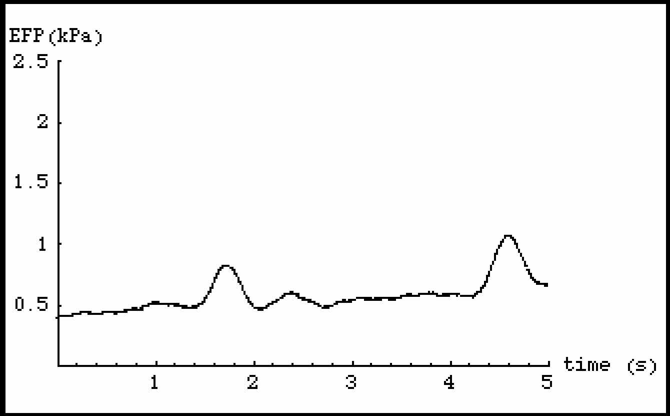

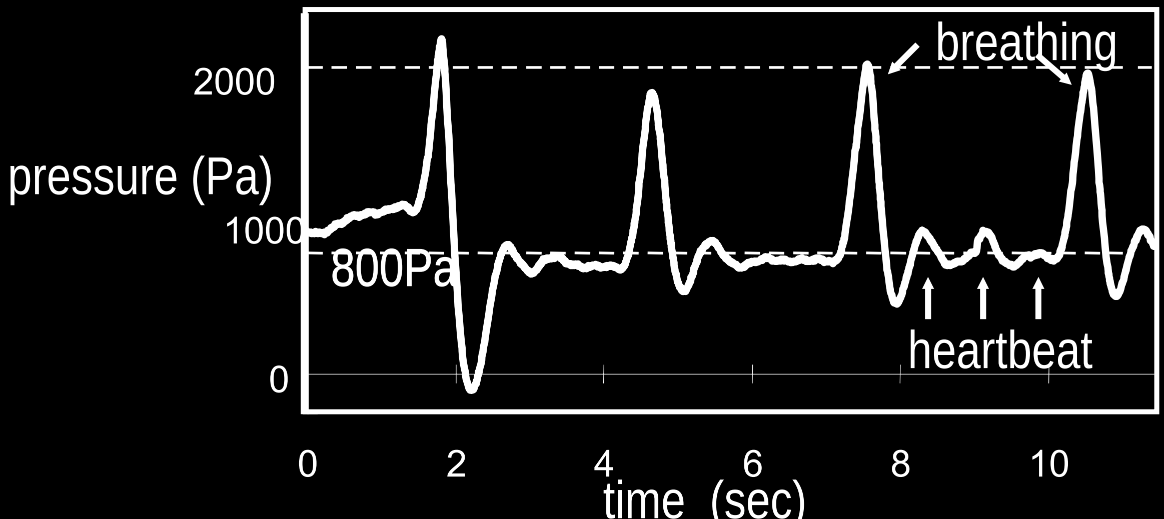

Layton, B.E., Sastry, A.M., "A Mechanical Model for Collagen Fibril Load Sharing in the Peripheral Nerve of Diabetics and Non-Diabetics." *to appear* ASME Biomechanical Engineering Journal

- molecular to tissue scale models of diabetic neuropathy

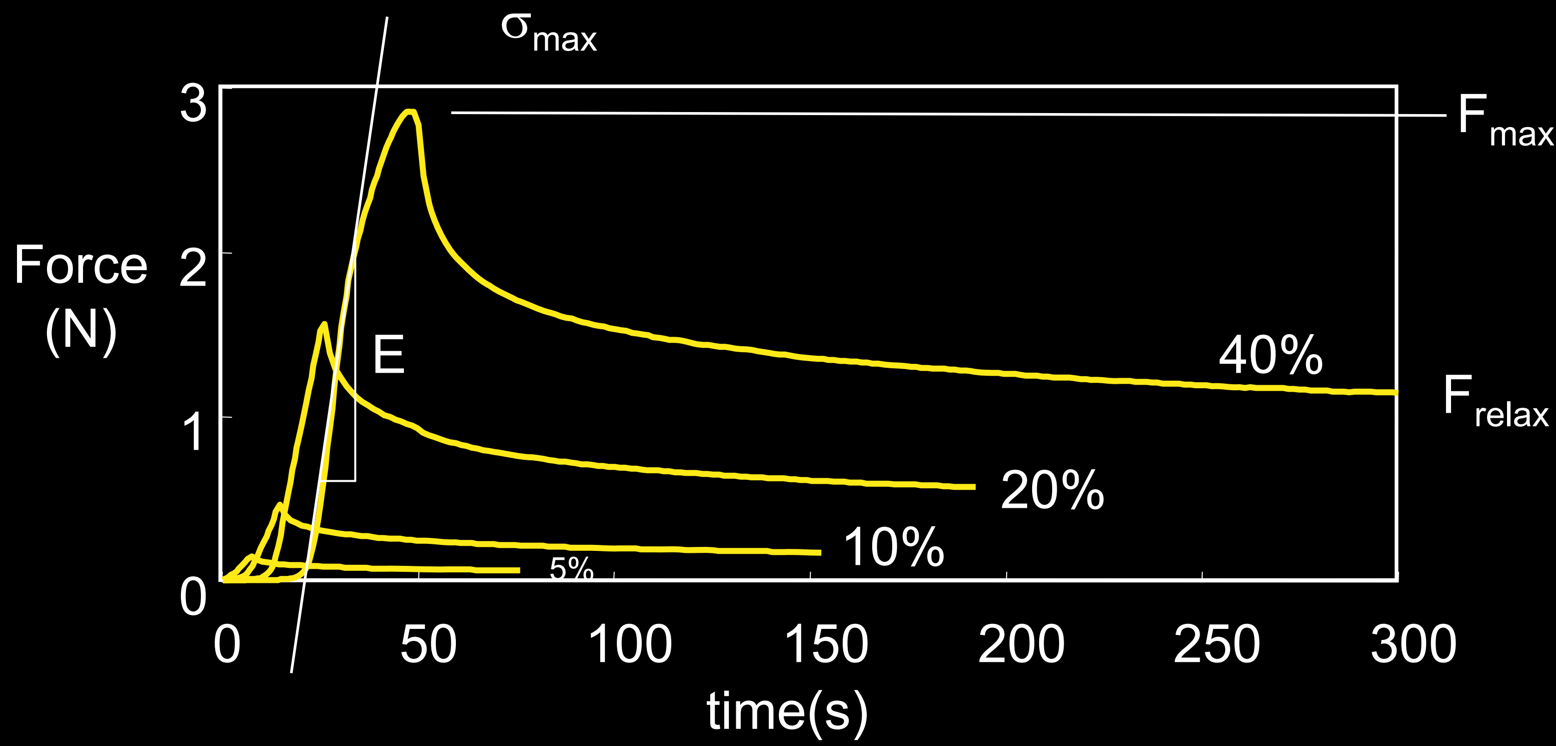

Brad Layton, Drexel University

- molecular to tissue scale models of diabetic neuropathy

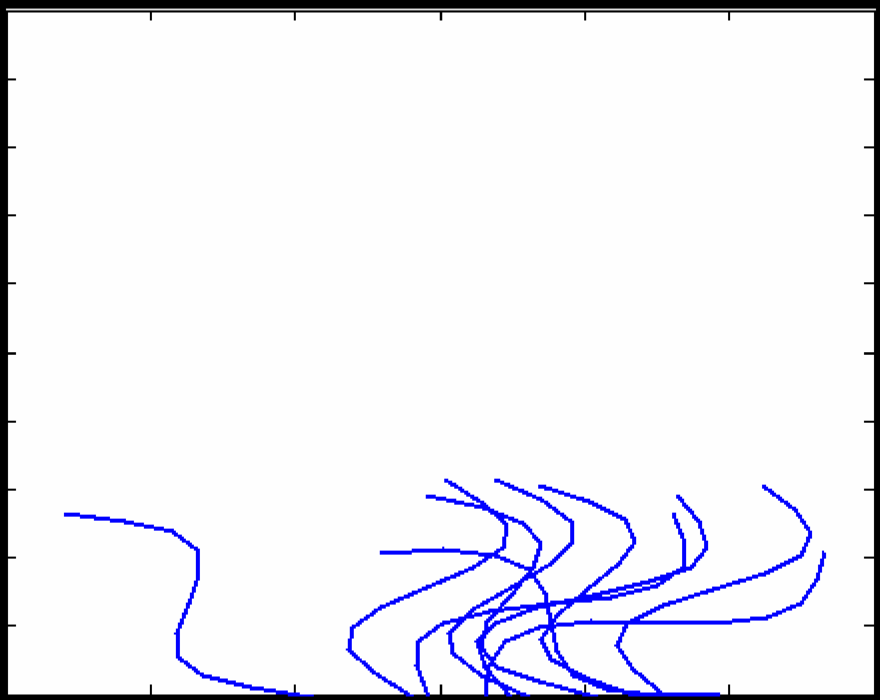

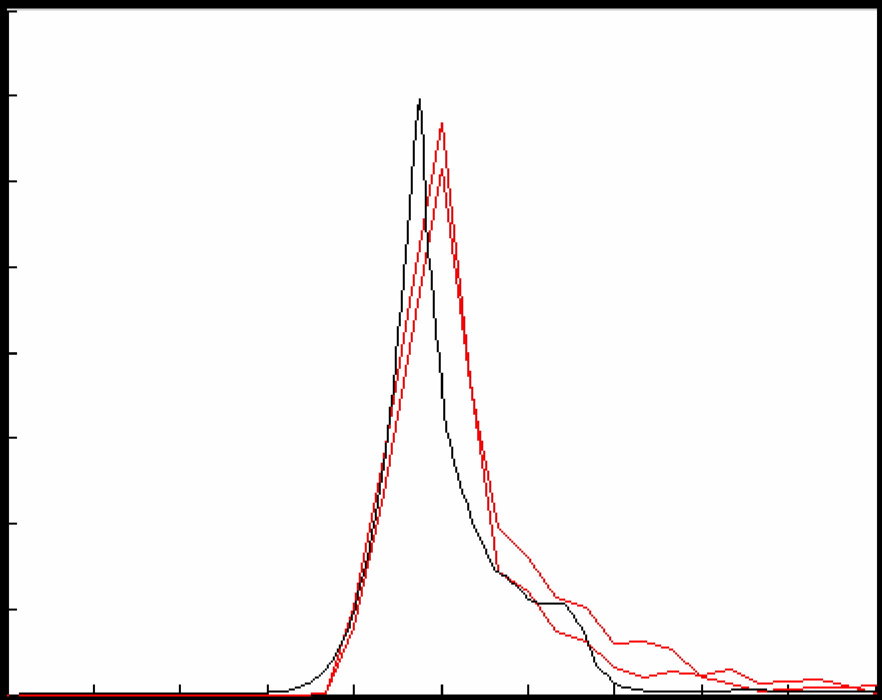

results: tissue scale

yield duration

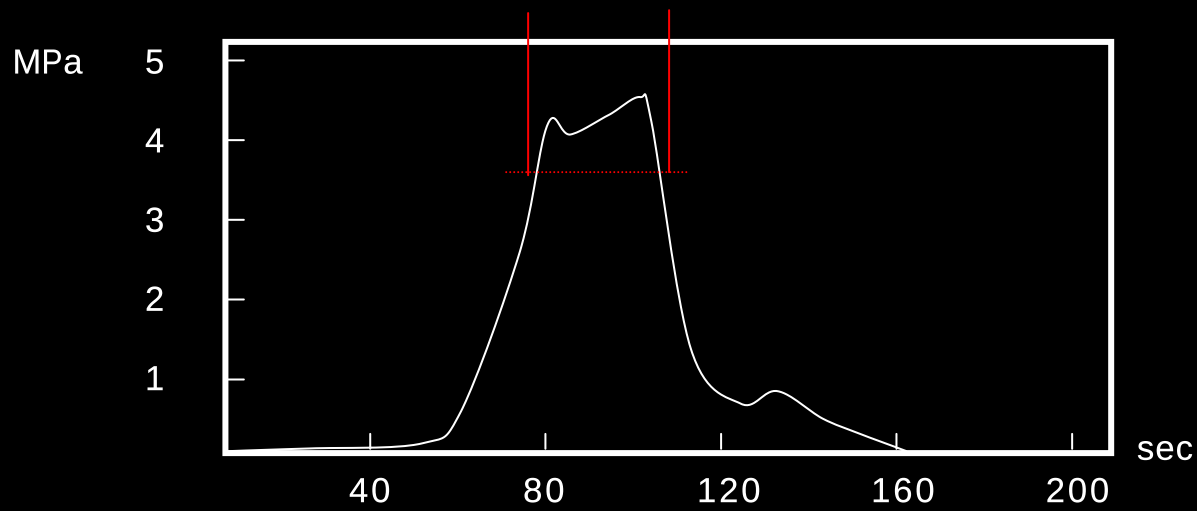

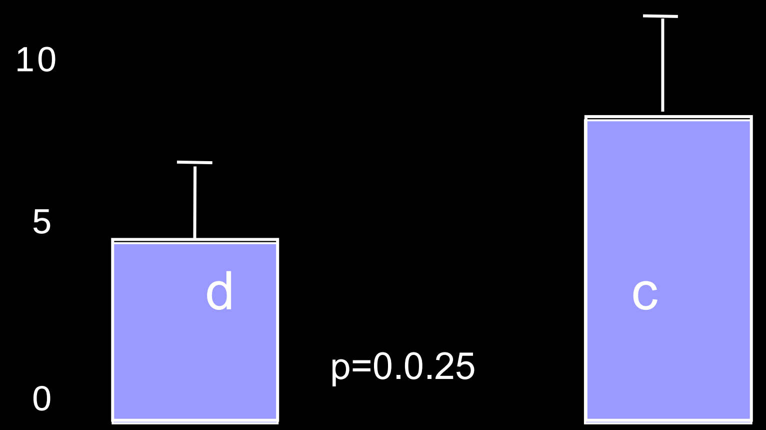

whole nerve uniaxial failure test

t-tests

- Student’s assumes normal distribution

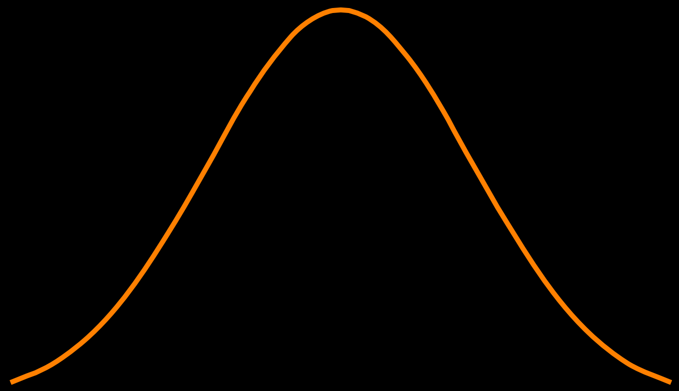

- Wilcoxon (non-parametric) assumes symmetric population

- Mann-Whitney assumes same-shape populations

Student, 1908. The probable error of a mean. Biometricka 6, 1-25. Weiss, N.A., 2002. Introductory Statistics 6th Ed. Addison-Wesley.

one-tailed vs. two-tailed

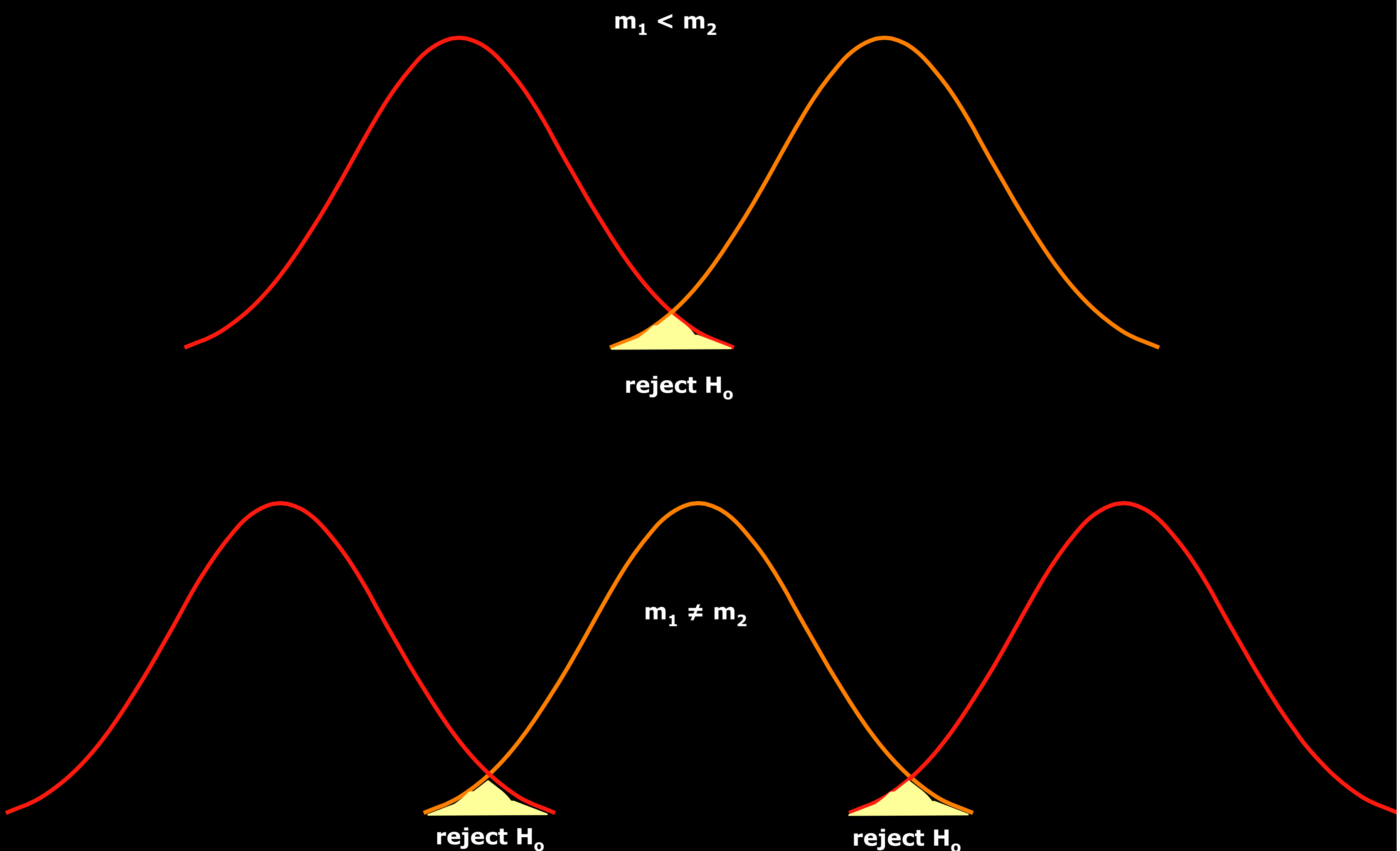

Student's t-test test

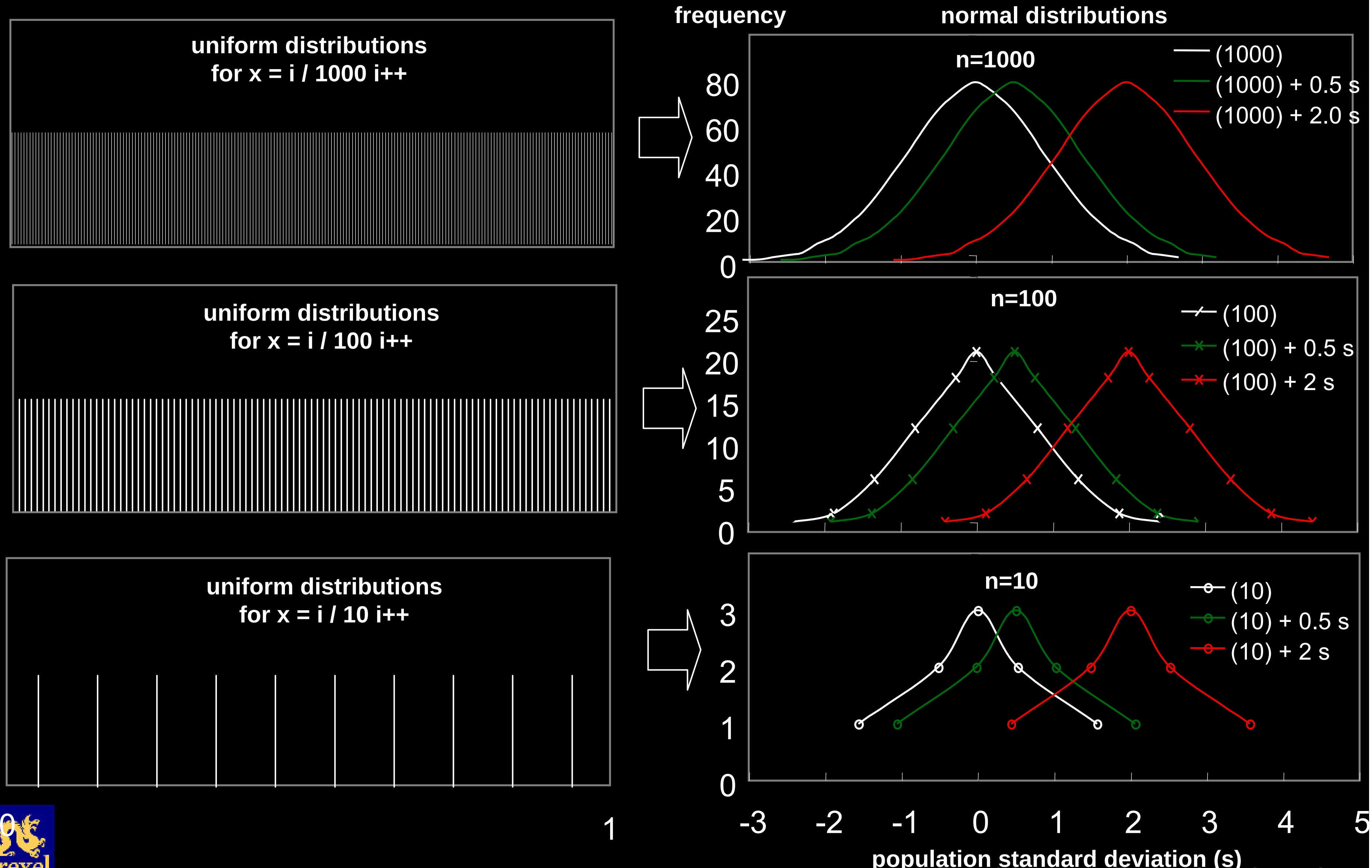

Brad Layton,Drexel University

Student’s t-test example result

n	1000		100		10	
± σ	0.5	2	0.5	2	0.5	2
one tailed	1.82E-28	2.9E-303	0.00027	7.66E-32	0.152	0.000056
two tailed	3.64E-28	5.7E-303	0.00054	1.53E-31	0.305	0.000112

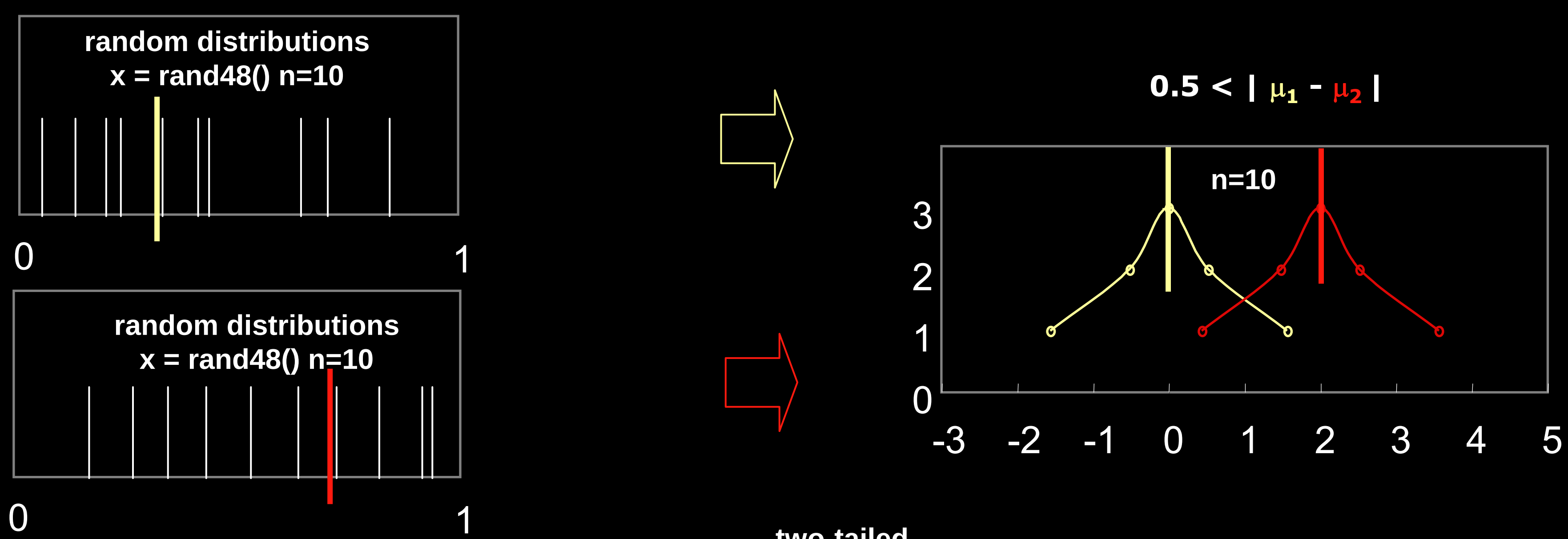

two-tailed

$0 < \mu_1 - \mu_2 < 0.25$	438
$0.25 < \mu_1 - \mu_2 < 0.5$	295
$0.5 < \mu_1 - \mu_2$	267
	1000

composite fibrous material failure

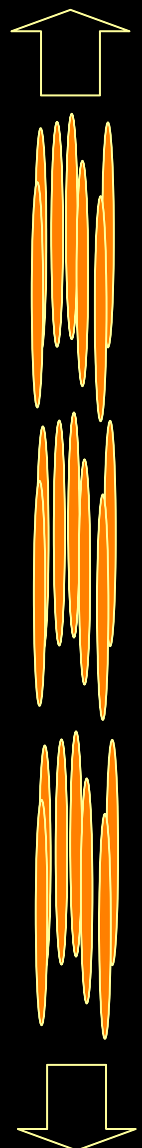

m = 3
n = 7

$$H_{m,n}(x) = 1 - \left[1 - G_n(x)\right]^m \quad for \quad x \geq 0$$

$$G_n(x) = \sum_{i=1}^{n} (-1)^{i+1} \binom{n}{i} F(x)^i G_{n-1}\left(\frac{nx}{n-i}\right)$$

(ELS rule

$$F(x) = 1 - e^{-\left(\frac{x}{x_o}\right)^{\rho}}$$

H = probability of failure of a composite consisting of a chain with m linked bundles of n fibers each
G = probability of failure of a bundle with n fibers
F = probability of failure of a single fiber

x_o = scale parameter of Weibull distribution
ρ = shape parameter of Weibull distribution

Harlow and Phoenix 1978

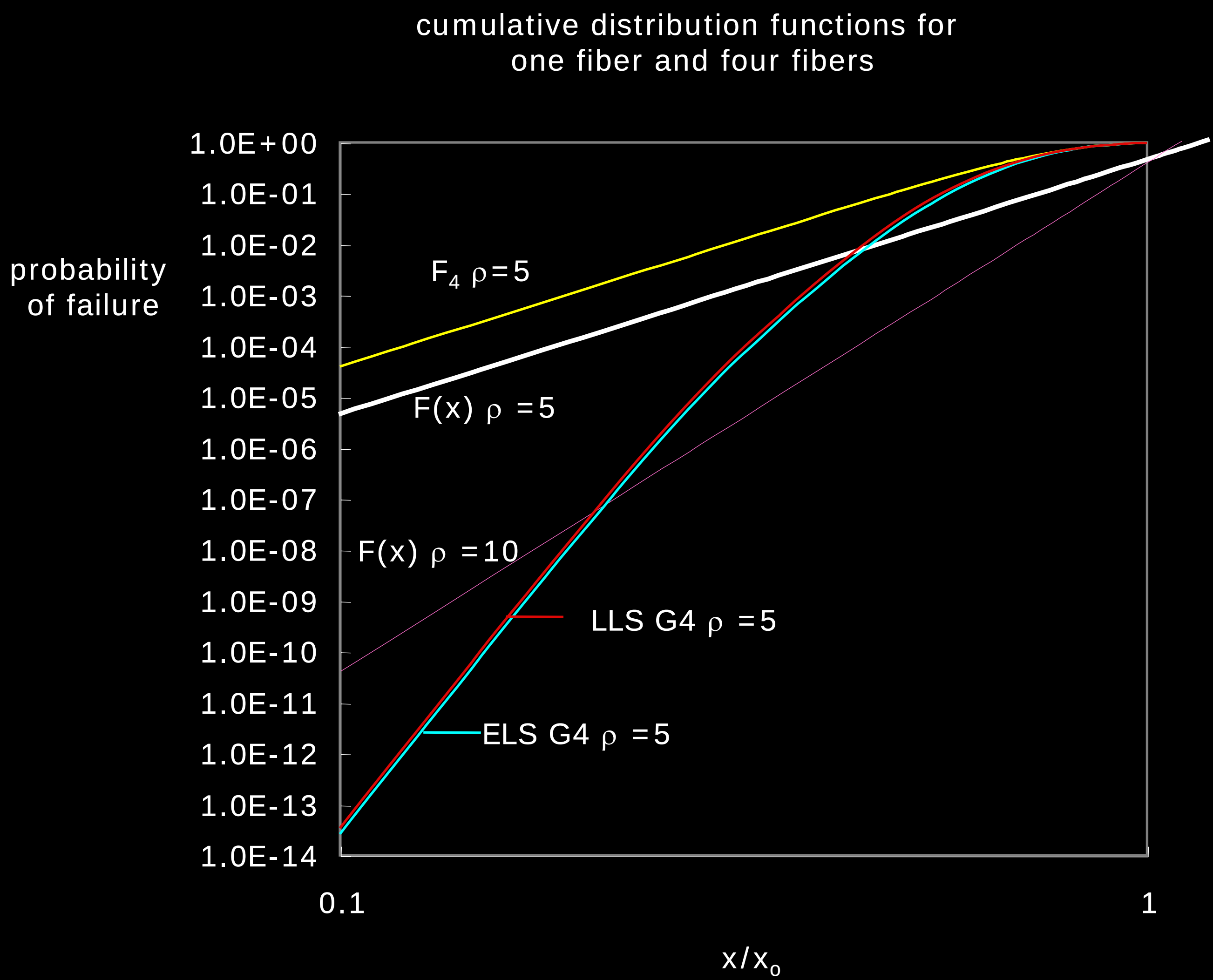

ELS vs LLS

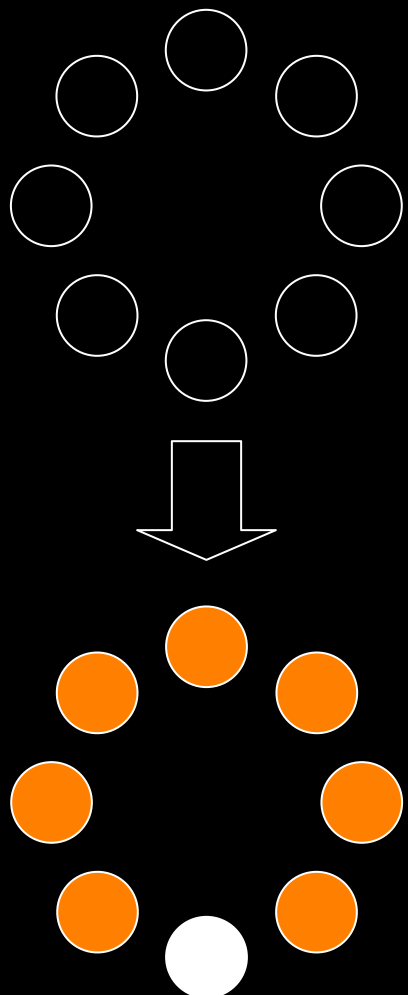

ELS

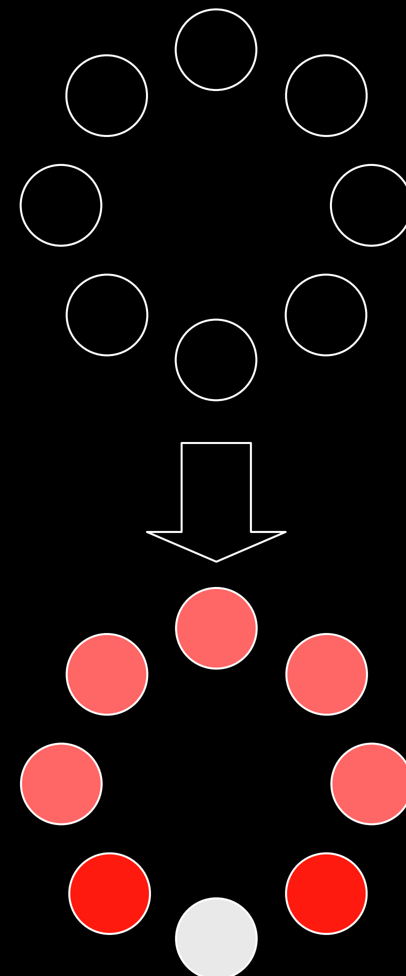

LLS

ELS vs LLS

Harlow and Phoenix use a circular array with uniform spacing

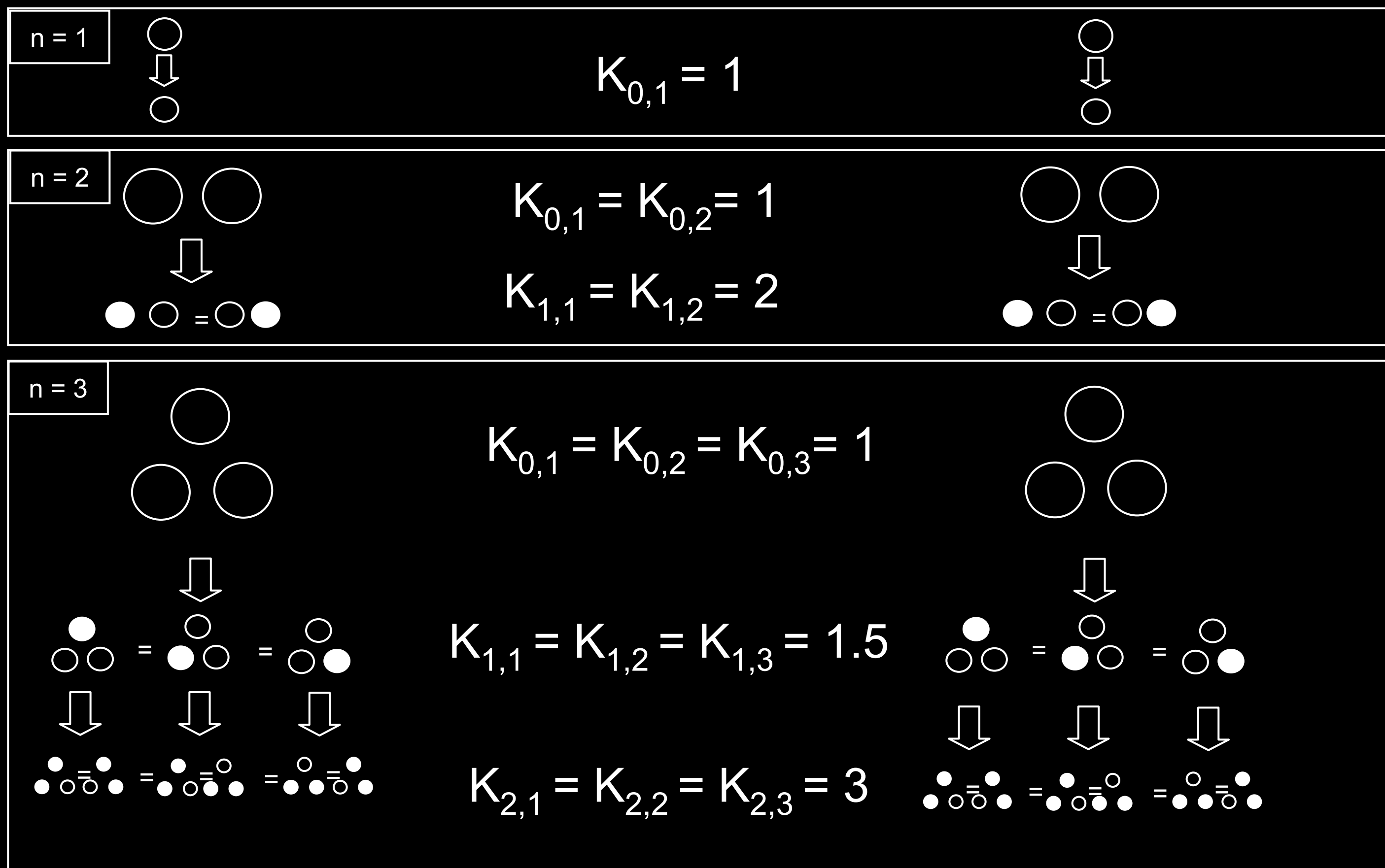

$K_b = n/(n-b)$

equal load sharing

$K_{b,i}$ = load concentration factor for i^{th} surviving fiber in bundle with *b* broken fibers

b = number of broken fibers in bundle

$K_r = 1 + r/2$

local load sharing

$K_{r,i}$ = load concentration factor for i^{th} surviving fiber adjacent to *r* broken fibers (both sides)

r = number of broken fibers immediately adjacent to unbroken fiber

ELS vs LLS

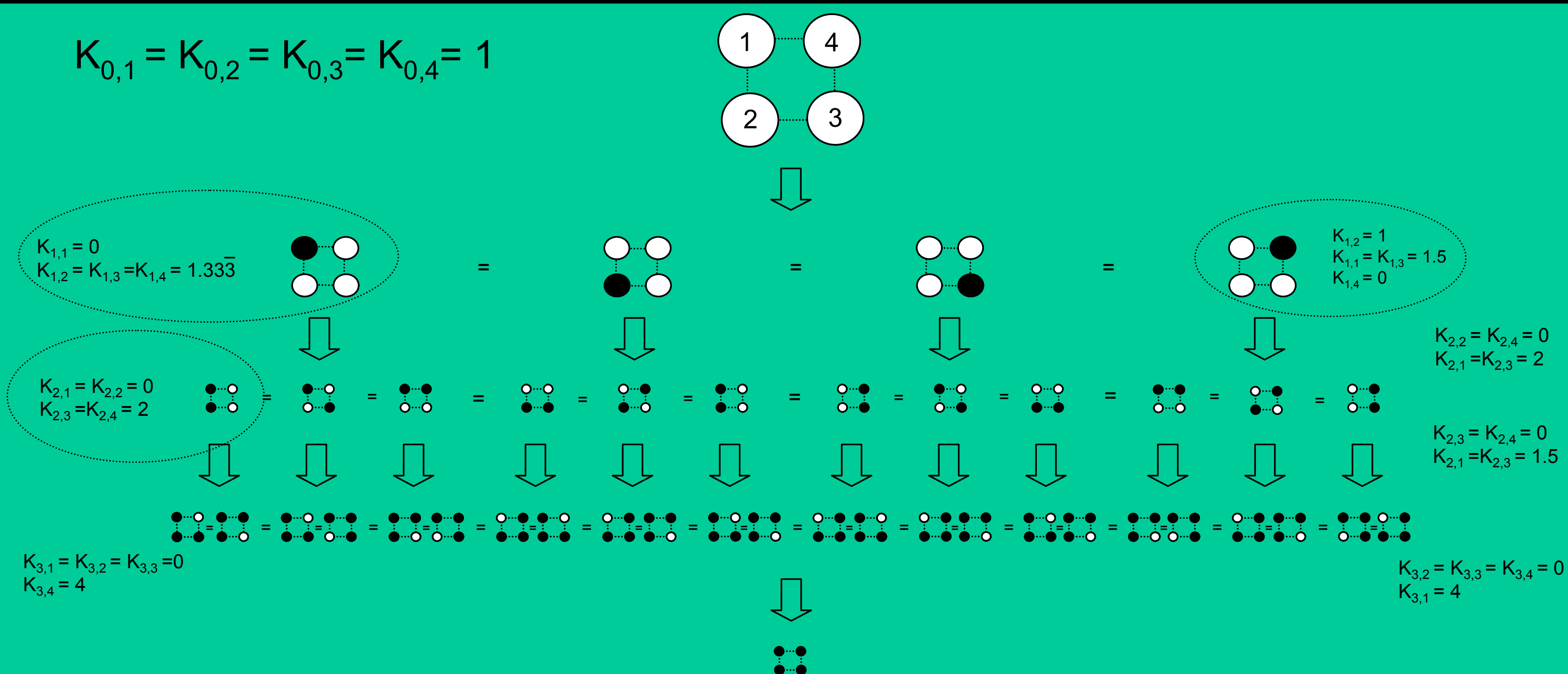

$K_b = n/(n-b)$

At first glance, it may appear that in load concentration factor for i^{th} surviving fiber adjacent to *r* broken fibers (both sides)
r = number of broken fibers immediately adjacent to unbroken fiber

$K_r = 1 + r/2$

equal load sharing

$K_{b,i}$ = load concentration factor for i^{th} surviving fiber in bundle with *b* broken fibers
b = number of broken fibers in bundle

local load sharing

$K_{r,i}$ = load concentration factor for i^{th} surviving fiber adjacent to *r* broken fibers (both sides)
r = number of broken fibers immediately adjacent to unbroken fiber

- molecular to tissue scale models of diabetic neuropathy

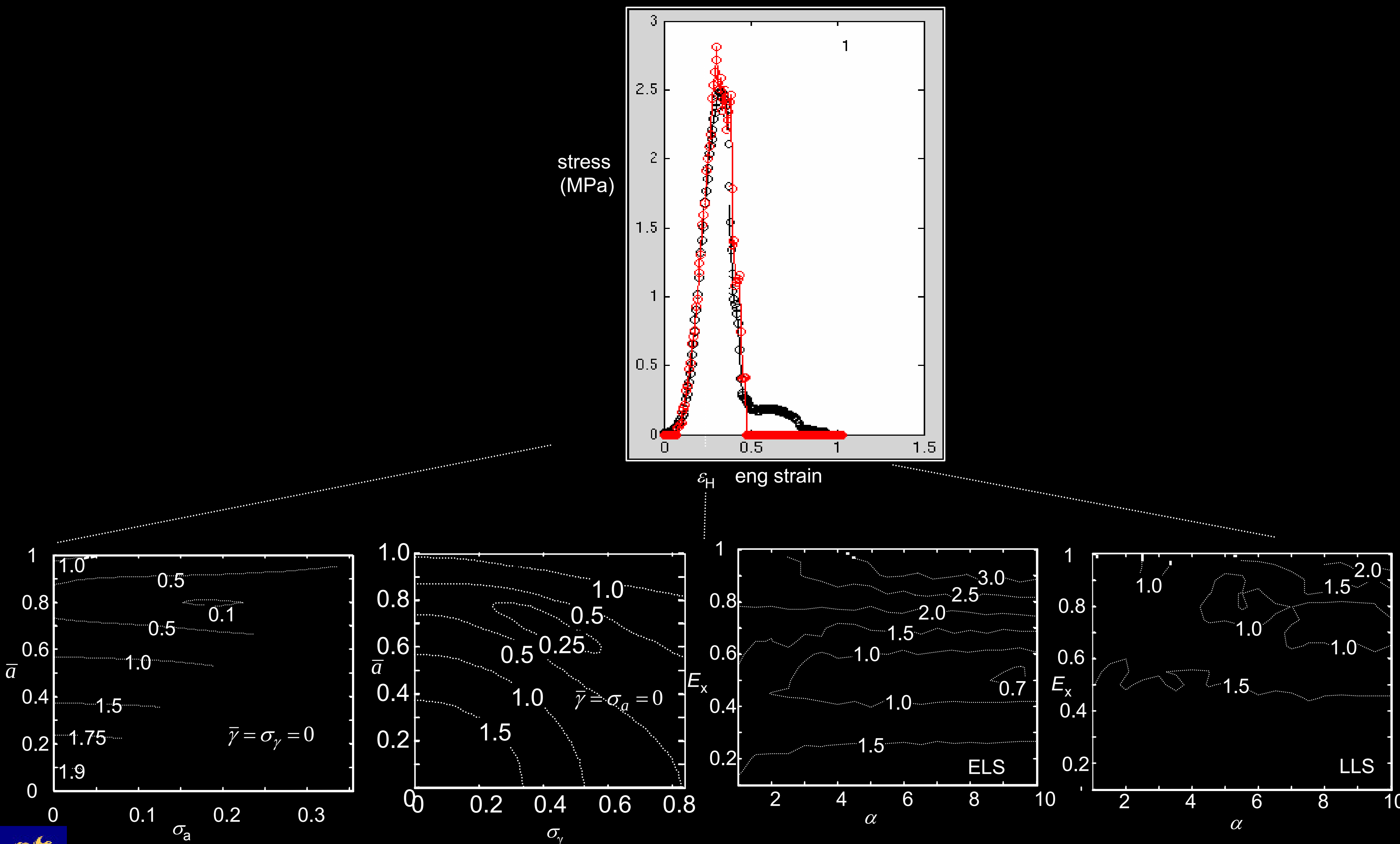

- molecular to tissue scale models of diabetic neuropathy

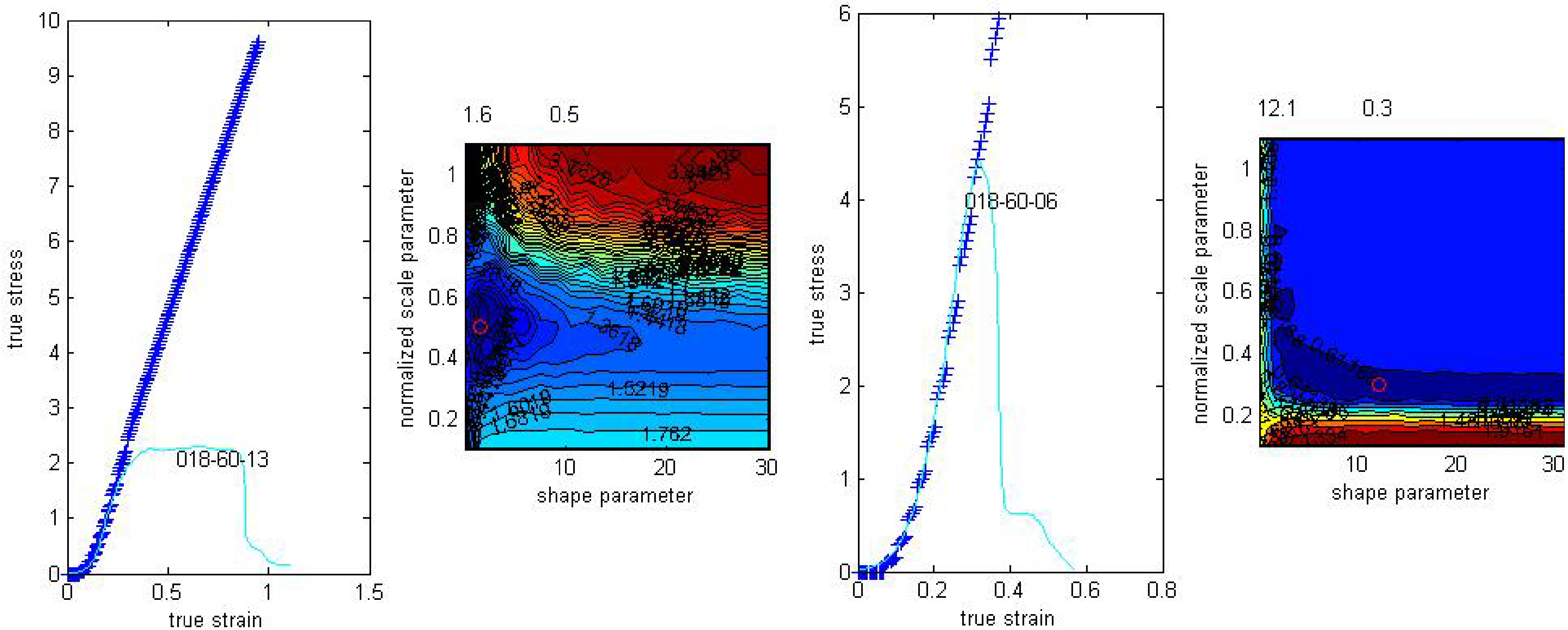

typical control *typical diabetic*

a lower shape parameter indicates greater variance
a lower scale parameter means a lower UTS – E ratio

OUTLINE

NANOMETROLOGY OF COLLAGEN

- molecular to tissue scale models of diabetic neuropathy

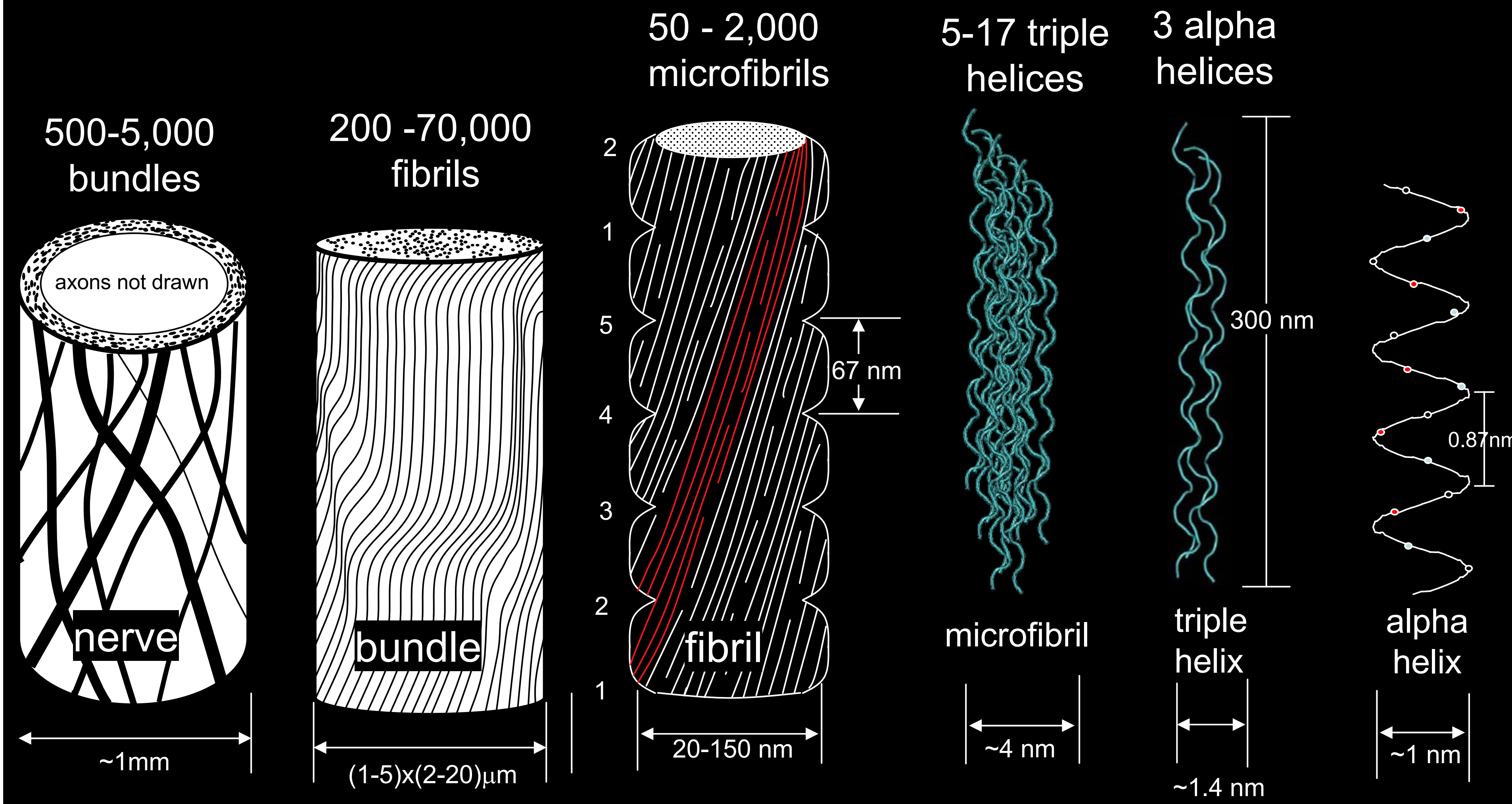

Brad Layton, Drexel University

- single molecule and single fibril experiments

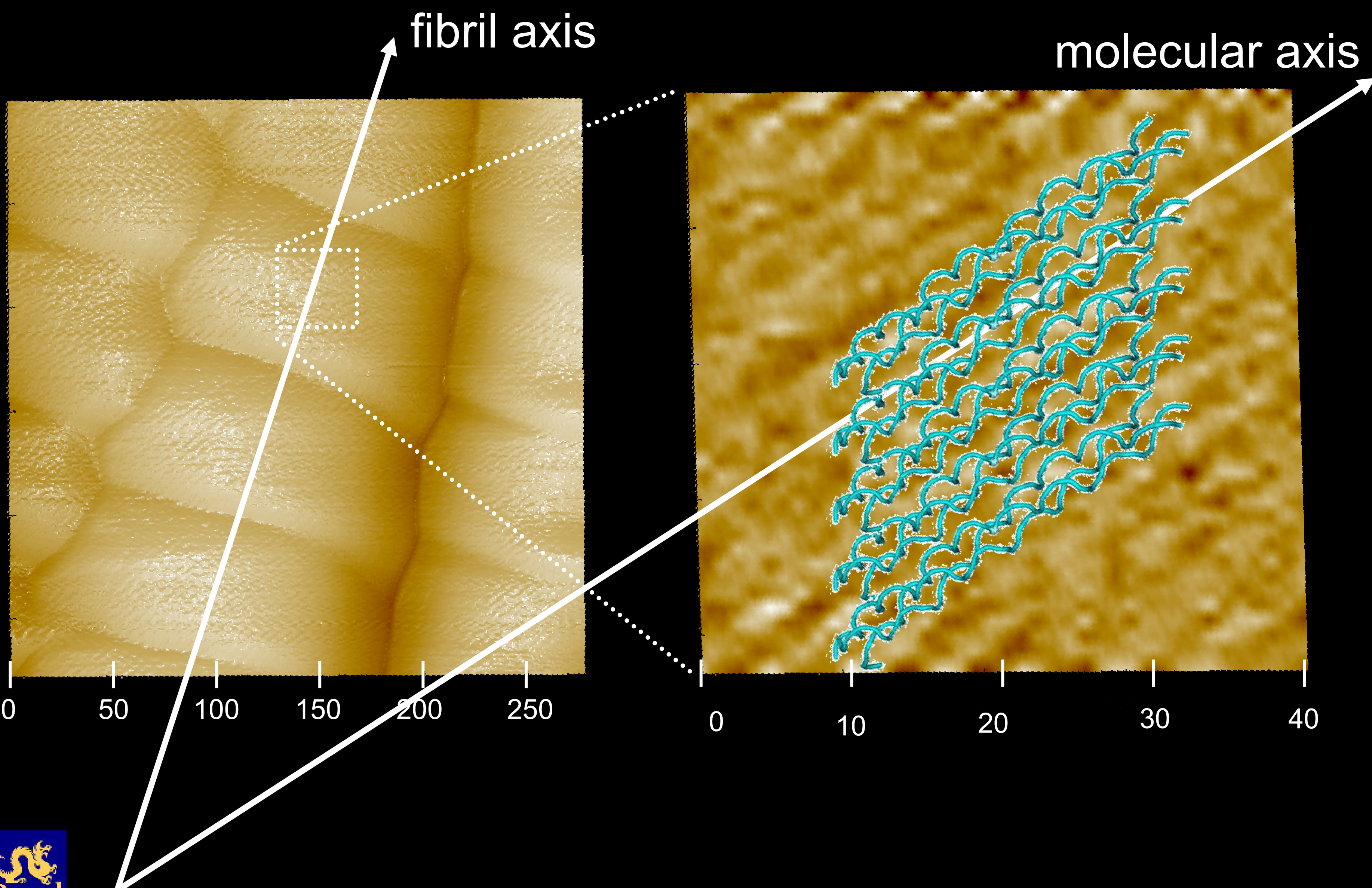

- single molecule and single fibril experiments

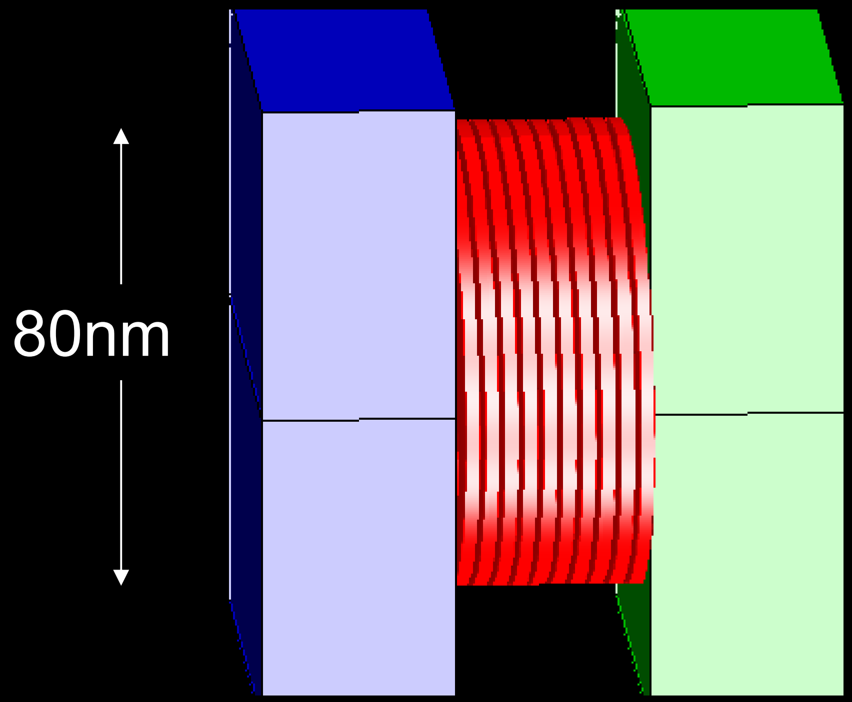

single collagen fibril testing

- single molecule and single fibril experiments

```
MFSFVDLRLLLLLAATALLTHGQEEGQVEGQDEDIPPITCVQNGLRYHDR
DVWKPEPCRICVCDNGKVLCDDVICDETKNCPGAEVPEGECCPVCPDGSE
SPTDQETTGVEGPKGDTGPRGPRGPAGPPGRDGIPGQPGLPGPPGPPGPP
GPPGLGGNFAPQLSYGYDEKSTGGISVPGPMGPSGPRGLPGPPGAPGPQG
FQGPPGEPGEPGASGPMGPRGPPGPPGKNGDDGEAGKPGRPGERGPPGPQ
GARGLPGTAGLPGMKGHRGFSGLDGAKGDAGPAGPKGEPGSPGENGAPGQ
MGPRGLPGERGRPGAPGPAGARGNDGATGAAGPPGPTGPAGPPGFPGAVG
AKGEAGPQGPRGSEGPQGVRGEPGPPGPAGAAGPAGNPGADGQPGAKGAN
GAPGIAGAPGFPGARGPSGPQGPGGPPGPKGNSGEPGAPGSKGDTGAKGE
PGPVGVQGPPGPAGEEGKRGARGEPGPTGLPGPPGERGGPGSRGFPGADG
VAGPKGPAGERGSPGPAGPKGSPGEAGRPGEAGLPGAKGLTGSPGSPGPD
GKTGPPGPAGQDGRPGPPGPPGARGQAGVMGFPGPKGAAGEPGKAGERGV
PGPPGAVGPAGKDGEAGAQGPPGPAGPAGERGEQGPAGSPGFQGLPGPAG
PPGEAGKPGEQGVPGDLGAPGPSGARGERGFPGERGVQGPPGPAGPRGAN
GAPGNDGAKGDAGAPGAPGSQGAPGLQGMPGERGAAGLPGPKGDRGDAGP
KGADGSPGKDGVRGLTGPIGPPGPAGAPGDKGESGPSGPAGPTGARGAPG
DRGEPGPPGPAGFAGPPGADGQPGAKGEPGDAGAKGDAGPPGPAGPAGPP
GPIGNVGAPGAKGARGSAGPPGATGFPGAAGRVGPPGPSGNAGPPGPPGP
AGKEGGKGPRGETGPAGRPGEVGPPGPPGPAGEKGSPGADGPAGAPGTPG
PQGIAGQRGVVGLPGQRGERGFPGLPGPSGEPGKQGPSGASGERGPPGPM
GPPGLAGPPGESGREGAPGAEGSPGRDGSPGAKGDRGETGPAGPPGAPGA
PGAPGPVGPAGKSGDRGETGPAGPAGPVGPAGARGPAGPQGPRGDKGETG
EQGDRGIKGHRGFSGLQGPPGPPGSPGEQGPSGASGPAGPRGPPGSAGAP
GKDGLNGLPGPIGPPGPRGRTGDAGPVGPPGPPGPPGPPGPPSAGFDFSF
LPQPPQEKAHDGGRYYRADDANVVRDRDLEVDTTLKSLSQQIENIRSPEG
SRKNPARTCRDLKMCHSDWKSGEYWIDPNQGCNLDAIKVFCNMETGETCV
YPTQPSVAQKNWYISKNPKDKRHVWFGESMTDGFQFEYGGQGSDPADVAI
QLTFLRLMSTEASQNITYHCKNSVAYMDQQTGNLKKALLLKGSNEIEIRA
EGNSRFTYSVTVDGCTSHTGAWGKTVIEYKTTKTSRLPIIDVAPLDVGAP
DQEFGFDVGPVCFL
```

- single molecule and single fibril experiments

MFSFVDLRLLLLLAATALLTH|QEE|QVE|QDEDIPPITCVQN|LRYHDR
DVWKPEPCRICVCDN|KVLCDDVICDETKNCP|AEVPE|ECCPVCPD|SESPTDQETT
|VE|PK|DT|PR|PR|PA|PP|RD|IP|QP|LP|PP|PP|PP|PP|L||NFAPQLSY|YDEKST
||ISVP|PM|PS|PR|LP|PP|AP|PQ|FQ
|PP|EP|EP|AS|PM|PR|PP|PP|KN|DD|EA|KP|RP|ER|PP|PQ
|AR|LP|TA|LP|MK|HR|FS|LD|AK|DA|PA|PK|EP|SP|EN|AP|QM
|PR|LP|ER|RP|AP|PA|AR|ND|AT|AA|PP|PT|PA|PP|FP|AV|AK
|EA|PQ|PR|SE|PQ|VR|EP|PP|PA|AA|PA|NP|AD|QP|AK|AN
|AP|IA|AP|FP|AR|PS|PQ|P||PP|PK|NS|EP|AP|SK|DT|AK|EP
|PV|VQ|PP|PA|EE|KR|AR|EP|PT|LP|PP|ER||P|SR|FP|AD|VA
|PK|PA|ER|SP|PA|PK|SP|EA|RP|EA|LP|AK|LT|SP|SP|PD
|KT|PP|PA|QD|RP|PP|PP|AR|QA|VM|FP|PK|AA|EP|KA|ER|VP
|PP|AV|PA|KD|EA|AQ|PP|PA|PA|ER|EQ|PA|SP|FQ|LP|PA|PP
|EA|KP|EQ|VP|DL|AP|PS|AR|ER|FP|ER|VQ|PP|PA|PR|AN
|AP|ND|AK|DA|AP|AP|SQ|AP|LQ|MP|ER|AA|LP|PK|DR|DA|PK
|AD|SP|KD|VR|LT|PI|PP|PA|AP|DK|ES|PS|PA|PT|AR|AP|DR
|EP|PP|PA|FA|PP|AD|QP|AK|EP|DA|AK|DA|PP|PA|PA|PP
|PI|NV|AP|AK|AR|SA|PP|AT|FP|AA|RV|PP|PS|NA|PP|PP|PA
|KE||K|PR|ET|PA|RP|EV|PP|PP|PA|EK|SP|AD|PA|AP|TP|PQ
|IA|QR|VV|LP|QR|ER|FP|LP|PS|EP|KQ|PS|AS|ER|PP|PM
|PP|LA|PP|ES|RE|AP|AE|SP|RD|SP|AK|DR|ET|PA|PP|AP|AP
|AP|PV|PA|KS|DR|ET|PA|PA|PV|PA|AR|PA|PQ|PR|DK|ET|EQ
|DR|IK|HR|FS|LQ|PP|PP|SP|EQ|PS|AS|PA|PR|PP|SA|AP
|KD|LN|LP|PI|PP|PR|RT|DA|PV|PP|PP|PP|PP|PPSA|FDFSF
LPQPPQEKAHD||RYYRADDANVVRDRDLEVDTTLKSLSQQIENIRSPE|
SRKNPARTCRDLKMCHSDWKS|EYWIDPNQ|CNLDAIKVFCNMET|ETCV
YPTQPSVAQKNWYISKNPKDKRHVWF|ESMTD|FQFEY||Q|SDPADVAI
QLTFLRLMSTEASQNITYHCKNSVAYMDQQT|NLKKALLLK|SNEIEIRA
E|NSRFTYSVTVD|CTSHT|AW|KTVIEYKTTKTSRLPIIDVAPLDV|AP
DQEF|FDV|PVCFL

- bioinformatics correlations

```
MLSFVDTRTLLLLAVTLCLATCQSLQEETVRKGPAGDRGPRGERG
PPGPPGRDGEDGPTGPPGPPGPPGPPGLGGNFAAQYDGKGVGLGP
GPMGLMGPRGPPGAAGAPGPQGFQGPAGEPGEPGQTGPAGARGPAGPPGKAGEDGHPGKPGRPGERGVVGPQGAR
GFPGTPGLPGFKGIRGHNGLDGLKGQPGAPGVKGEPGAPGENGTPGQTGARGLPGERGRVGAPGPAGARGSDGSV
GPVGPAGPIGSAGPPGFPGAPGPKGEIGAVGNAGPAGPAGPRGEVGLPGLSGPVGPPGNPGANGLTGAKGAAGLP
GVAGAPGLPGPRGIPGPVGAAGATGARGLVGEPGPAGSKGESGNKGEPGSAGPQGPPGPSGEEGKRGPNGEAGSA
GPPGPPGLRGSPGSRGLPGADGRAGVMGPPGSRGASGPAGVRGPNGDAGRPGEPGLMGPRGLPGSPGNIGPAGKE
GPVGLPGIDGRPGPIGPAGARGEPGNIGFPGPKGPTGDPGKNGDKGHAGLAGARGAPGPDGNNGAQGPPGPQGVQ
GGKGEQGPPGPPGFQGLPGPSGPAGEVGKPGERGLHGEFGLPGPAGPRGERGPPGESGAAGPTGPIGSRGPSGPP
GPDGNKGEPGVVGAVGTAGPSGPSGLPGERGAAGIPGGKGEKGEPGLRGEIGNPGRDGARGAPGAVGAPGPAGAT
GDRGEAGAAGPAGPAGPRGSPGERGEVGPAGPNGFAGPAGAAGQPGAKGERGAKGPKGENGVVGPTGPVGAAGPA
GPNGPPGPAGSRGDGGPPGMTGFPGAAGRTGPPGPSGISGPPGPPGPAGKEGLRGPRGDQGPVGRTGEVGAVGPP
GFAGEKGPSGEAGTAGPPGTPGPQGLLGAPGILGLPGSRGERGLPGVAGAVGEPGPLGIAGPPGARGPPGAVGSP
GVNGAPGEAGRDGNPGNDGPPGRDGQPGHKGERGYPGNIGPVGAAGAPGPHGPVGPAGKHGNRGETGPSGPVGPA
GAVGPRGPSGPQGIRGDKGEPGEKGPRGLPGLKGHNGLQGLPGIAGHHGDQGAPGSVGPAGPRGPAGPSGPAGKD
GRTGHPGTVGPAGIRGPQGHQGPAGPPGPPGPPGPPGVSGGGYDFGYDGD
FYRADQPRSAPSLRPKDYEVDATLKSLNNQIETLLTPEGSRKNPARTCRD
LRLSHPEWSSGYYWIDPNQGCTMDAIKVYCDFSTGETCIRAQPENIPAKN
WYRSSKDKKHVWLGETINAGSQFEYNVEGVTSKEMATQLAFMRLLANYAS
QNITYHCKNSIAYMDEETGNLKKAVILQGSNDVELVAEGNSRFTYTVLVD
GCSKK1TNEWGKTIIEYKTNKPSRLPFLDIAPLDIGGADQEFFVDIGPVCFK
(a)
MLVCVFVALYTMMGLLTDIKQL
QSDFDDEMFEFRAITKDTWQRI
VTKHTYPGGVDEETIESHPPTF
ETLFGTRKARQAYPEQCNCGPKSE
GCPAGPPGPPGEGGQSGEPGHDGDDGKP
GAPGVIVAITHDIPGGCIKCPPGRPGPR
GPSGLVGPAGPAGDQGRHGPPGPTGGQGGP
GEQGDAGRPGAAGRPGPPGPRGEPGTEYRP
GQAGRAGPPGPRGPPGPEGNPGGAGEDGNQ
GPVGHPGVPGRPGIPGKSGTCGEHGGPGEP
GPDAGYCPCPGRSYKA
(b)
```

vertebrate

worm

- molecular evolution

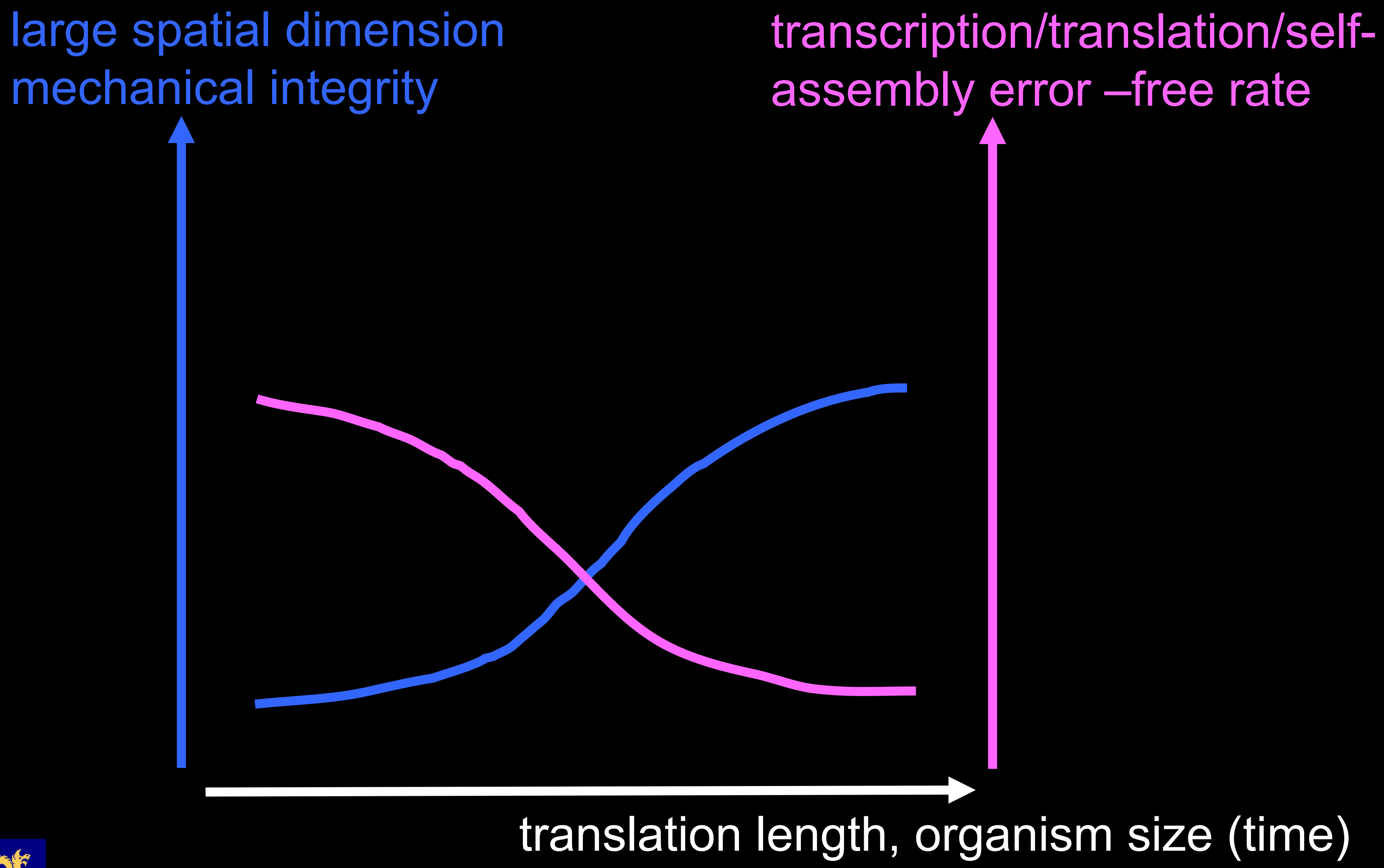

OUTLINE

NANOMETROLOGY OF MITOCHONDRIA

introduction: mitochondria physiology

- predominant mitochondrial membrane protein: VDAC

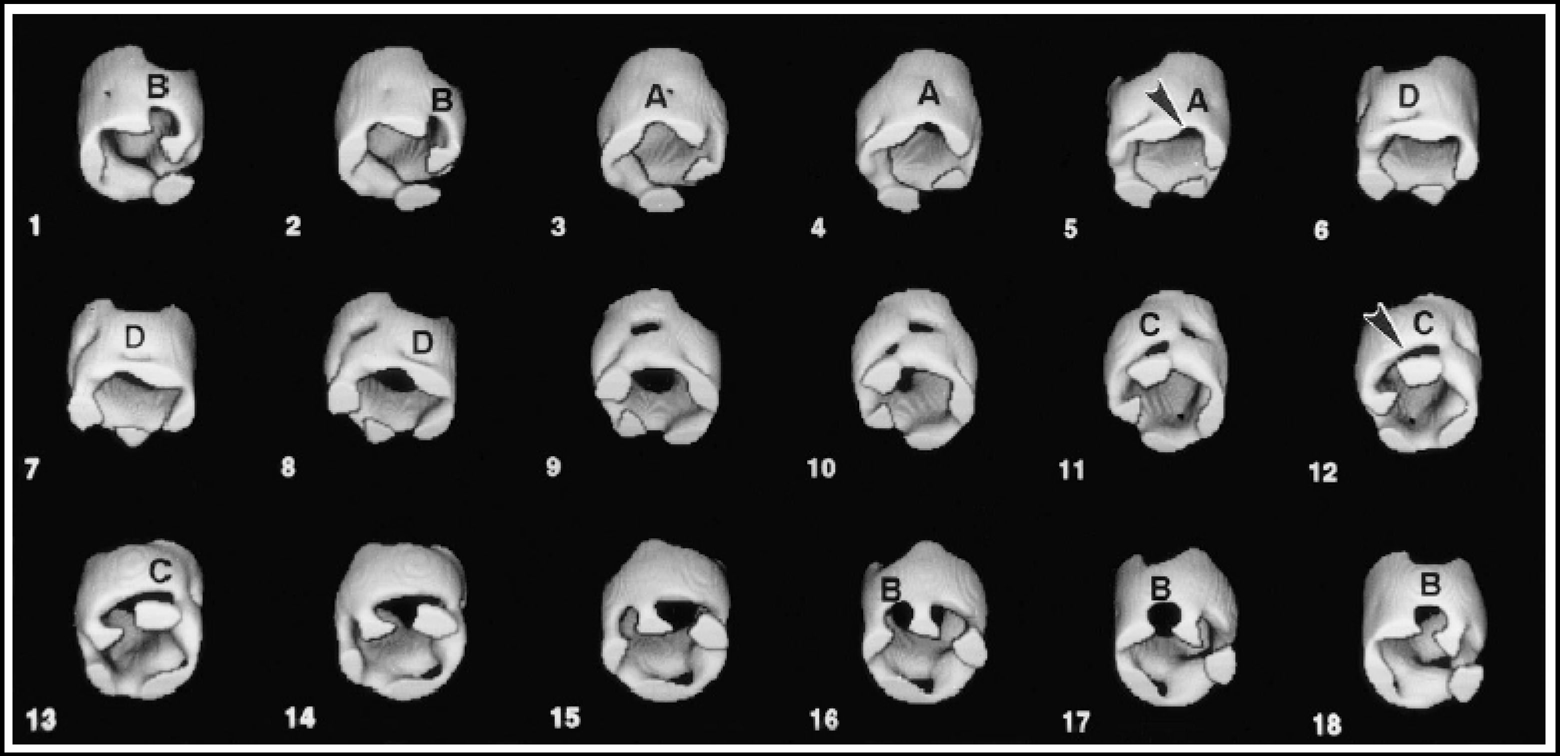

single VDAC pore
electron crystallography.
height=4.6nm
OD=5.2nm

Fig. 7 from Mannella, J. 1998. Struct. Biol. 121 207.

methods – isolation and verification

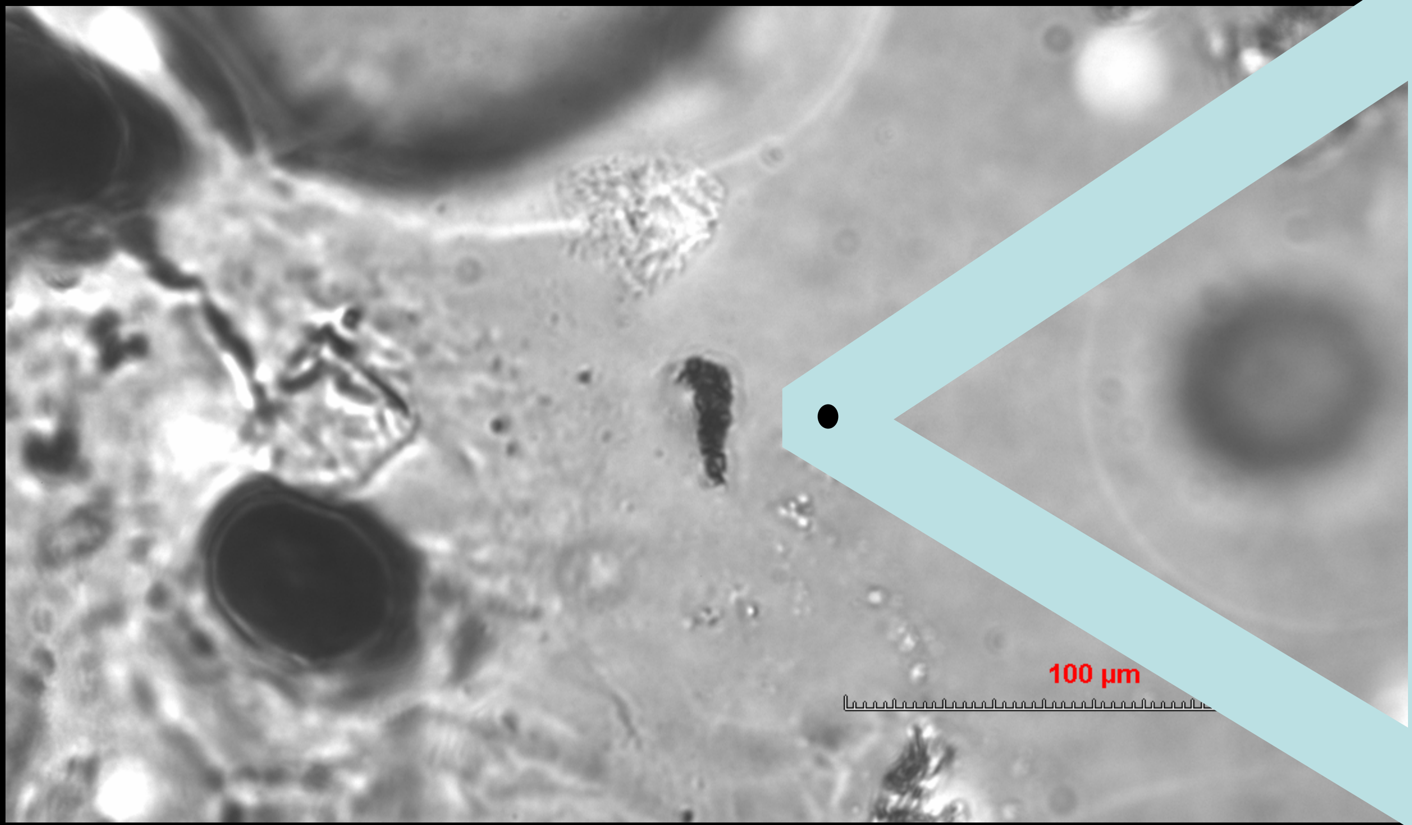

methods – isolation and verification

mitotracker

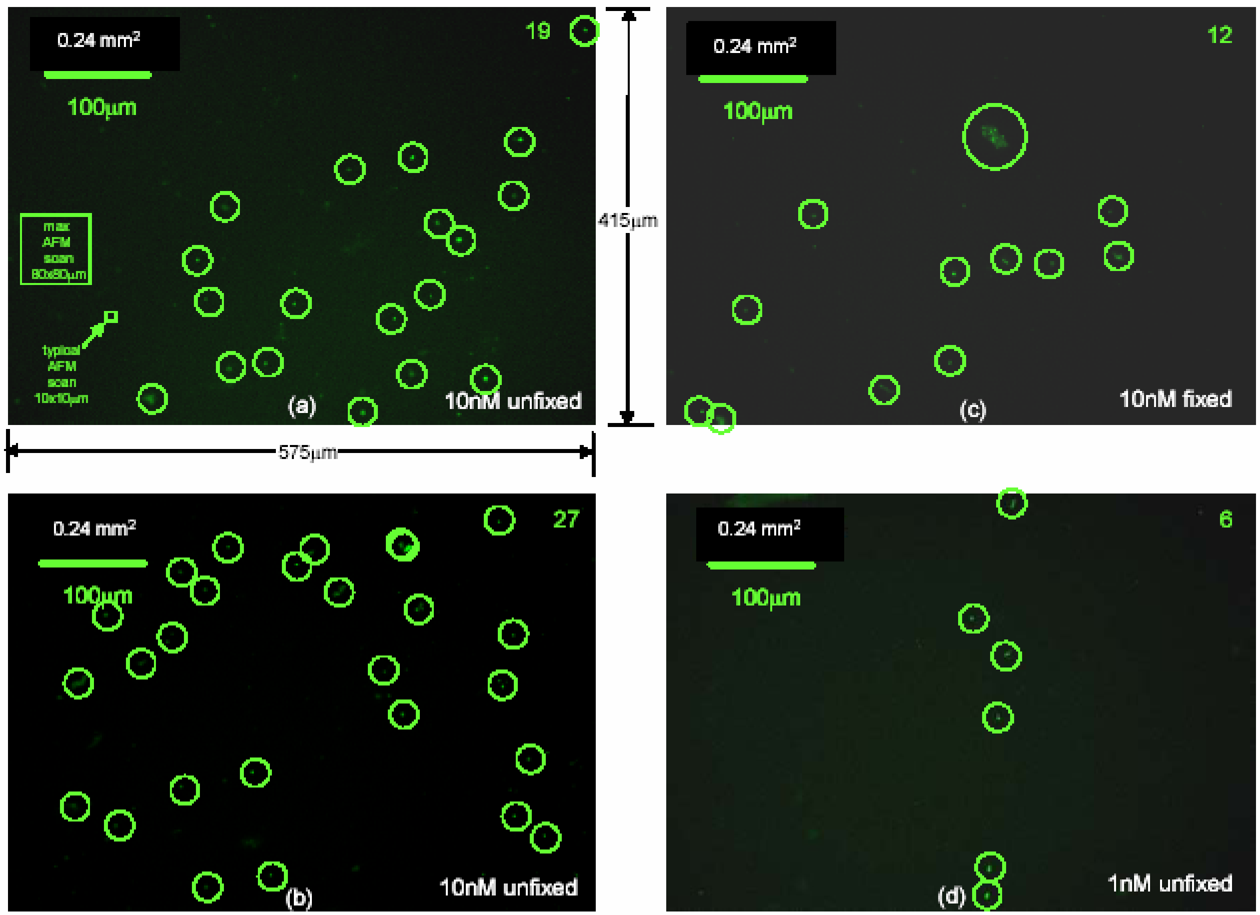

64 clusters per mm²; 10,000 10μm² scans per mm²; $p_{hit} = 0.0064$. $q = p_{miss} = 0.9936$. $P(N) = 1-q^N$ $P(10)=1-0.9936^{10}=0.06$

methods – isolation and verification

• air contact or fluid tapping atomic force microscopy on poly-L-lysine slides with DNP-S tips

• find pores ***in situ***

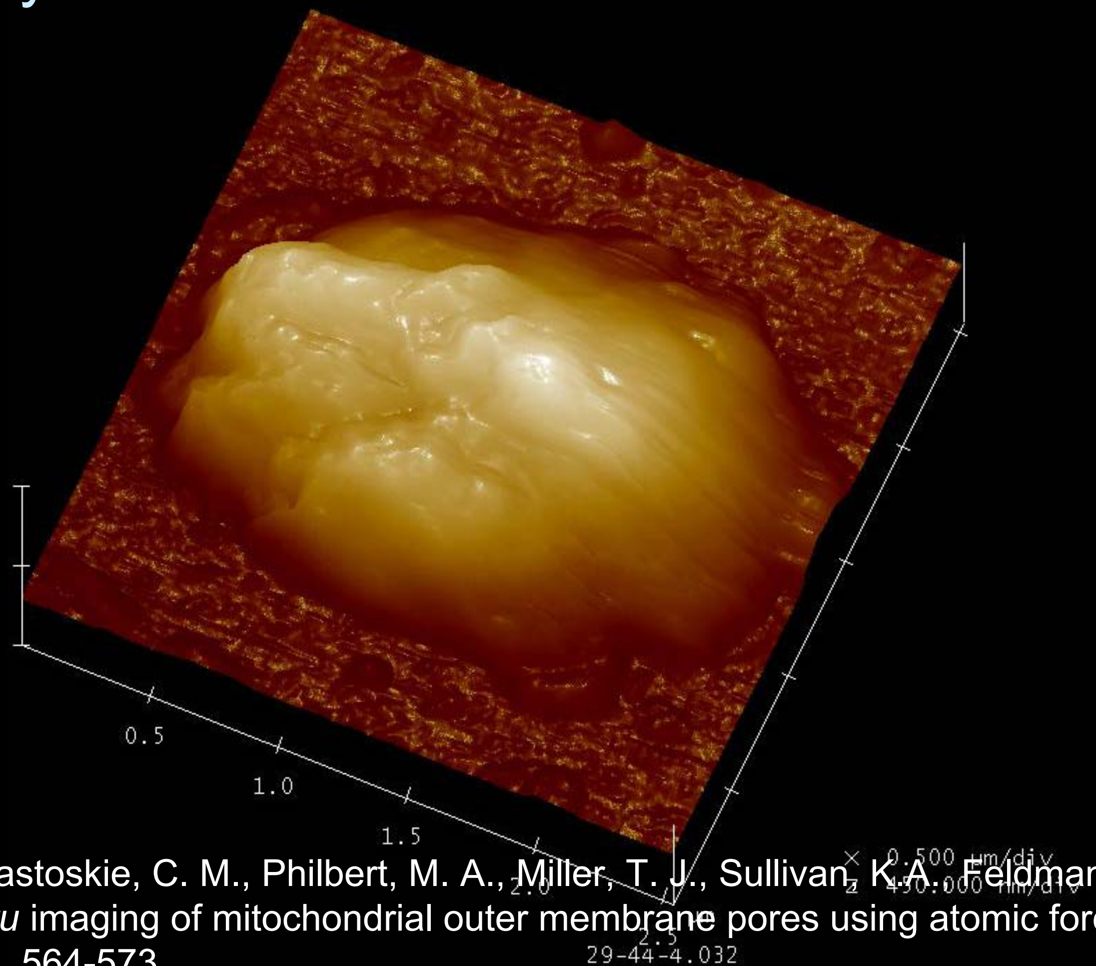

Layton, B. E., Sastry, A. M., Lastoskie, C. M., Philbert, M. A., Miller, T. J., Sullivan, K.A., Feldman, E.L., Wang C.-W., 2004. "*In situ* imaging of mitochondrial outer membrane pores using atomic force microscopy." Biotechniques 37, 564-573.

results

fixed
glucose

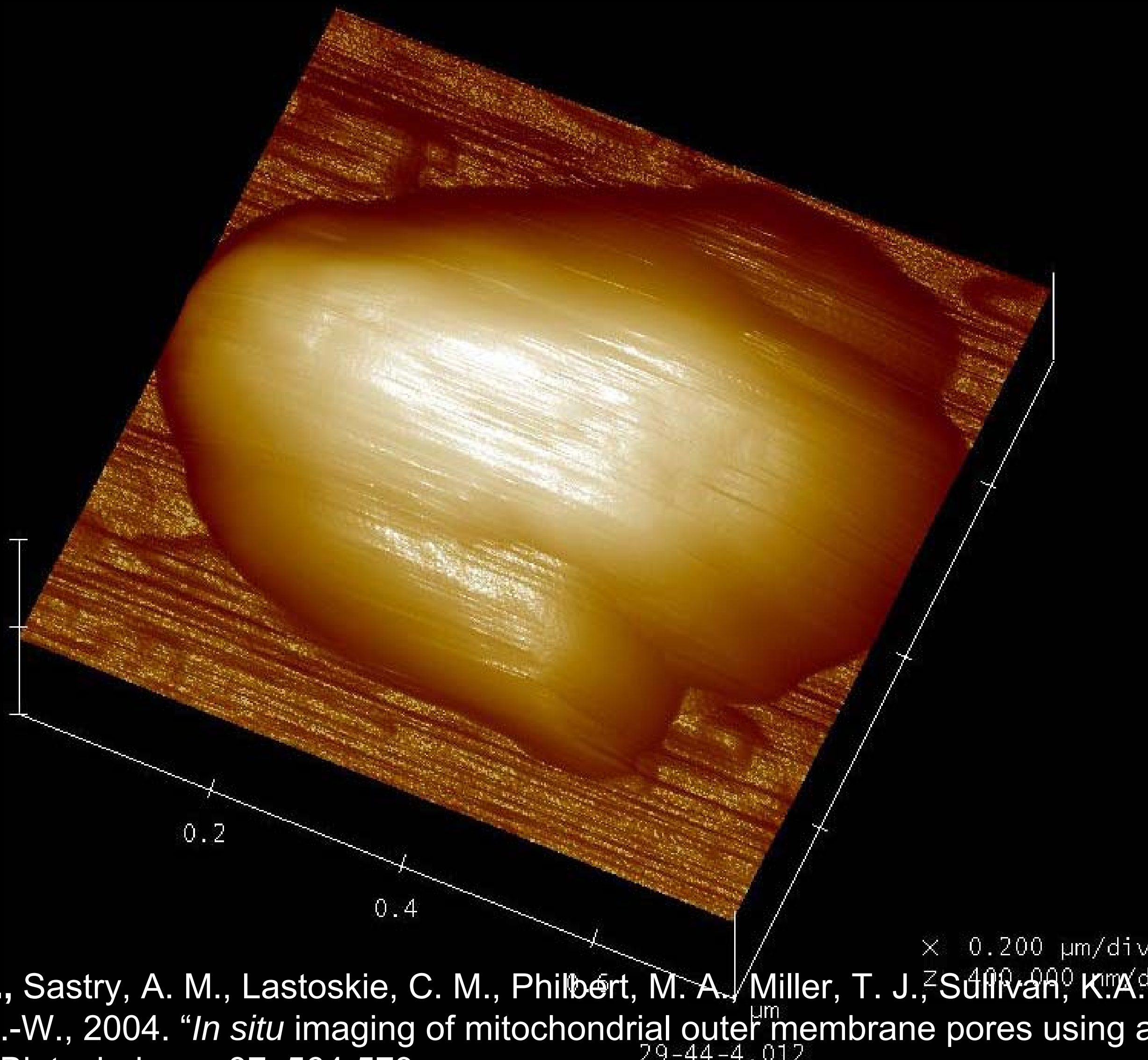

Layton, B. E., Sastry, A. M., Lastoskie, C. M., Philbert, M. A., Miller, T. J., Sullivan, K.A., Feldman, E.L., Wang C.-W., 2004. "*In situ* imaging of mitochondrial outer membrane pores using atomic force microscopy." Biotechniques 37, 564-573.

29-44-4.012

results

fixed
glucose

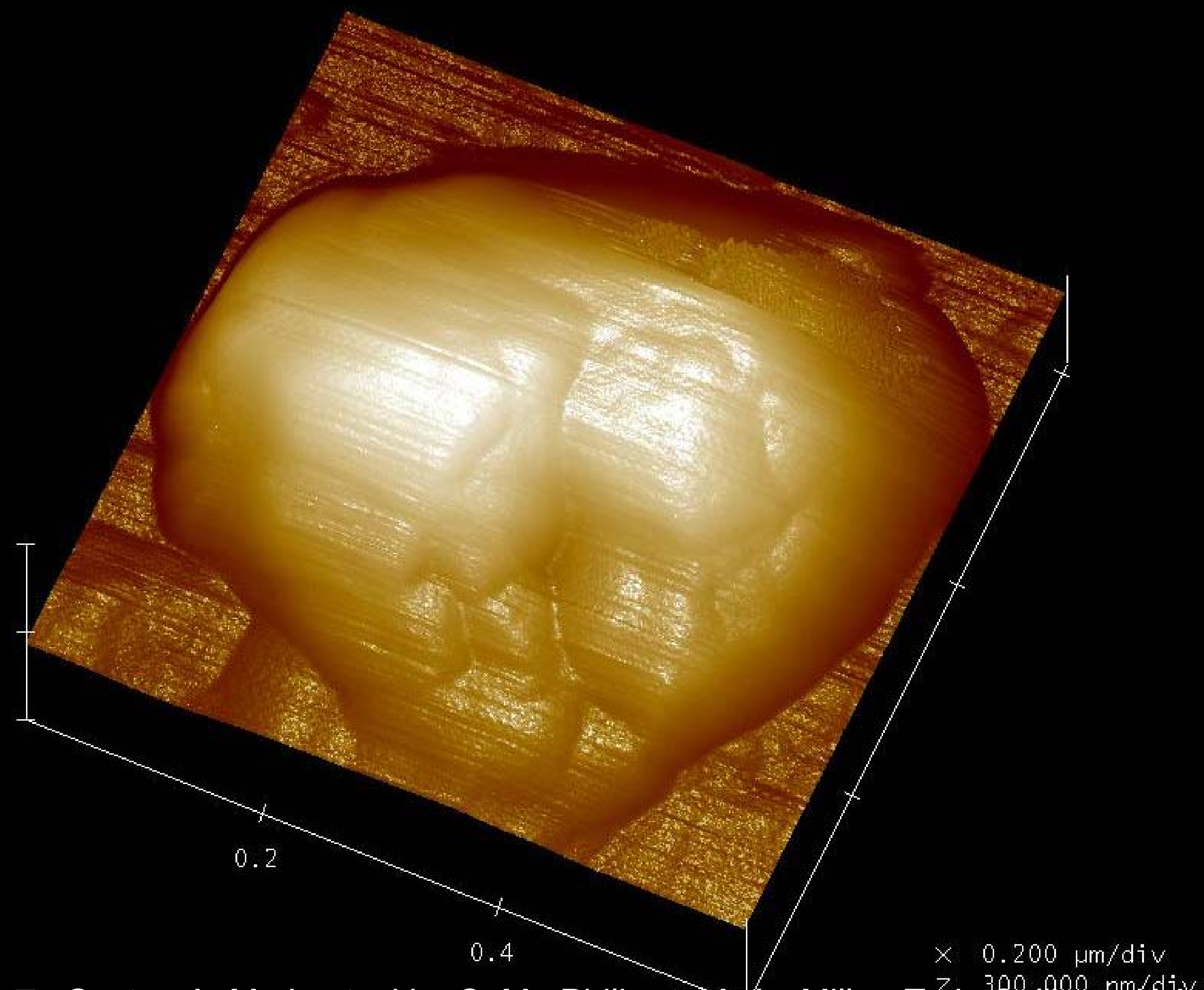

Layton, B. E., Sastry, A. M., Lastoskie, C. M., Philbert, M. A., Miller, T. J., Sullivan, K.A., Feldman, E.L., Wang C.-W., 2004. "*In situ* imaging of mitochondrial outer membrane pores using atomic force microscopy." Biotechniques 37, 564-573.

29-44-4.020

methods – isolation and verification

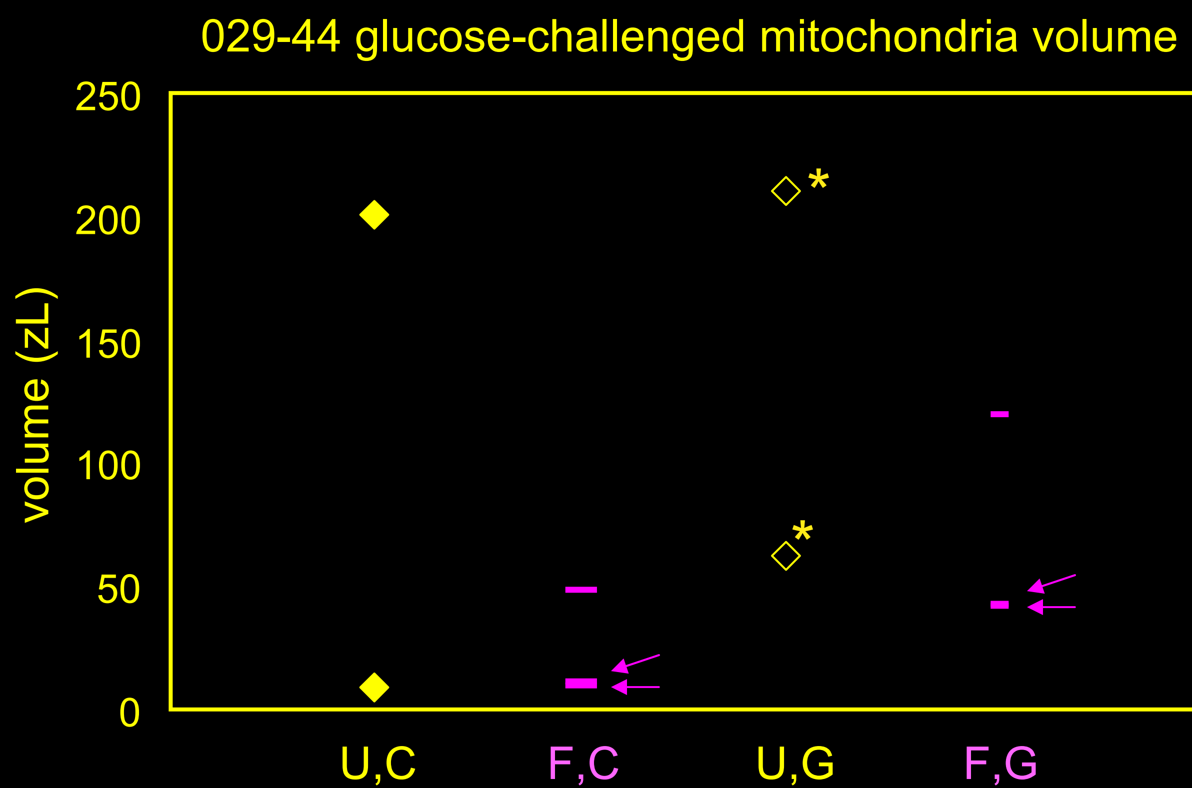

* not clear that mitochondria were present in this prep

results - pores

unfixed
glucose

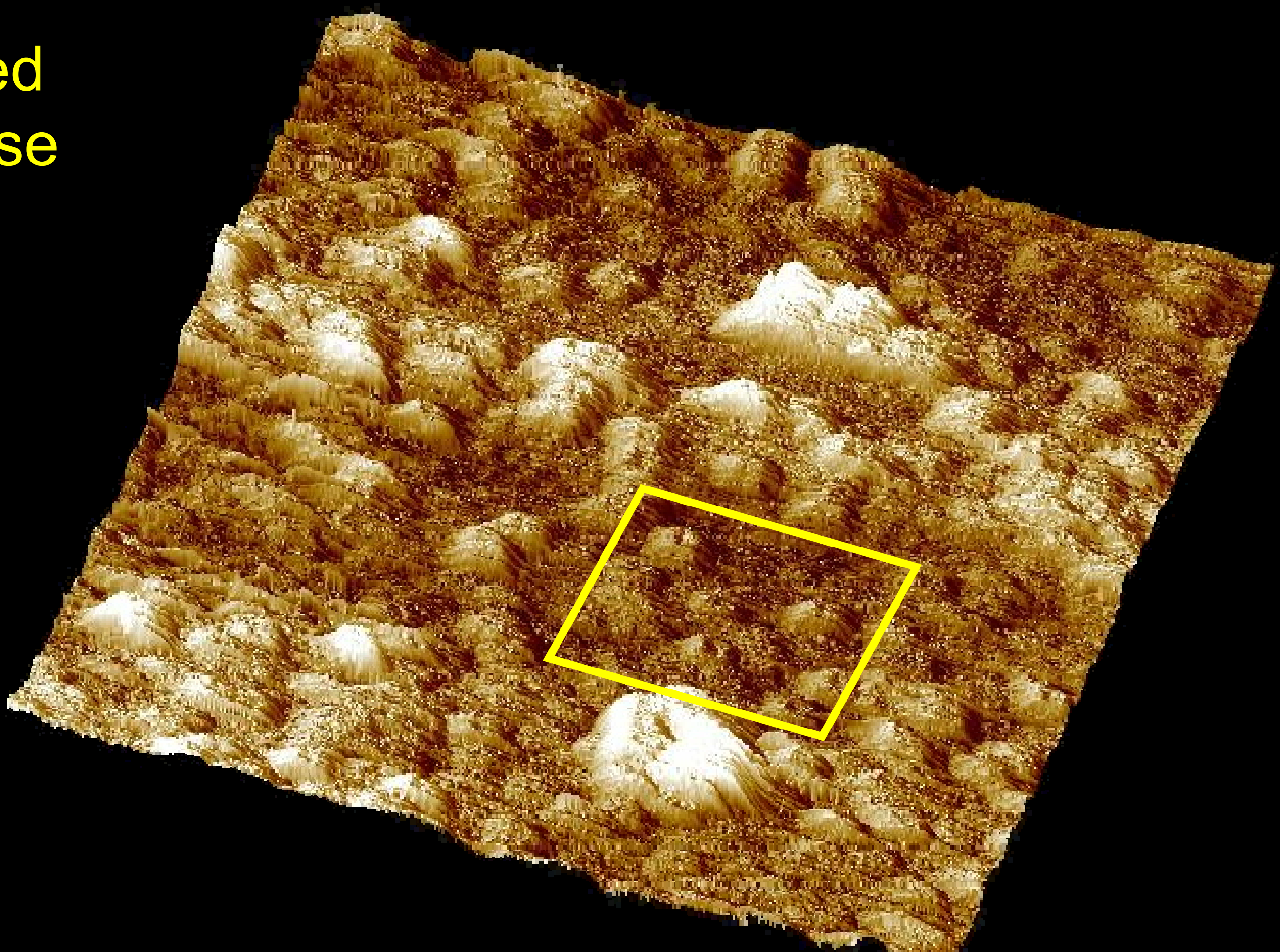

Layton, B. E., Sastry, A. M., Lastoskie, C. M., Philbert, M. A., Miller, T. J., Sullivan, K.A., Feldman, E.L., Wang C.-W., 2004. "*In situ* imaging of mitochondrial outer membrane pores using atomic force microscopy." Biotechniques 37, 564-573.

29-44-3.040 **2x2μm**

results - pores

possibly nuclear membrane

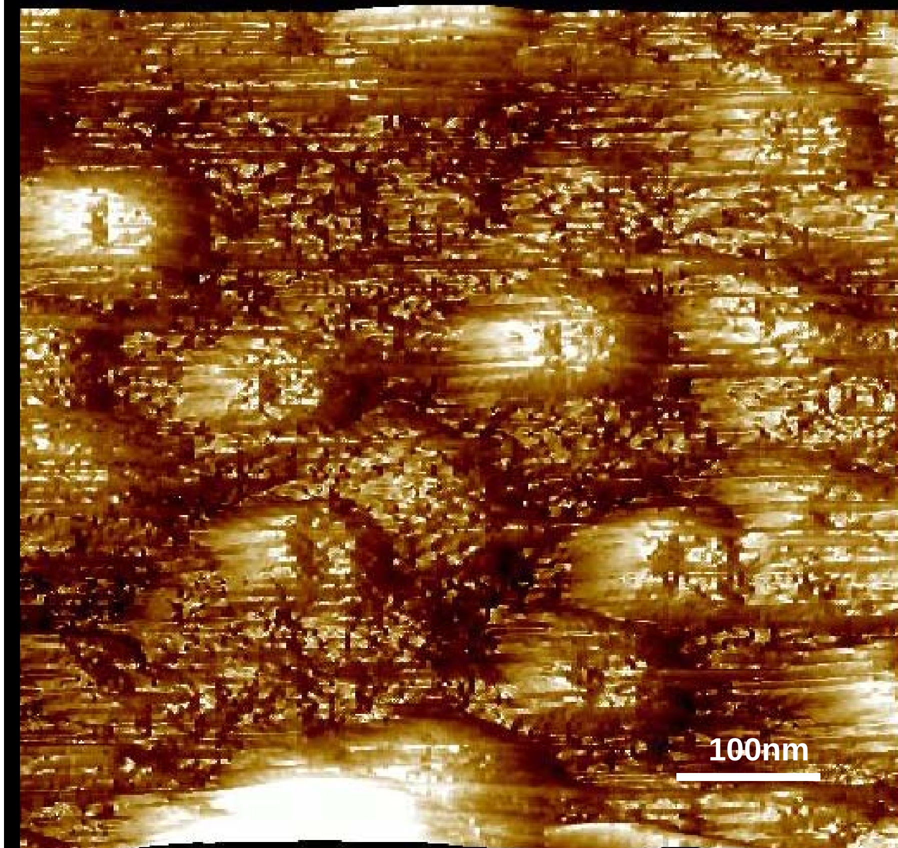

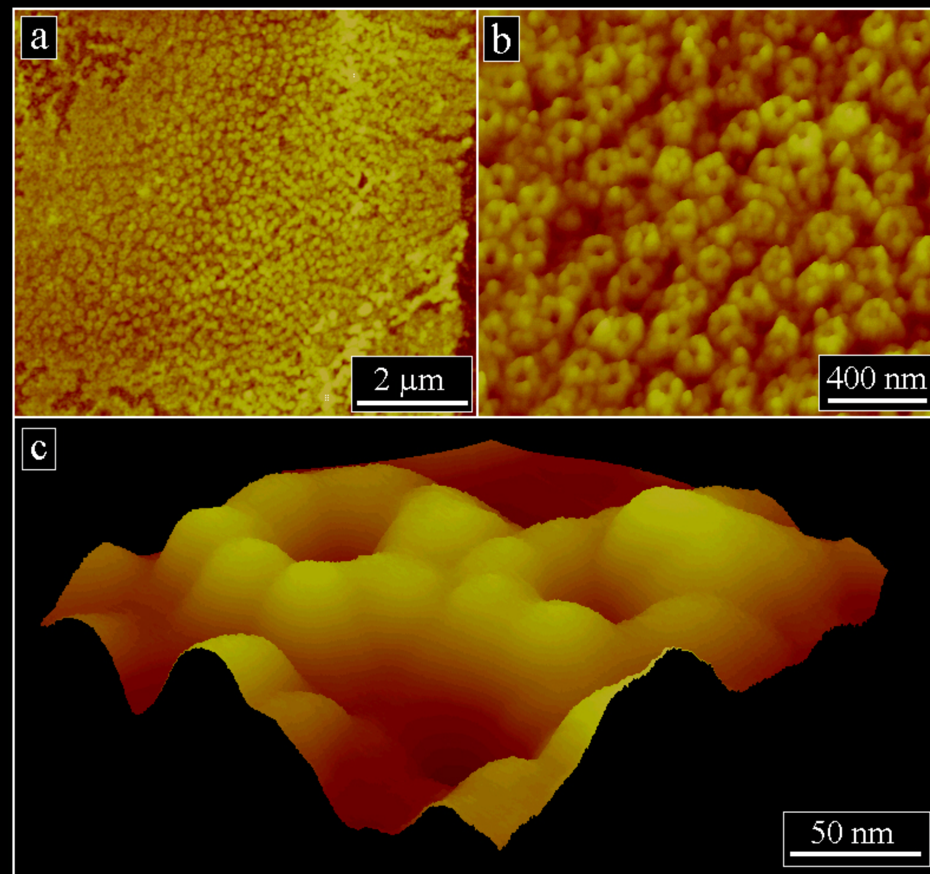

unfixed
glucose

29-44-3.040 500x500nm

http://medweb.uni-muenster.de/institute/phys/vegphys/research/pore5.htm

results - pores

probably VDAC

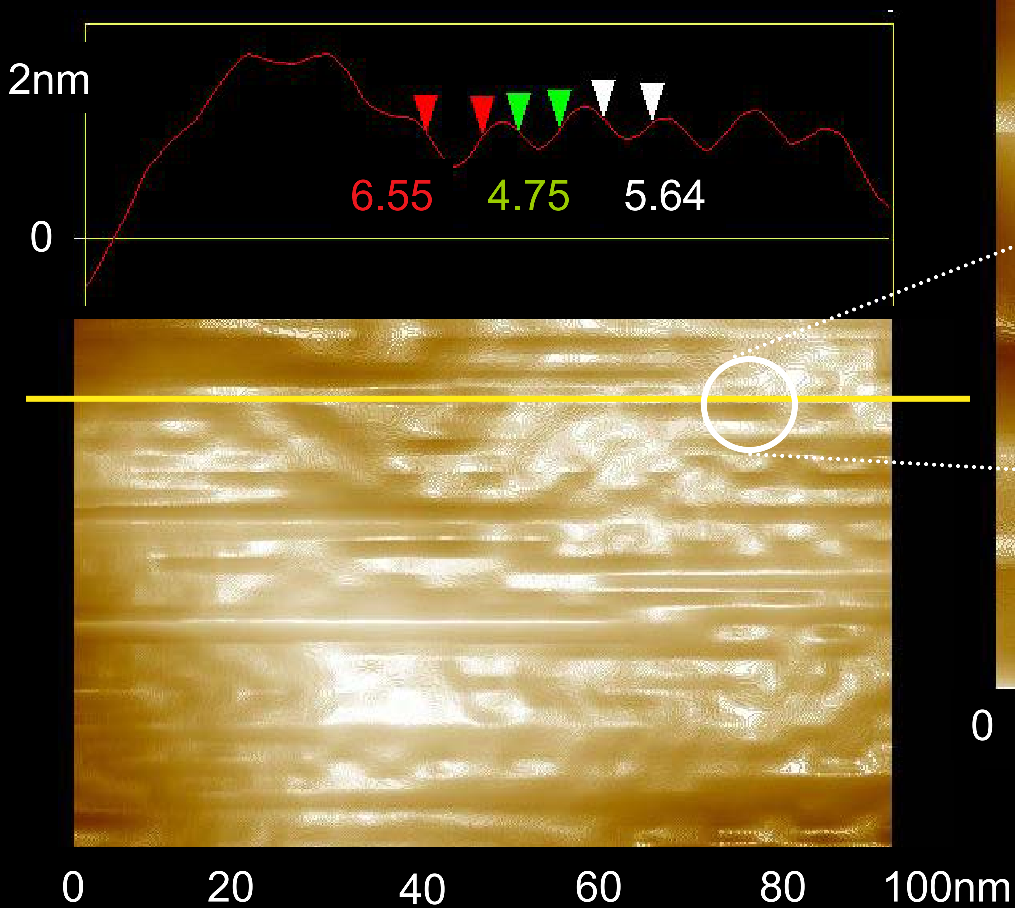

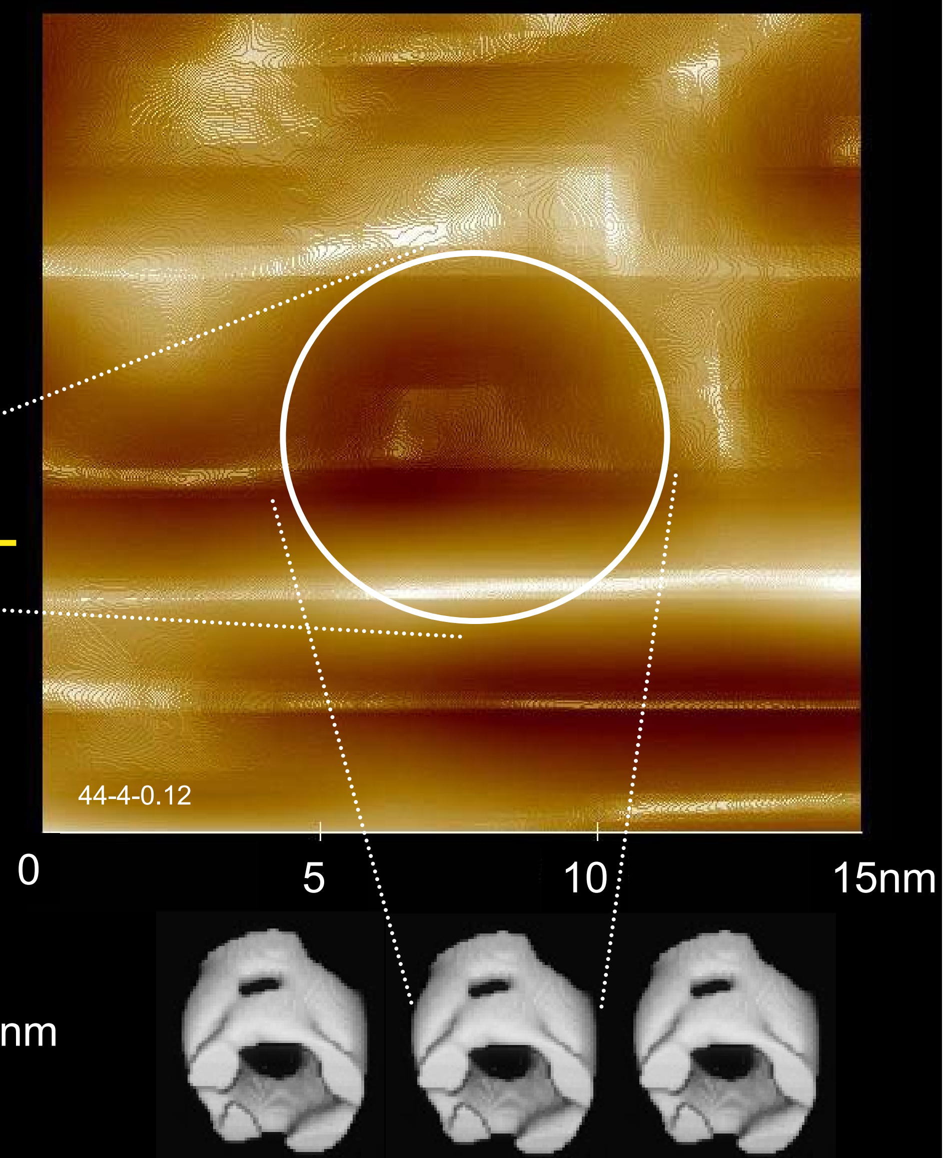

fixed
glucose

Brad Layton,Drexel University

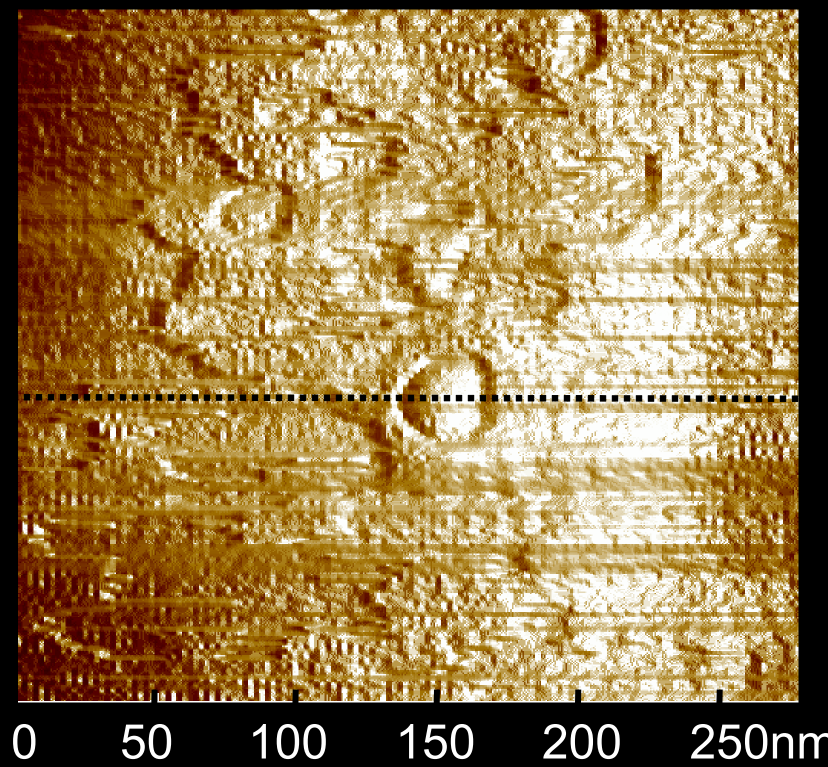

(b)

Layton, B. E., Sastry, A. M., Lastoskie, C. M., Philbert, M. A., Miller, T. J., Sullivan, K.A., Feldman, E.L., Wang C.-W., 2004. "*In situ* imaging of mitochondrial outer membrane pores using atomic force microscopy." Biotechniques 37, 564-573.

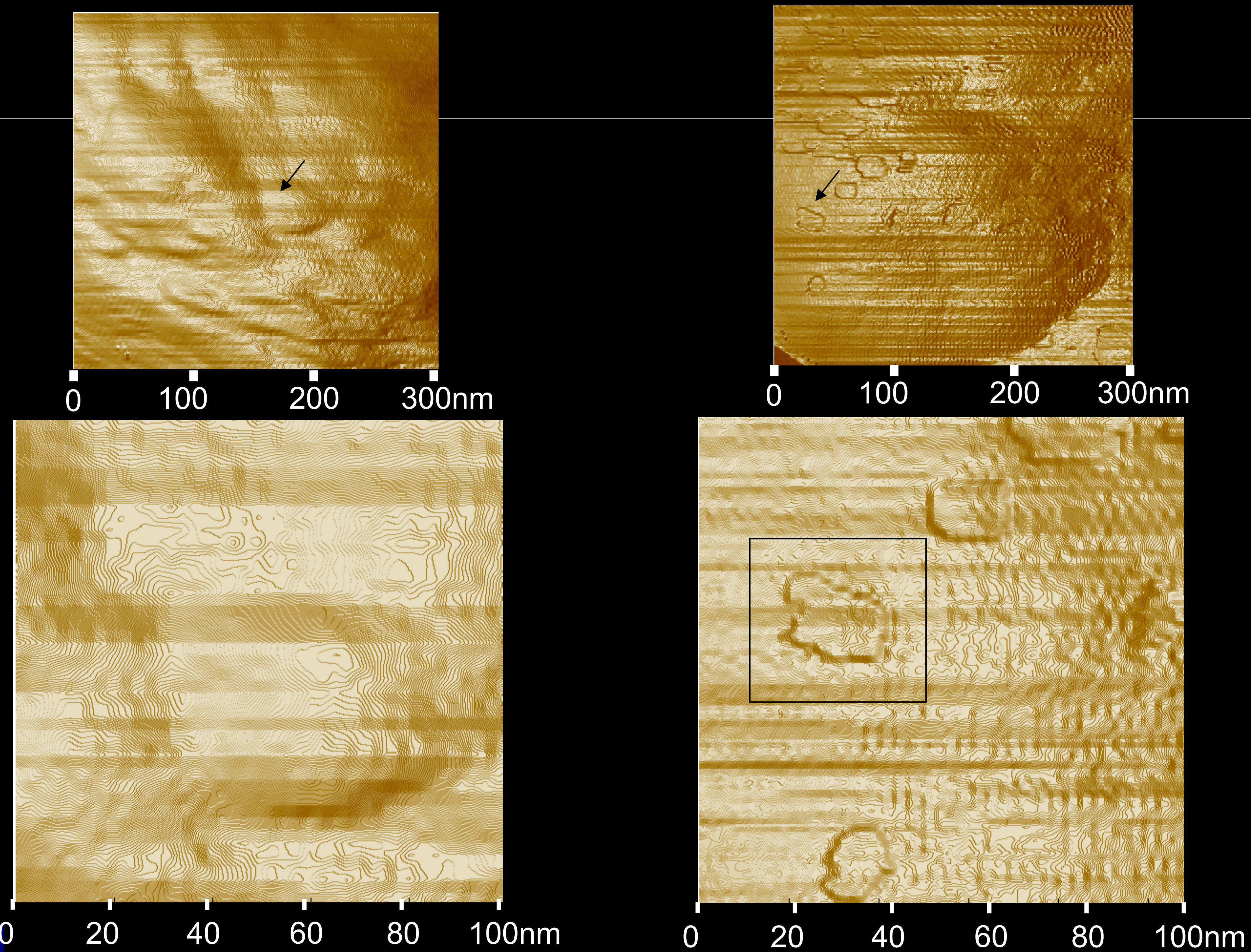

Figure 5

Brad Layton, Drexel University

OUTLINE

ERROR REDUCTION
IN
NANOMANIPULATION

- Zyvex L100 nanomanipulator interfaced with DI AFM

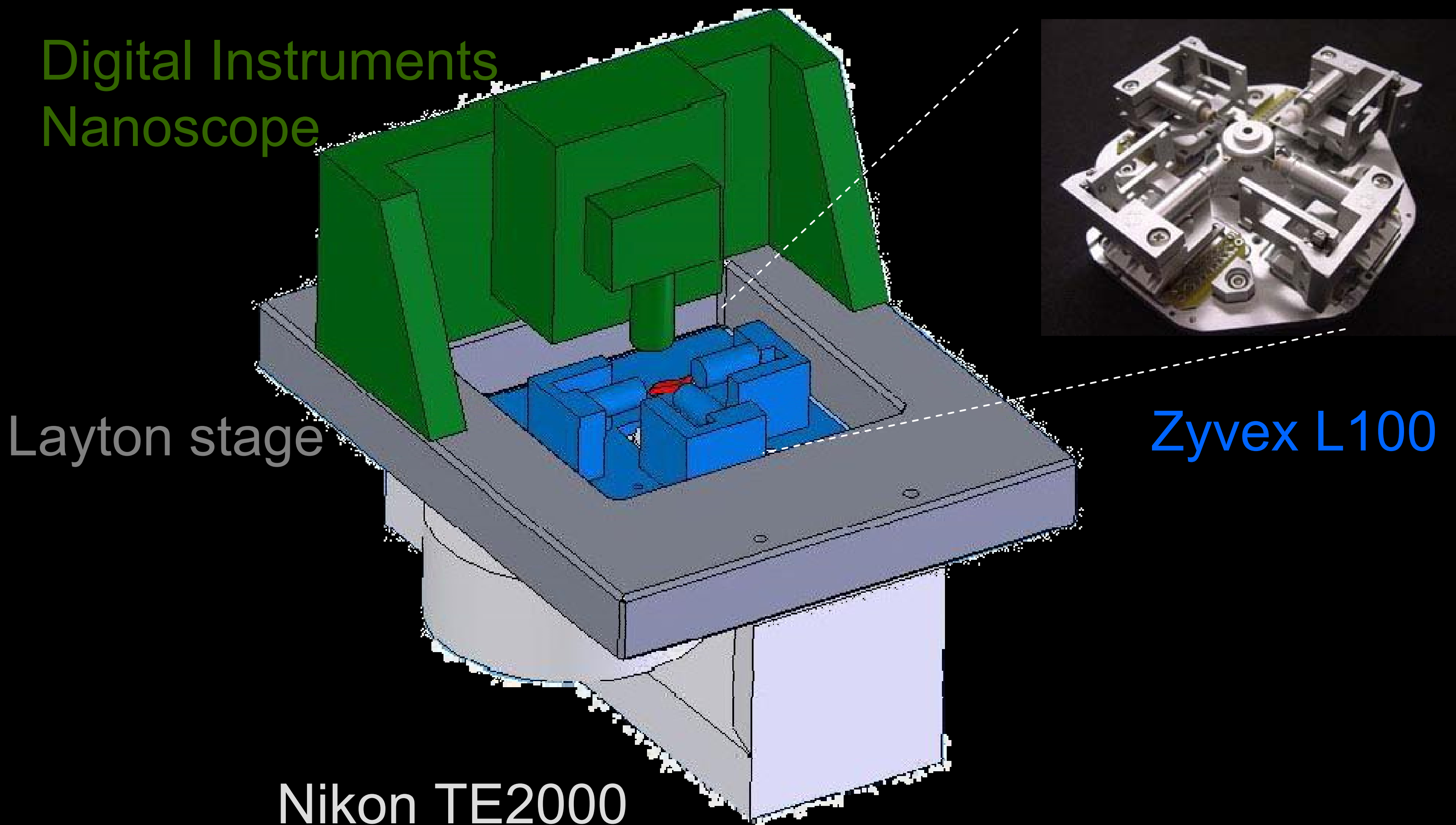

- Zyvex L100 nanomanipulator

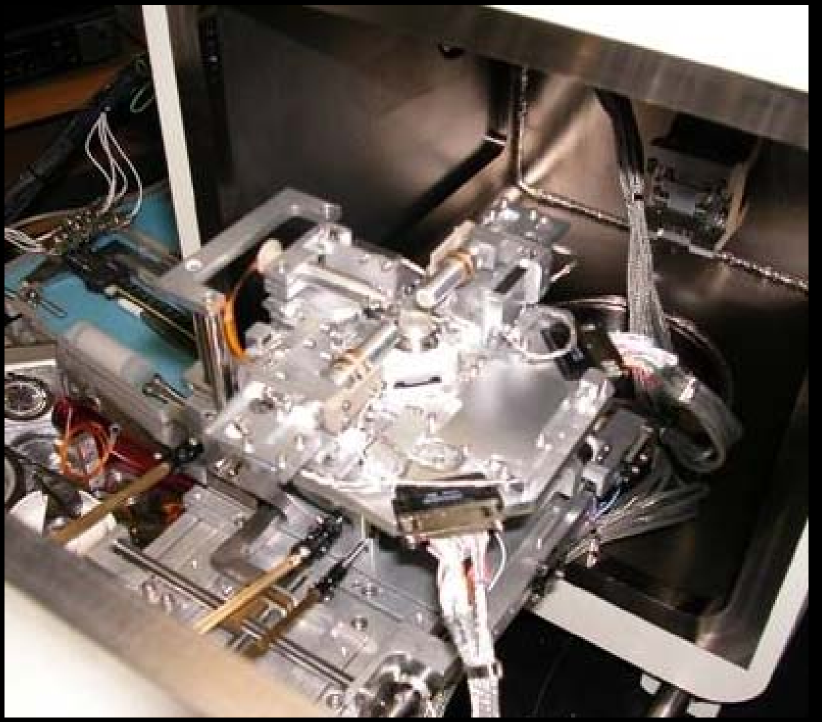

- single molecule and single fibril experiments

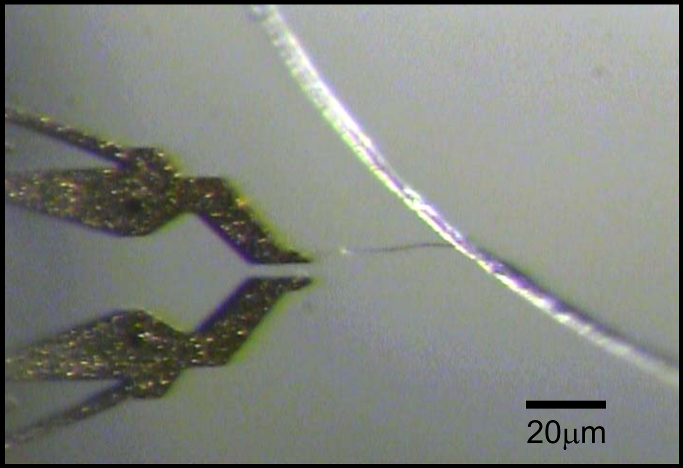

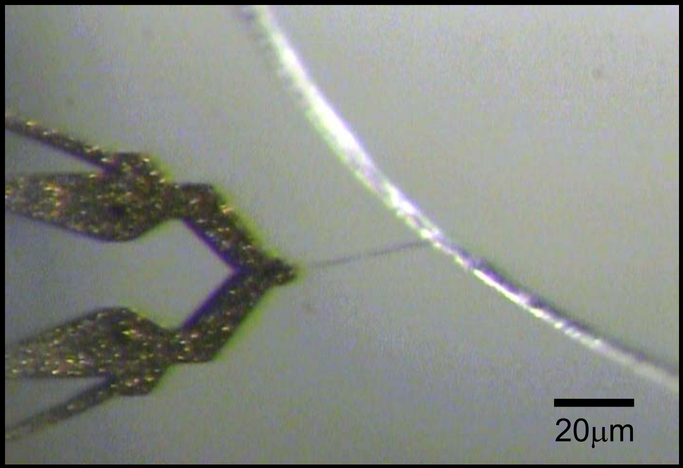

Zyvex L100 nanomanipulation system

- single molecule and single fibril experiments

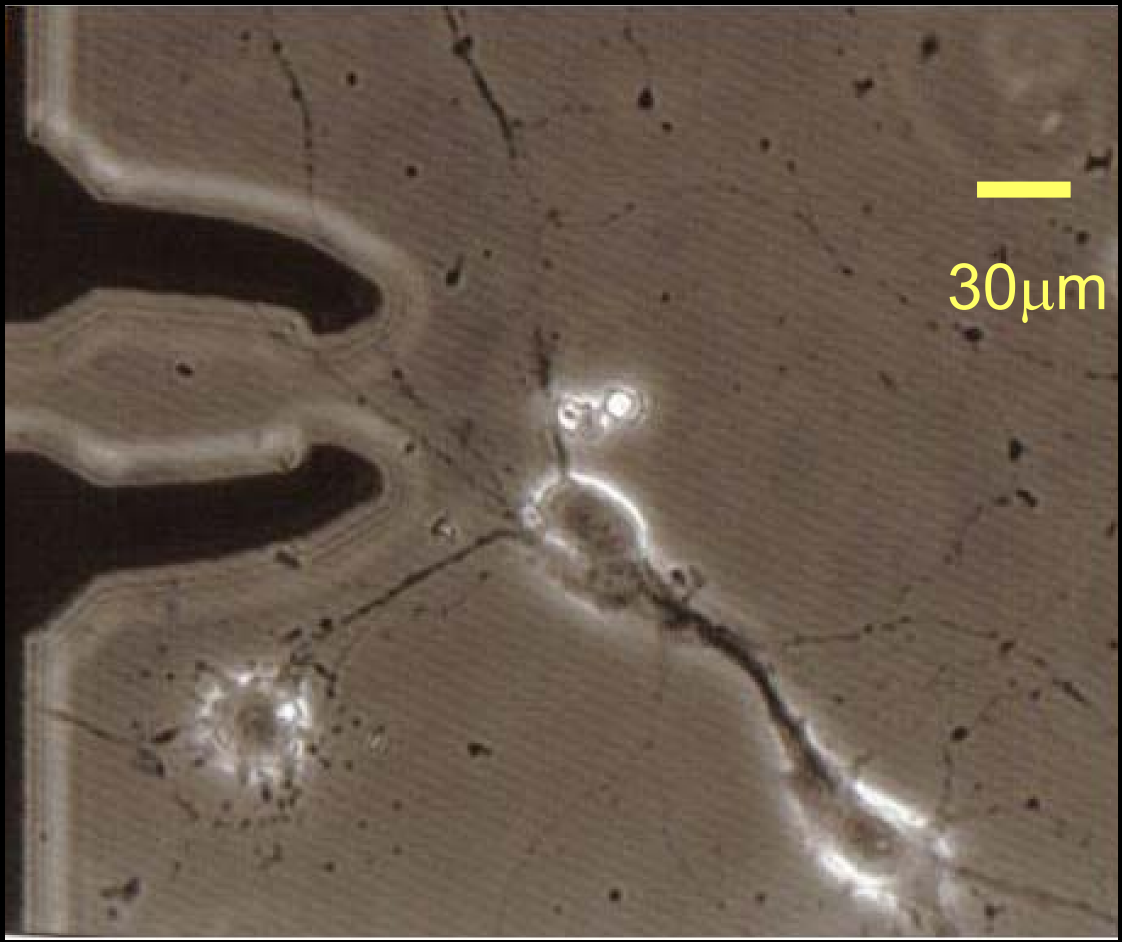

Layton, B.E. Baas, P.W., Allen, K.B. 2005. "The Use of Thermally Actuated Microgrippers to Stimulate Axonal Growth," 2nd Annual IEEE-EMBS Conference on Neural Engineering, March 16-19, Arlington, VA.

- Zyvex L100 nanomanipulator

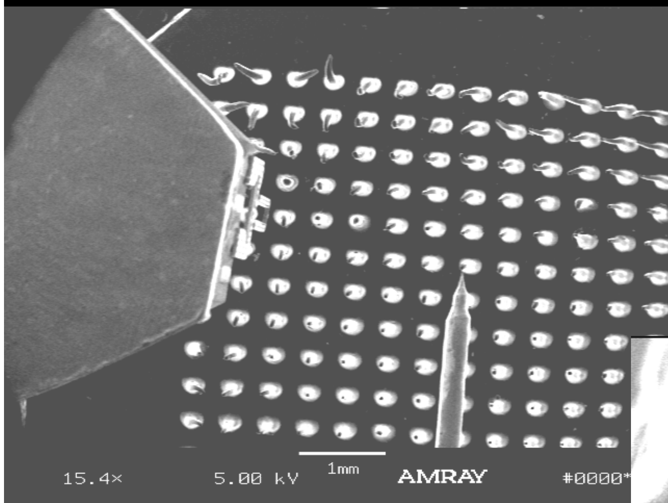

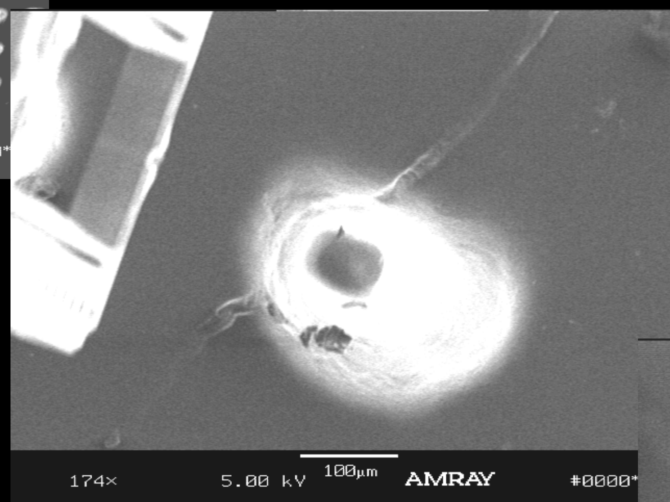

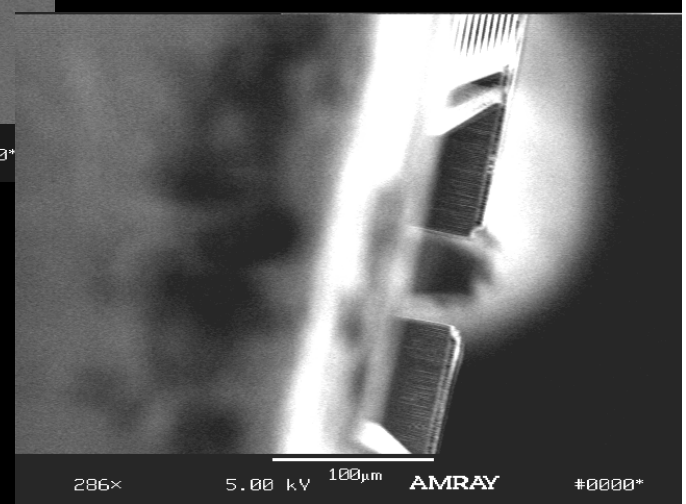

- Zyvex L100 nanomanipulator

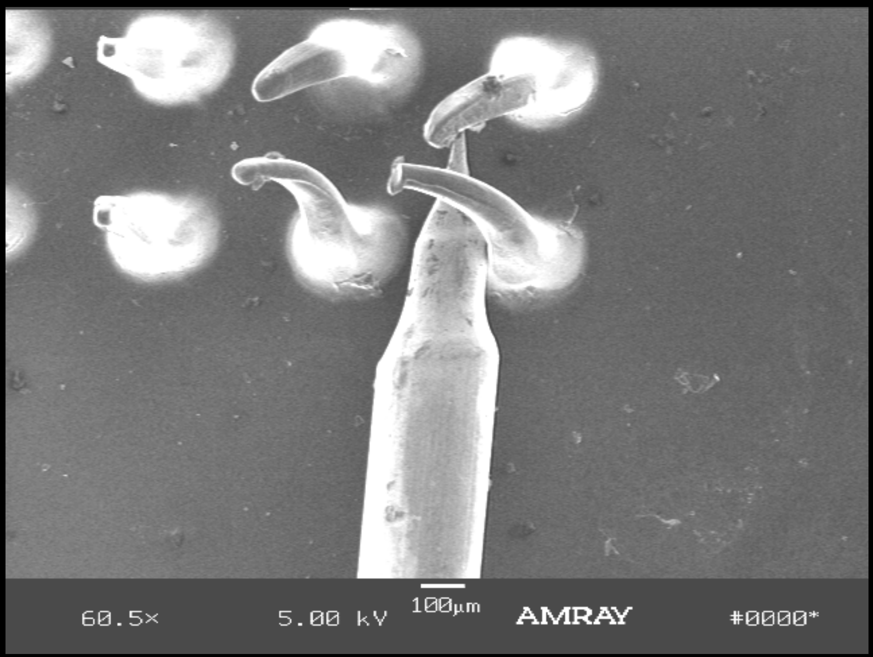

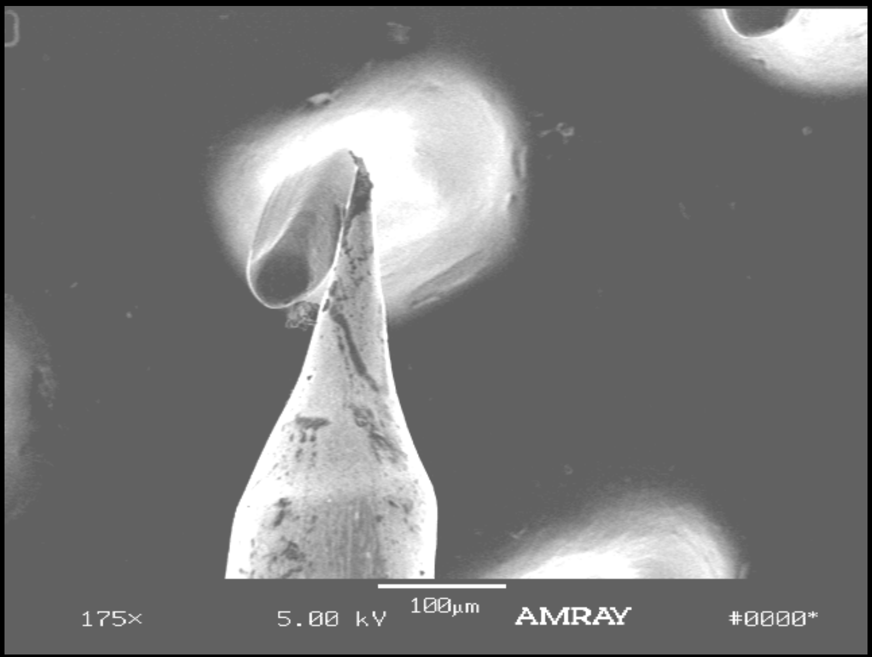

- Zyvex L100 nanomanipulator

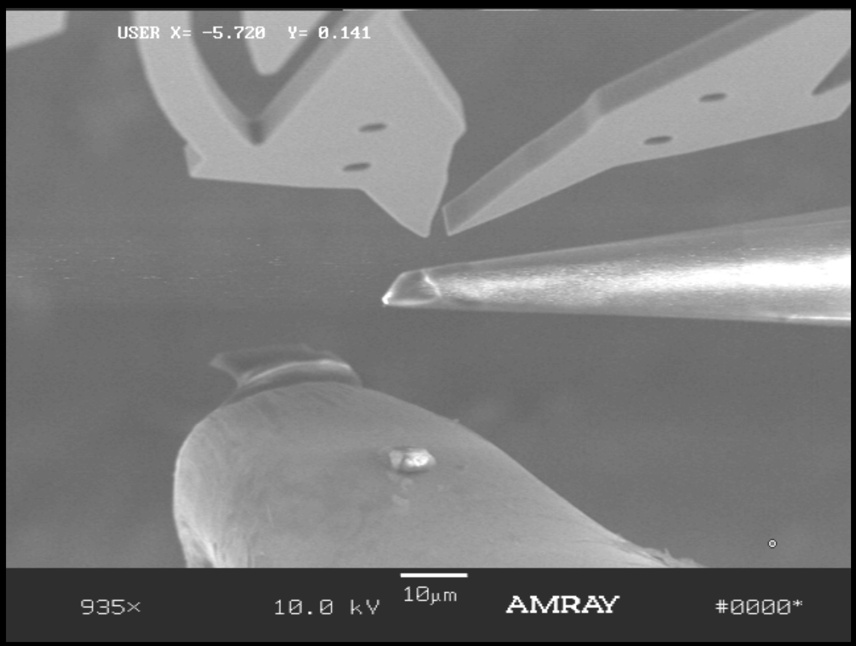

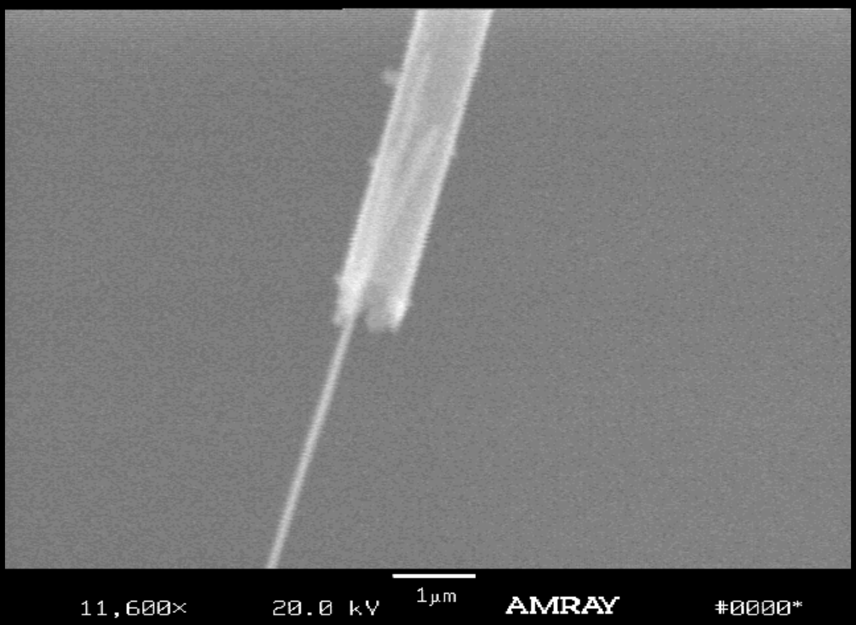

- Zyvex L100 nanomanipulator

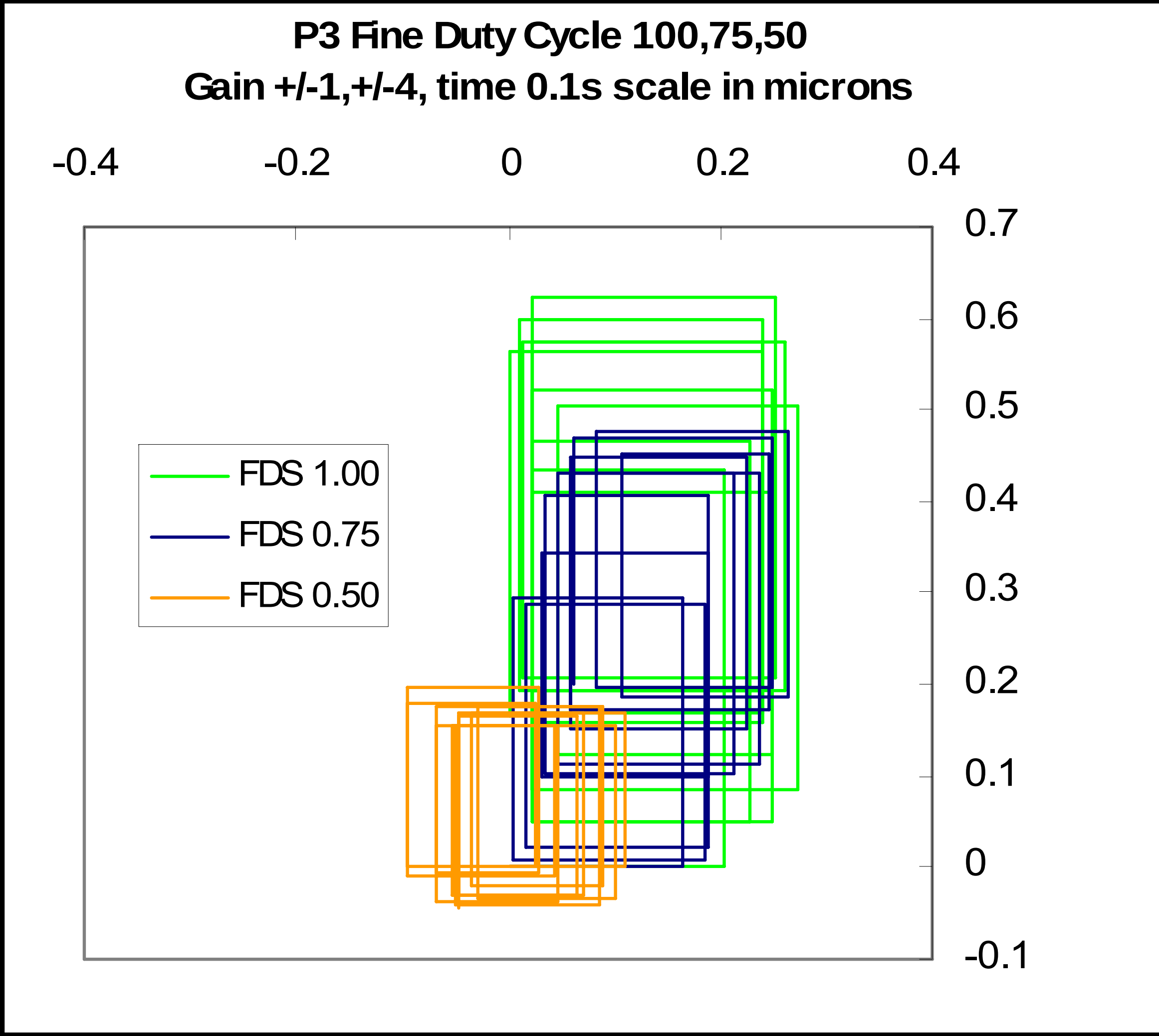

- Zyvex L100 nanomanipulator

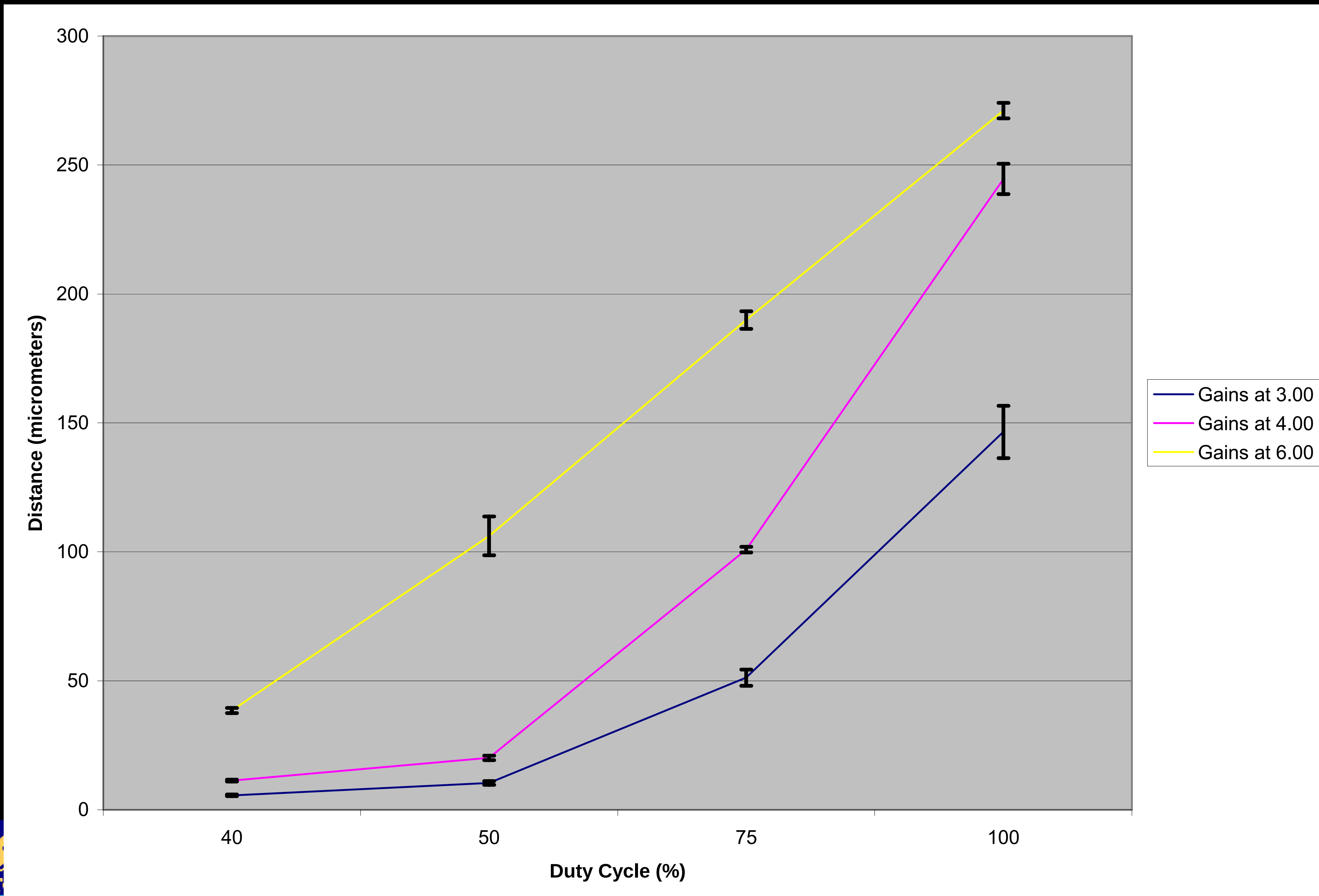

- Zyvex L100 nanomanipulator

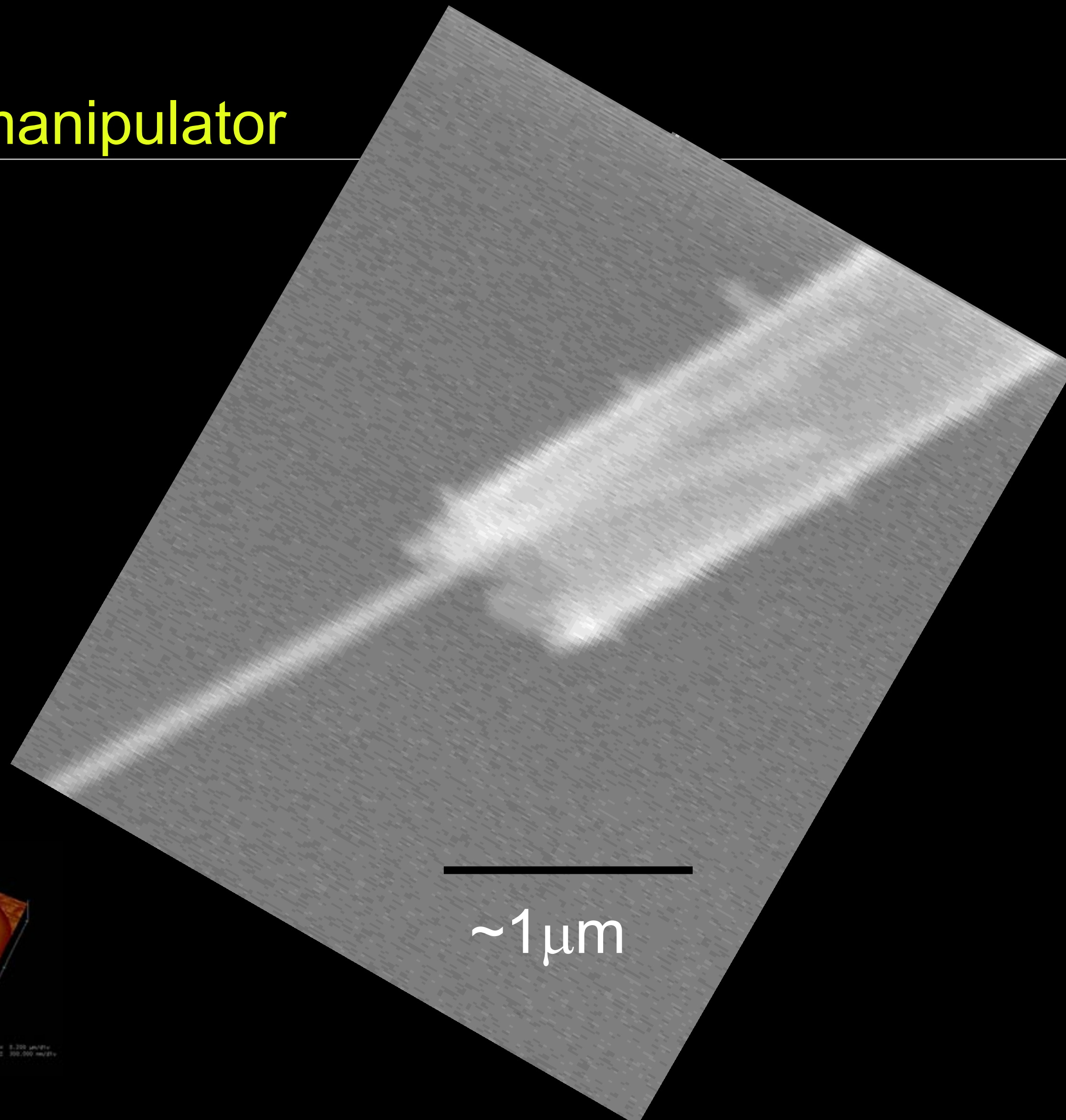

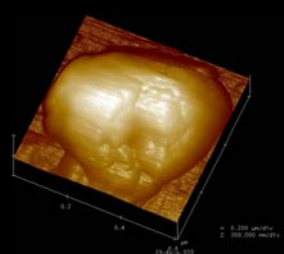

(to scale)

OUTLINE

BLOOD CELL SORTING

PROBLEM INTRODUCTION

- develop a blood profile device for extended space missions
- hematology parameters such as red blood cell volume fraction 40-50% or count (4.2-5.7 E6/μL), mean red blood cell volume 80-100fL, red blood cell volume distribution (11-15%) are important for determining human health and are an important indication of average red blood cell age in vitro
- most health profiles done on astronauts are done prior to and subsequent to launch[1]

1 *Kimzey, S.L., et al., Hematology and immunology studies: the second manned Skylab mission. Aviat Space Environ Med, 1976.* ***47****(4): p. 383-90.*

OBJECTIVES

- continuous (daily) monitoring of hematology parameters
- low volume sample size required (~1μL)
- low mass of device
- simple interface, probably electrical rather than optical
- disposable, single use
- minimally invasive
- quick, accurate

PRELIMINARY FINDINGS

trapped between beds

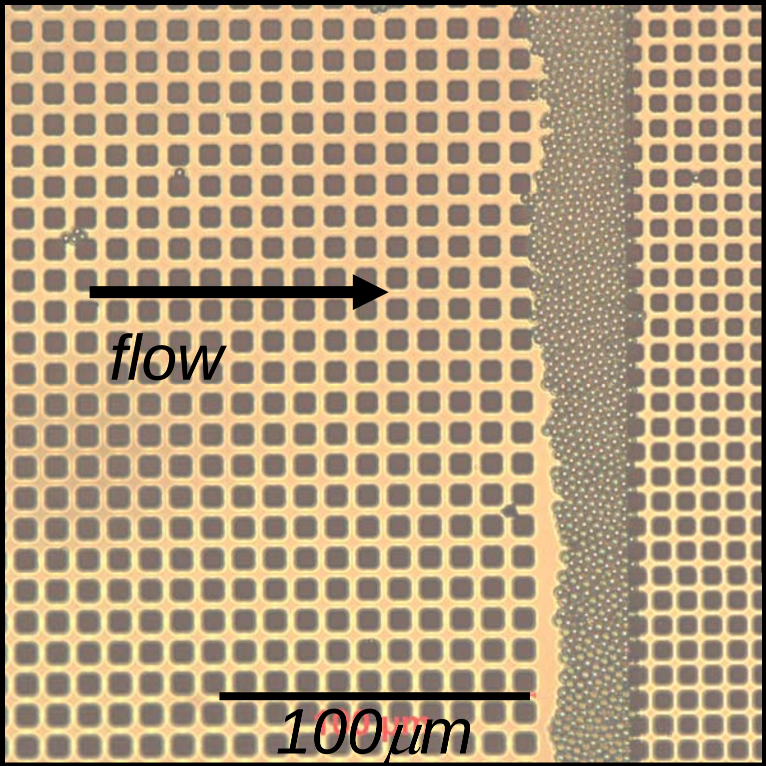

square grid
6 μm PS beads

trapped between and within beds

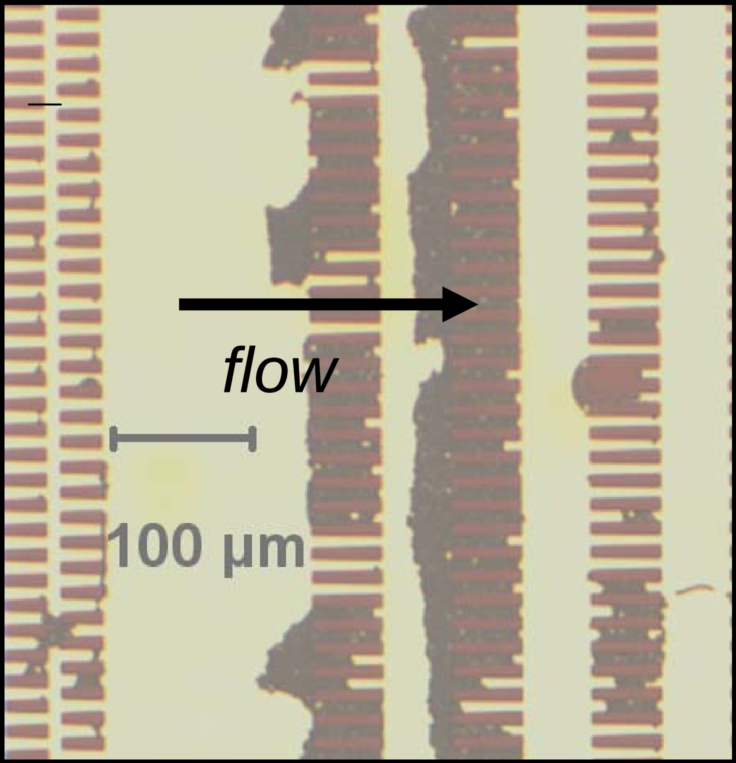

trapezoidal grid
6 μm PS beads

PRELIMINARY FINDINGS

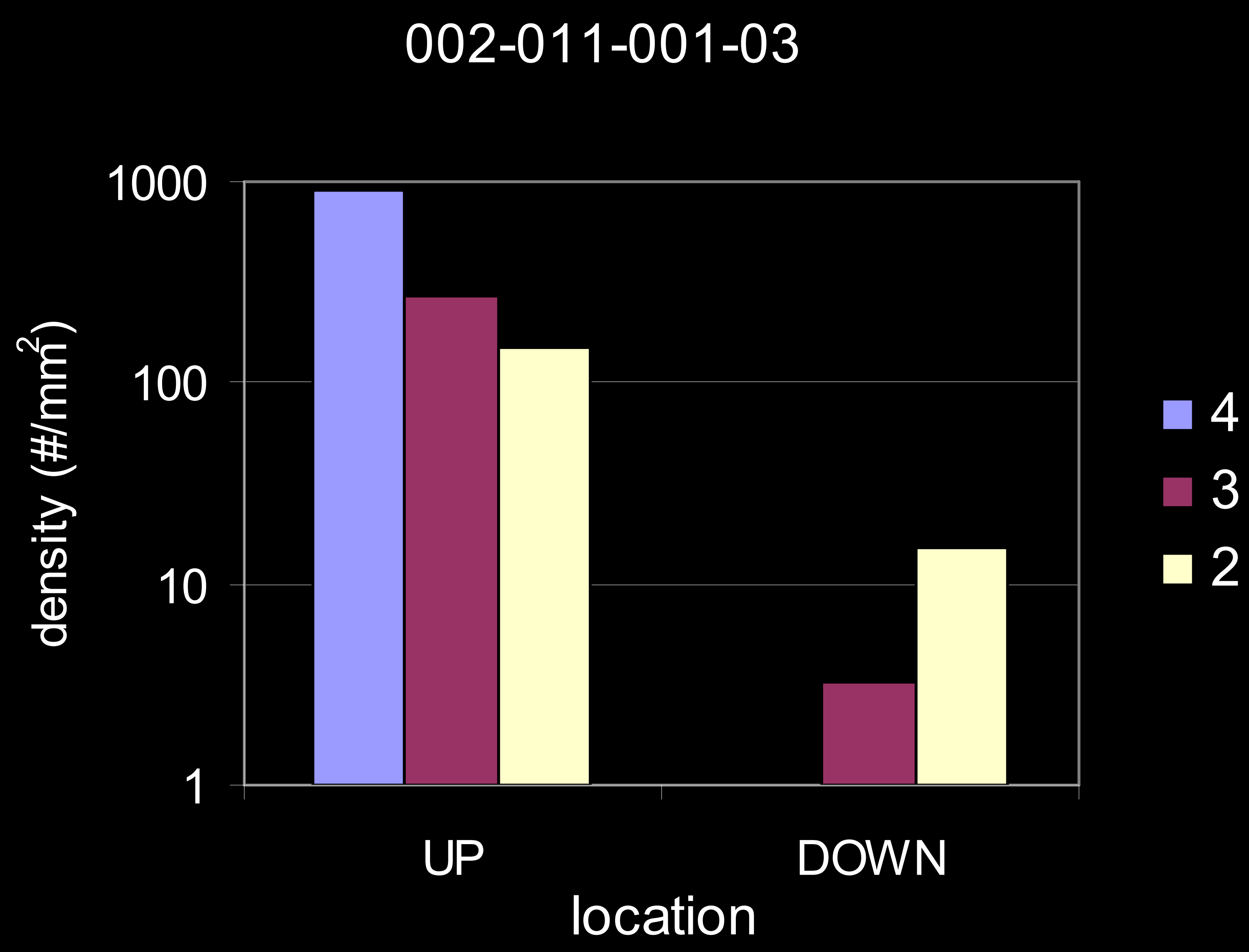

PREVIOUS WORK

- Coulter, 1950's[1] pioneer in cell counting
- Gifford *et al.*, 2003 single cell wedging[2]
- Cui *et al*., 2002 optical[3]
- Gawad, et al, electrical[4-13]
- Yamada et al 2005, pinched flow fractionation [14]

1 Coulter, W.H. High Speed Automatic Blood Cell Counter and Cell Size Analyzer. in Proc. Natl. Electronics Conf. 1956.
2 Gifford, S.C., et al., Parallel microchannel-based measurements of individual erythrocyte areas and volumes. Biophys J, 2003. 84(1): p. 623-33.
3 Cui, L., T. Zhang, and H. Morgan, Optical particle detection integrated in a dielectrophoretic lab-on-a-chip. Journal of Micromechanics and Microengineering, 2002. ***12****(1): p. 7-12*
4 Gawad, S., et al., Dielectric spectroscopy in a micromachined flow cytometer: theoretical and practical considerations. Lab on a Chip, 2004. 4(3): p. 241-251.
5 Ayliffe, H.E., B. S.D., and R.D. Rabbitt. Micro-electric Impedance Spectra of Isolated Cells Recorded in Micro-channels. in Proceedings of the second Joint EMBS/BMES Conference. 2002. Houston, TX.
6 Cui, L., T. Zhang, and H. Morgan, Optical particle detection integrated in a dielectrophoretic lab-on-a-chip. Journal of Micromechanics and Microengineering, 2002. 12(1): p. 7-12.
7 Heath, M.L., M.D. Vickers, and D. Dunlap, A simple method for simultaneous determination of plasma and red cell volume. Br J Anaesth, 1969. 41(8): p. 669-76.
8 Mohanty, S.K., L.L. Sohn, and D.J. Beebe. Hybrid Polymer/Thin Film Impedance System for Label Free Monitoring of Cells. in 26th Annual International Conference of the IEEE EMBS. 2004. San Francisco, CA.
9 Cheung, K., S. Gawad, and P. Renaud, Impedance spectroscopy flow cytometry: On-chip label-free cell differentiation. Cytometry A, 2005. 65A(2): p. 124-132.
10 Ayliffe, H.E. and R.D. Rabbitt, High frequency capacitance of vital and non-vital polymorphoneuclear leukocytes. Biophysical Journal, 1999. 76(1): p. A356-A356.
11 Gimsa, J., et al., Dielectric spectroscopy of single human erythrocytes at physiological ionic strength: Dispersion of the cytoplasm. Biophysical Journal, 1996. 71(1): p. 495-506.
12 Larsen, U.D., G. Blankenstein, and J. Branebjerg. Microchip Coulter particle counter. in International Conference on Solid State Sensors and Actuators. 1997. Chicago, IL.
13 Zhao, T.X., B. Jacobson, and T. Ribbe, Triple-Frequency Method for Measuring Blood Impedance. Physiological Measurement, 1993. 14(2): p. 145-156.
14 Yamada, M., M. Nakashima, and M. Seki, Pinched flow fractionation: continuous size separation of particles utilizing a laminar flow profile… Anal Chem, 2004. 76(18): p. 5465-71

EXPERIMENTAL DETAILS

NIST traceable particle size standard

sample number	sample description
mb06	6 μm microbead, pure PolySci
mb10	10 μm microbead, pure PolySci
mb06-10b	6 and 10 μm microbead, blended PolySci
mb06-10s	6 and 10 μm microbead, centrifuged PolySci
mb02	2 μm microbead, pure Bangs 640nm
mb03	3 μm microbead, pure Bangs
mb05	5 μm microbead, pure Bangs 420nm
mb02-03-05b	2,3,5 μm microbead, blended Bangs

EXPERIMENTAL DETAILS

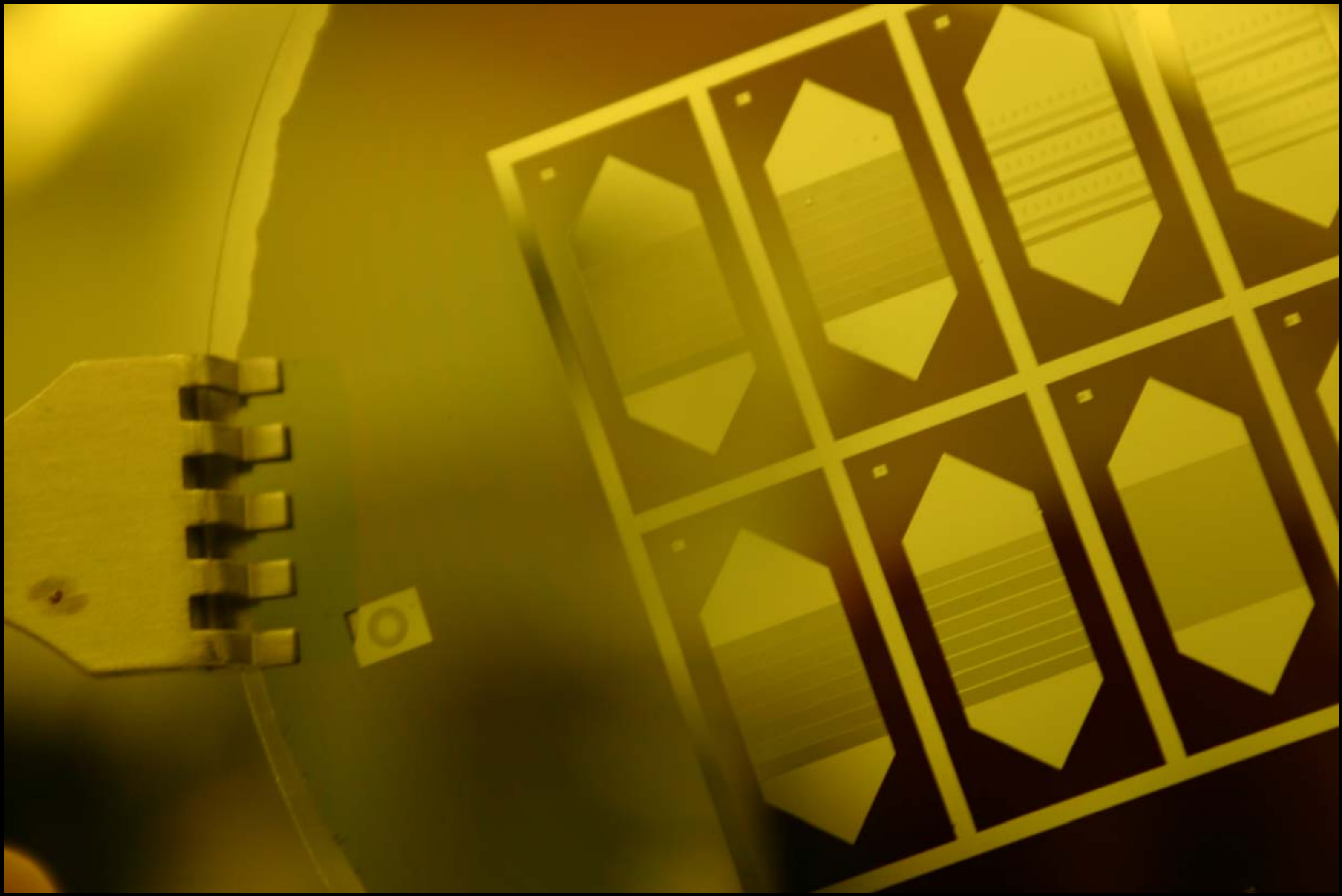

ANALYTICAL DETAILS

$$L = r\left(\frac{A}{2\pi r^2} - 1 - \left(\sqrt[3]{3\left(\frac{V}{\pi r^3} - \frac{A}{2\pi r^2} + 1\right)} + 1\right)^2\right)$$

r pore radius
A RBC surface area
V RBC volume

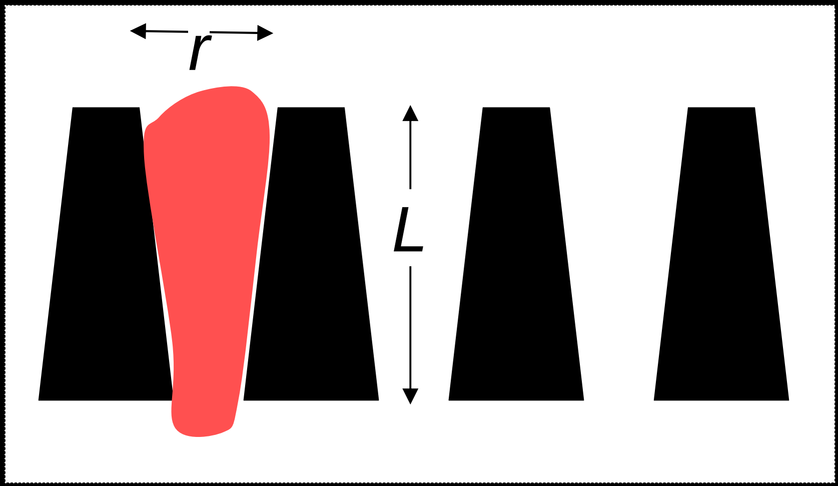

Abatti, P.J., Determination of the red blood cell ability to traverse cylindrical pores. IEEE Trans Biomed Eng, 1997. ***44****(3): p. 209-12.*

FLOW MODEL

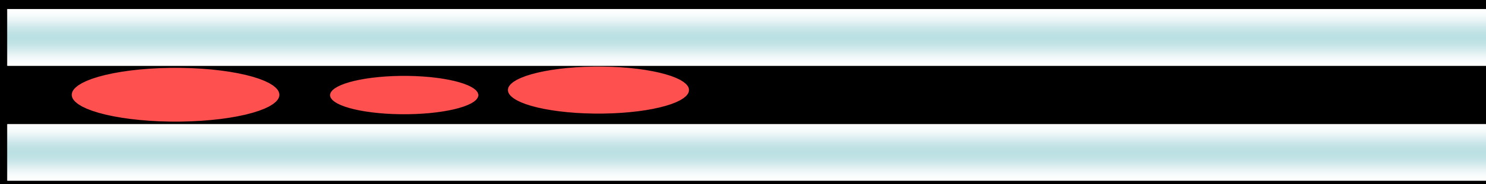

too shallow, all cell sizes impeded ~equally

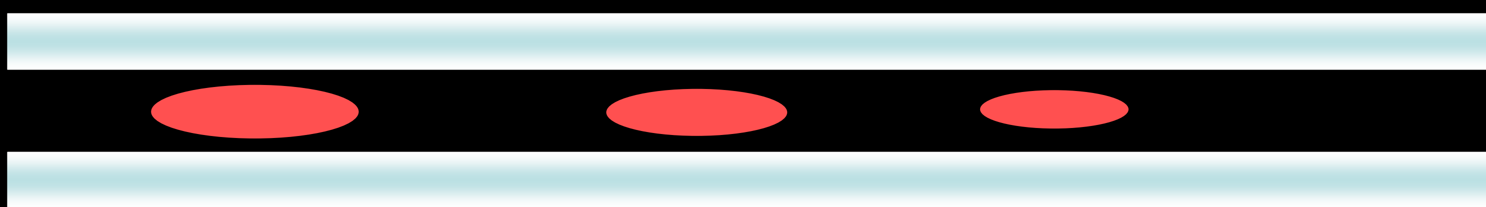

proper boundary layer interaction, presorting occurs

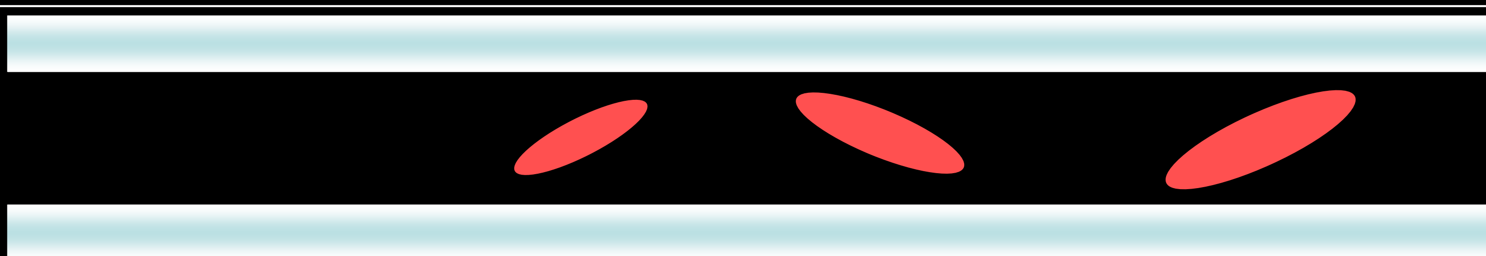

too deep, no BL effect, cells impeded equally

optimizing device depth for presorting in prebed region

FLOW MODEL

$$\sum F = \mu \dot{x}$$

μ_f = friction coefficient
μ = viscosity
ρ = density
E = modulus of elasticity
H = Heaviside step function
ℓ = characteristic length
R = Reynolds number
u = velocity

steady-state

$$F_{drag} + F_{flow} = 0$$

assume

$$F_{drag} \approx E\mu_f \left(d_{cell} - d_{channel}\right) H\left(d_{cell} - d_{channel}\right)$$

$$Re = \frac{\rho u l}{\mu} \approx \frac{\frac{1000kg}{\mathrm{m}^3} \cdot \frac{0.001m}{\mathrm{sec}} \cdot 0.00001m}{\frac{0.001N \cdot s}{m^2}} \approx 0.01$$

ow R number -> Stokes eqn

$$F_{flow} = 3\pi\mu d_{cell} u \approx 3\pi \cdot \frac{0.001N \cdot s}{m^2} \cdot 0.00001m \cdot \frac{0.001m}{s} = 1E-7 = 100E-9 = 100nN$$

$$F_{flow} \approx \frac{\mu d_{cell} u}{d_{channel}}$$

FLOW MODEL

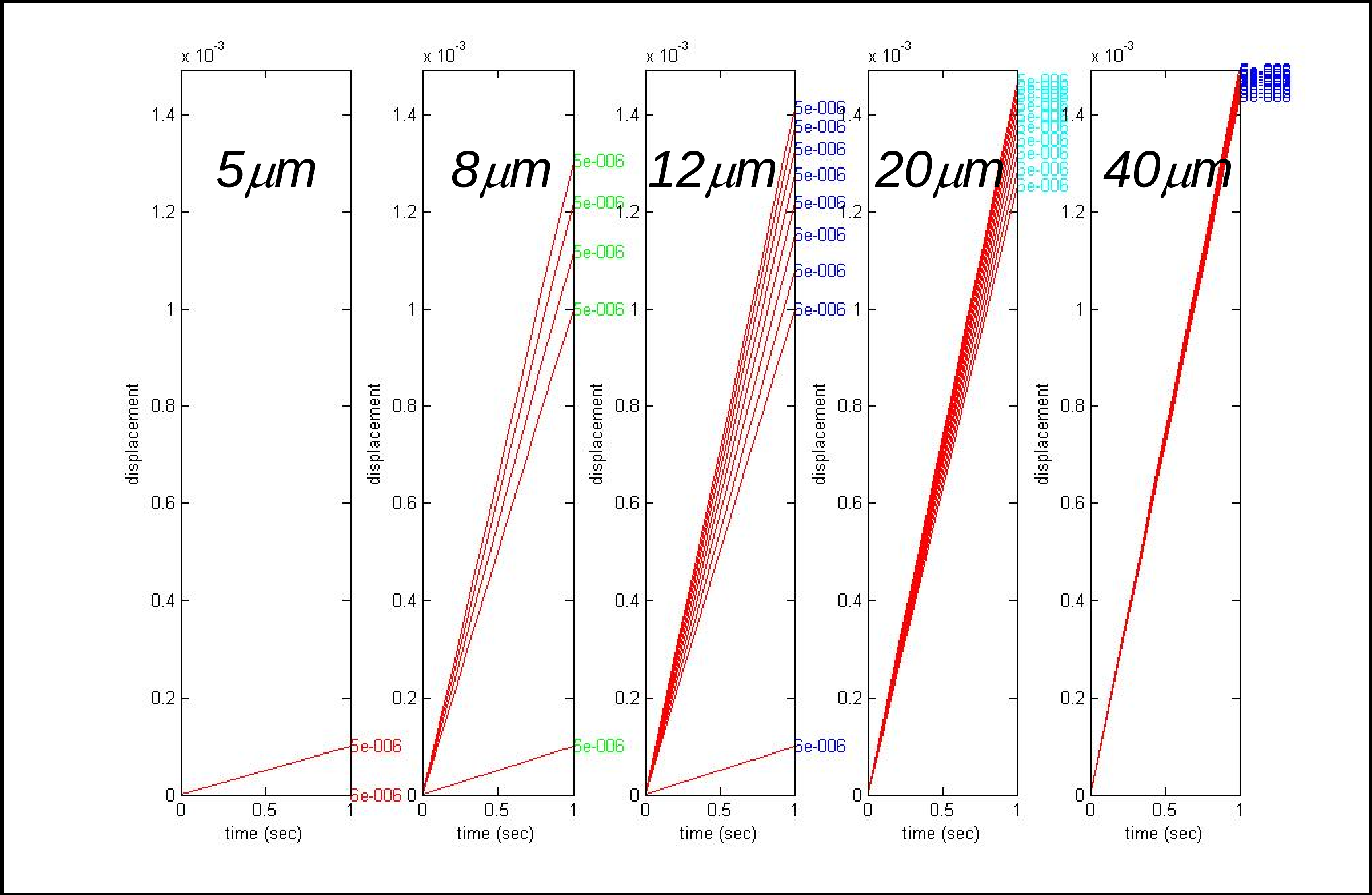

PRELIMINARY FLOW RESULTS

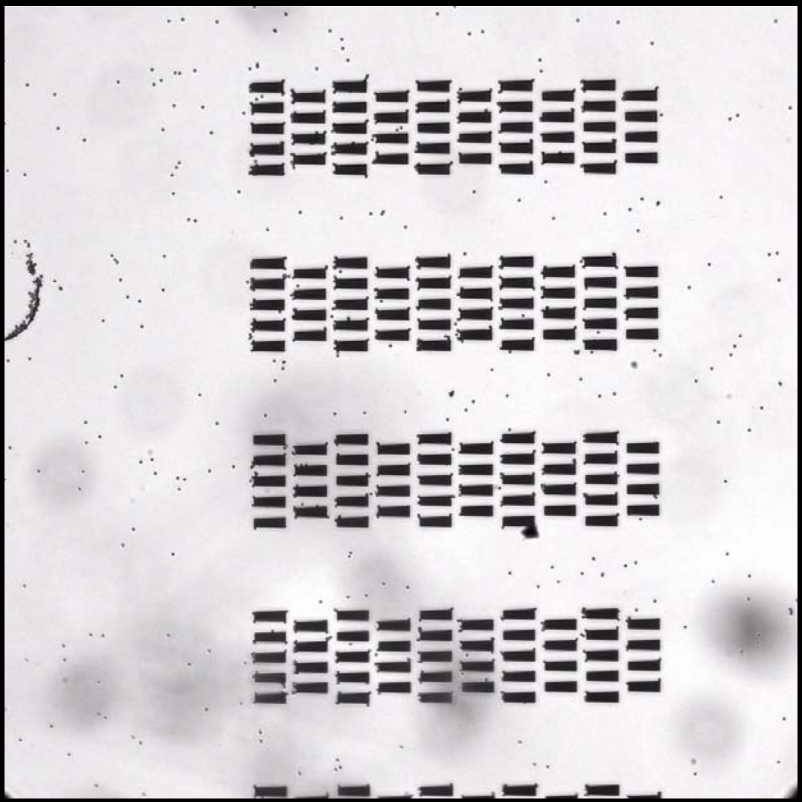

Mix of 2, 3, 4 μm microspheres
(~7500 beads/μl)

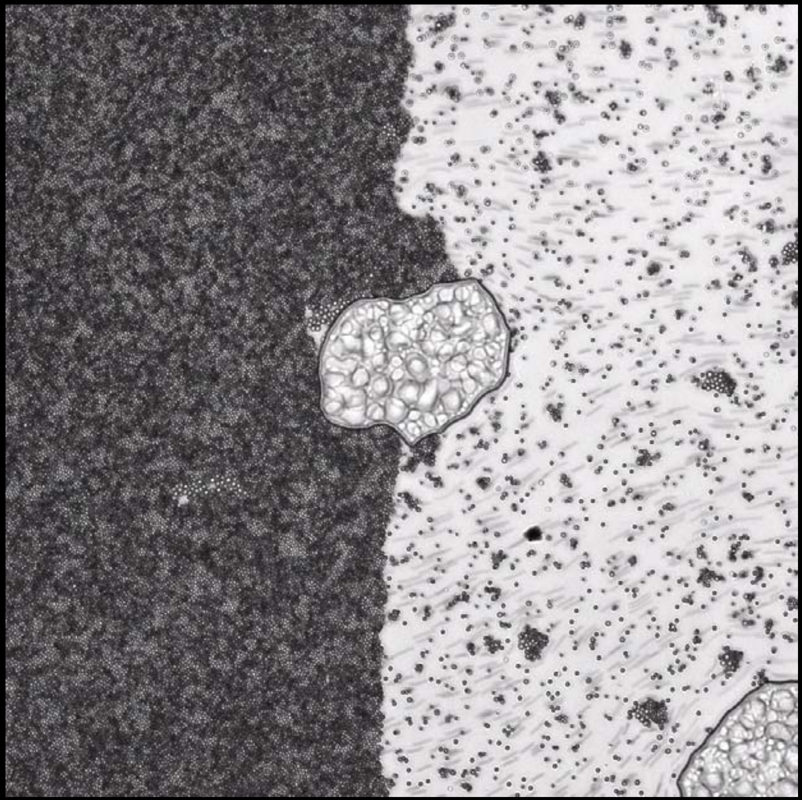

2 μm microspheres
(1.496 x 10^6 beads/μl)

CIRCUIT ANALYSIS MODEL

impedance spectroscopy

$$V_{OUT} = V_{IN}\left(\frac{Z_{R_2} + Z_C}{Z_{R_1} + Z_{R_2} + Z_C}\right) \qquad Z = R_e + \frac{R_t}{1 + R_t^2 C_d^2 \omega^2} - j\frac{R_t^2 C_d \omega}{1 + R_t^2 C_d^2}$$

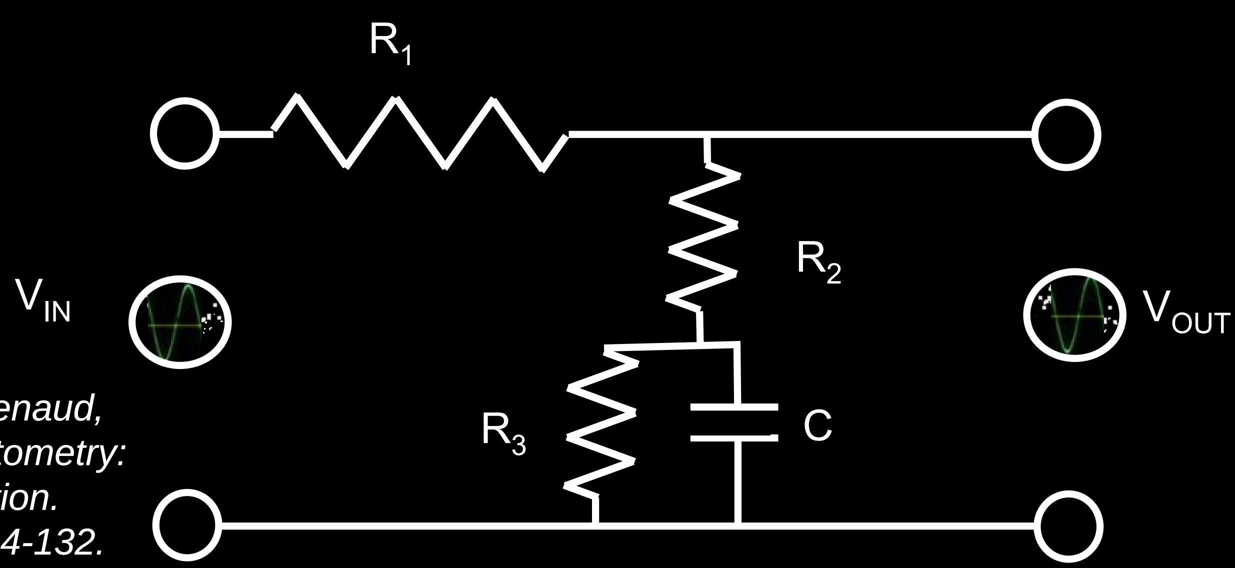

Cheung, K., S. Gawad, and P. Renaud, Impedance spectroscopy flow cytometry: On-chip label-free cell differentiation. Cytometry A, 2005. ***65A****(2): p. 124-132.*

CIRCUIT ANALYSIS RESULTS

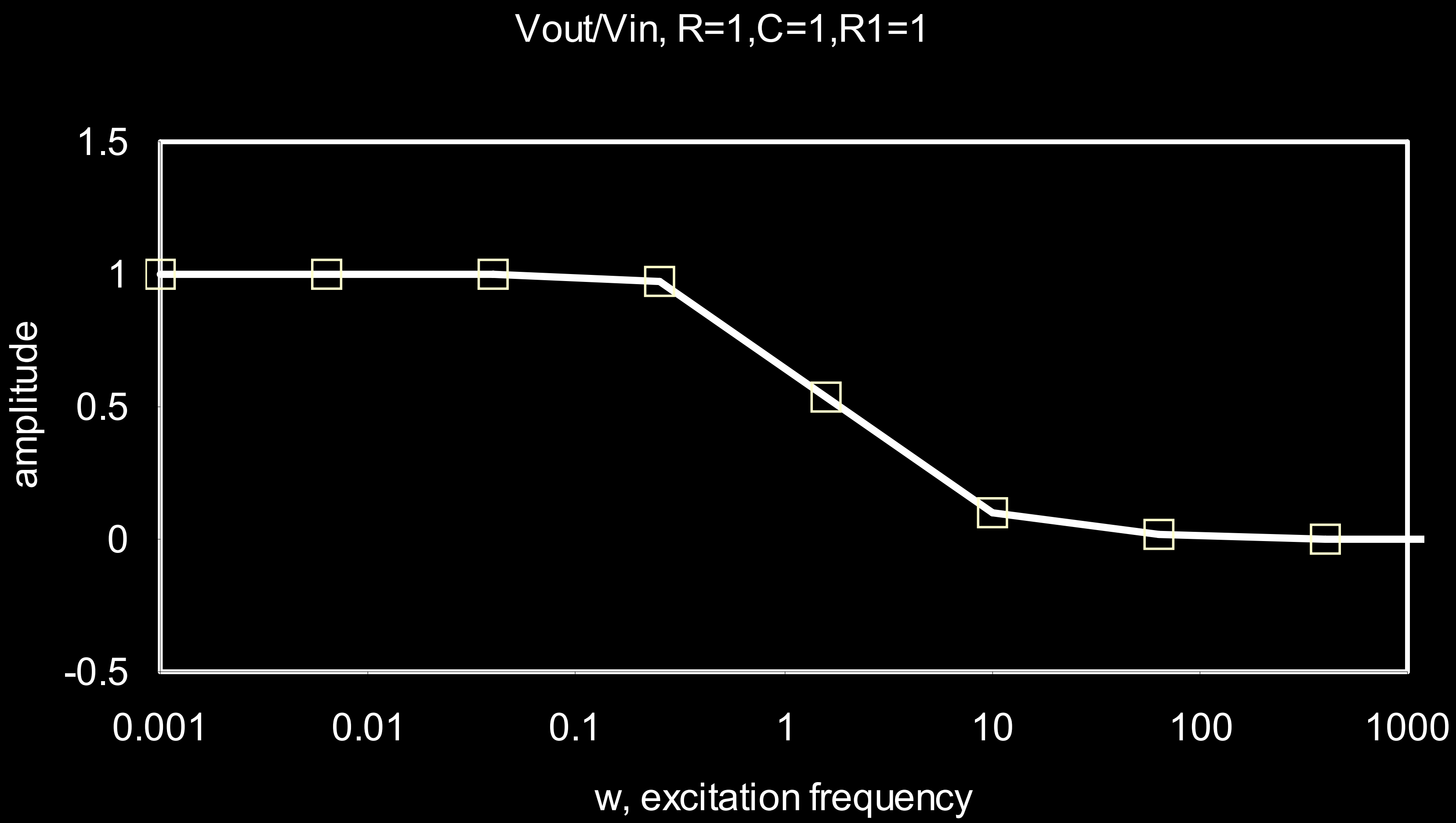

Cheung, K., S. Gawad, and P. Renaud, Impedance spectroscopy flow cytometry: On-chip label-free cell differentiation. Cytometry A, 2005. 65A(2): p. 124-132.

CONCLUSIONS AND FUTURE PLANS

- *integration with microneedles, for sample collection*
- *integration with other devices such as chemical analysis systems, presorting systems such as pinched flow*
- *other pumping methods, such as capillary, small centrifugal*

NEURITE STRETCHING

small scale cell-ECM experiments

- Microtubules are the main compressive structural support elements for the axon of a neuron.
- Actin filaments are the primary tensile support elements.

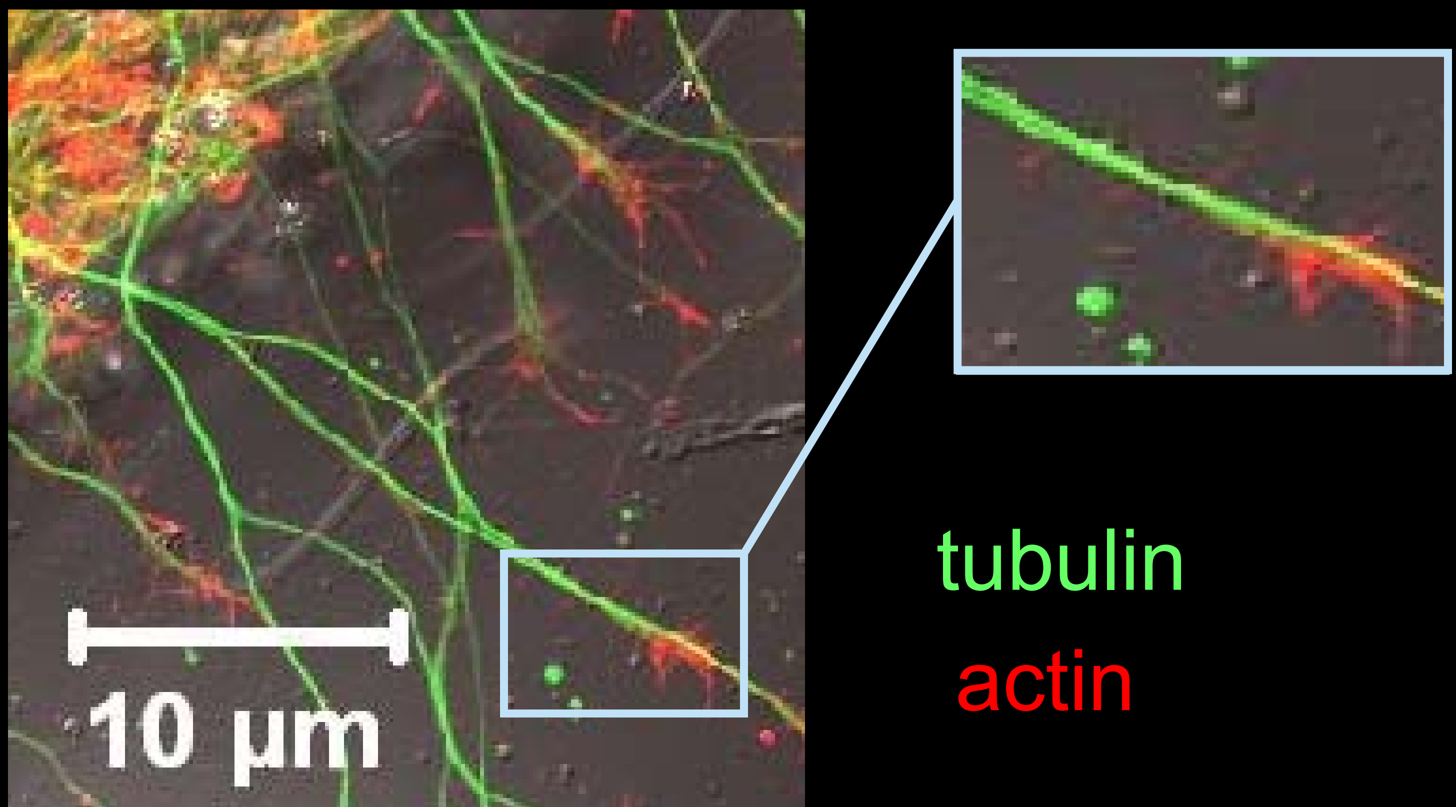

small scale cell-ECM experiments

- A plot of individual average microtubule lengths as a function of time for five preliminary simulations

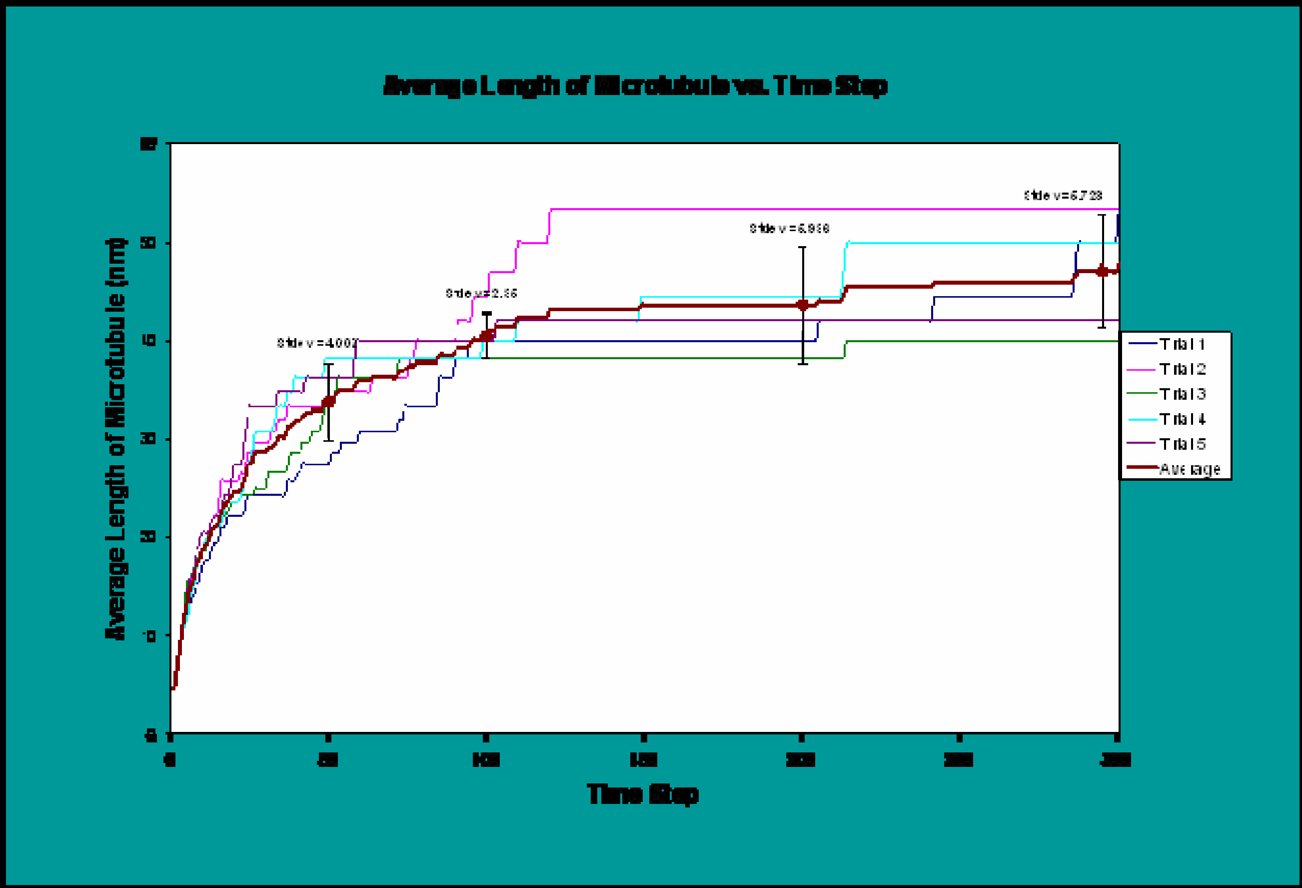

small scale cell-ECM experiments

- Trial simulation to determine the effects of membrane friction and thermal energy on the time required for a microtubule polymerizing to be forced into the same orientation as a microtubule supporting the shape of the cell

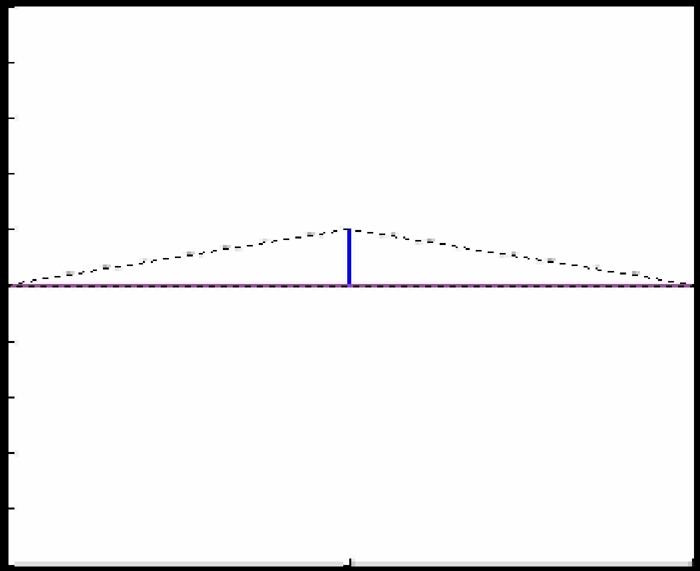

Movie 1: Large membrane friction, small thermal energy

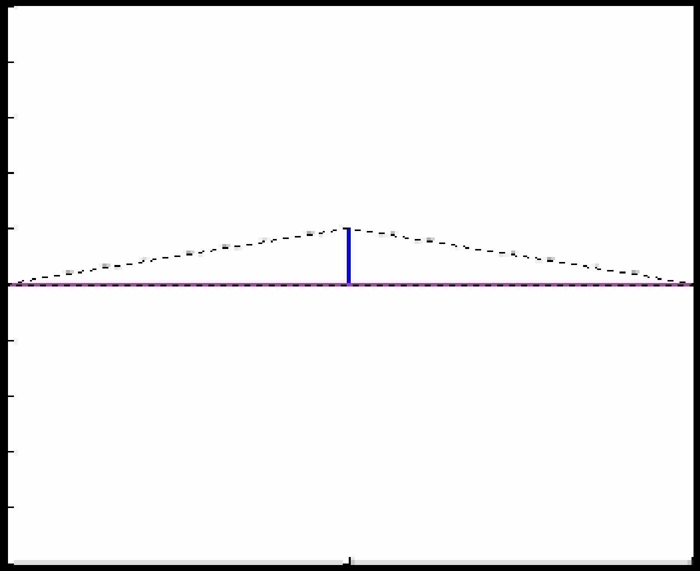

Movie 2: Small membrane friction, large thermal energy

small scale cell-ECM experiments

- alignment time

Deterministic Model

Time step = .05

Time (Time step*number of frames) for MT 1 align with MT 2

Dt\ μ	**0. 001**	**0.01**	**0.1**	**1**
0.001	6.2	6.7	15	33
0.01	4.6	4.7	5.3	12
0.1	3.00	3.00	3.05	3.80

Computational Time (seconds) for MT 1 to align with MT 2

Dt\ μ	**0. 001**	**0.01**	**0.1**	**1**
0.001	0.563	0.688	0.703	0.732
0.01	0.484	0.594	0.562	0.594
0.1	0.375	0.375	0.484	0.547

greater friction -> longer time constant
lower thermal energy -> longer time constant

μ ≈ friction coefficient with membrane
Dt ≈ temperature, energy of the system

small scale cell-ECM experiments

- Currently we are using the Heaviside step function, where *c* is a critical bonding radius, to model particle-particle interactions

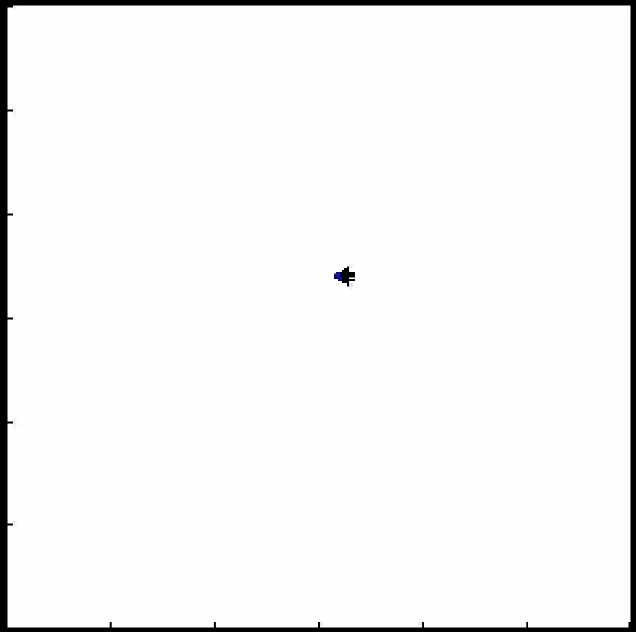

Movie 1: 100 dimers, initial spacing = random number from -1 to 1

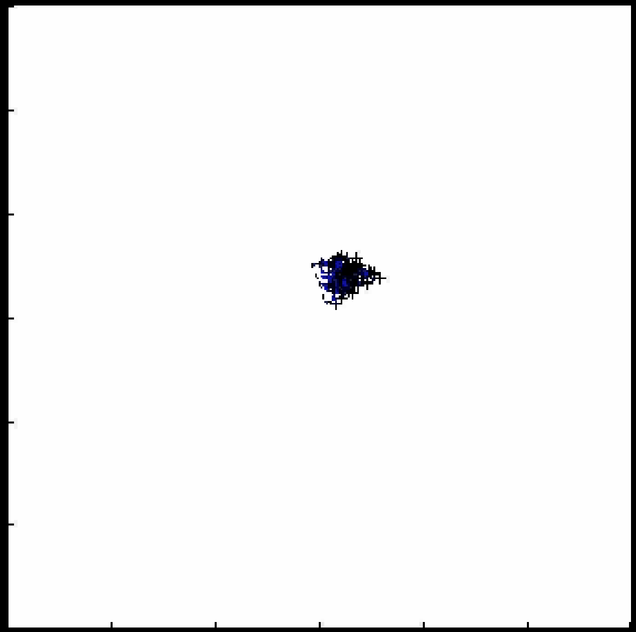

Movie 2: 100 dimers, initial spacing = 10 multiplied by random number from -1 to 1

small scale cell-ECM experiments

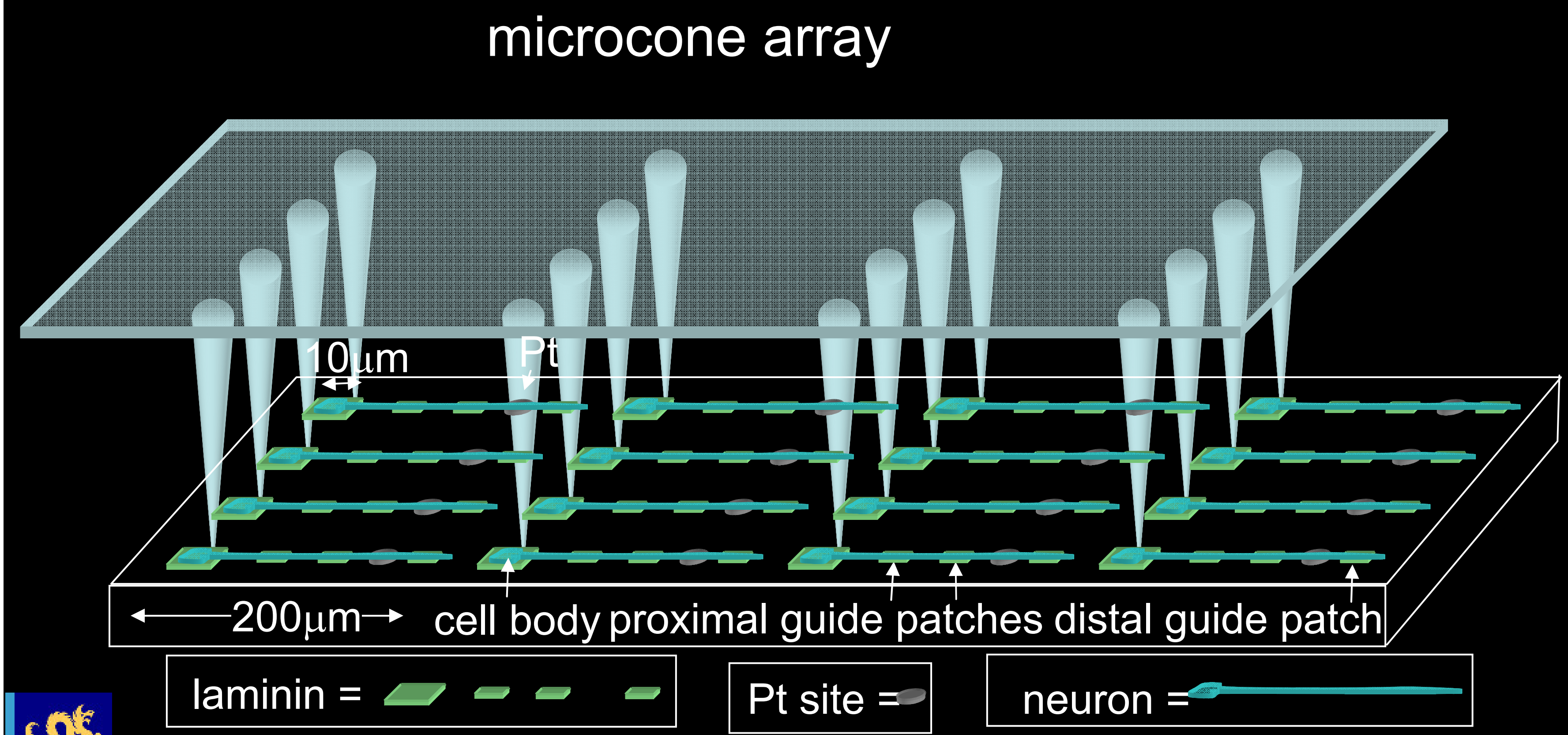

small scale cell-ECM experiments

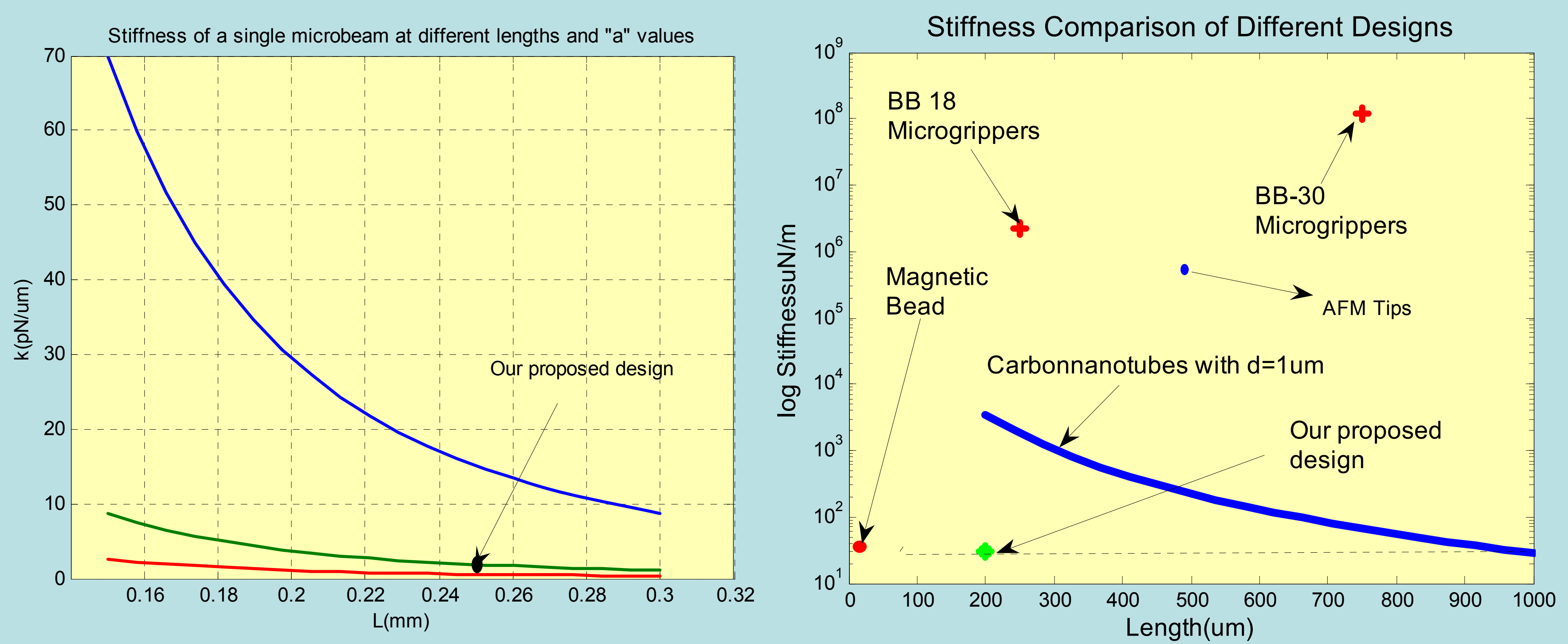

small scale cell-ECM experiments

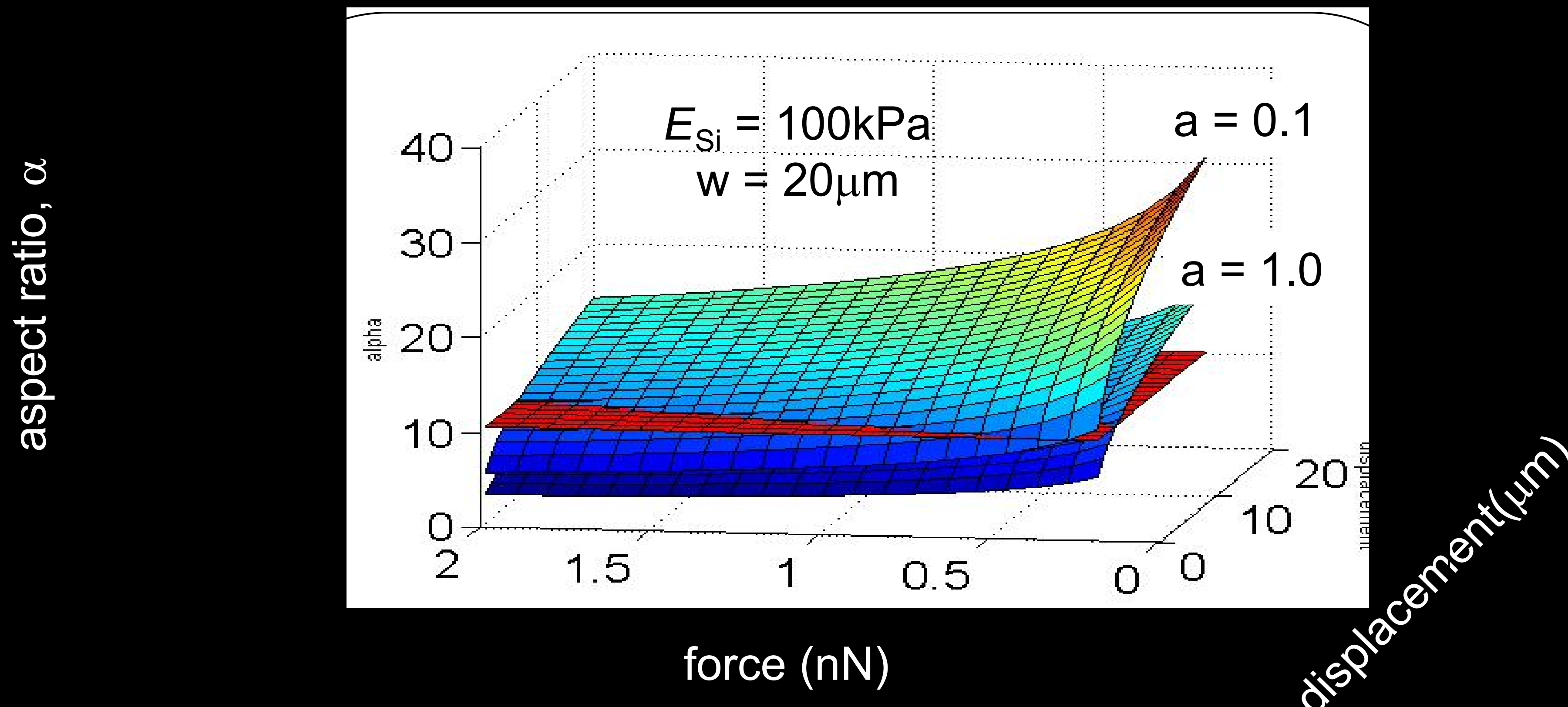

tapered PDMS mircobeam aspect ratio as a function of desired mechanical resolution (compliance)

small scale cell-ECM experiments

STEEL

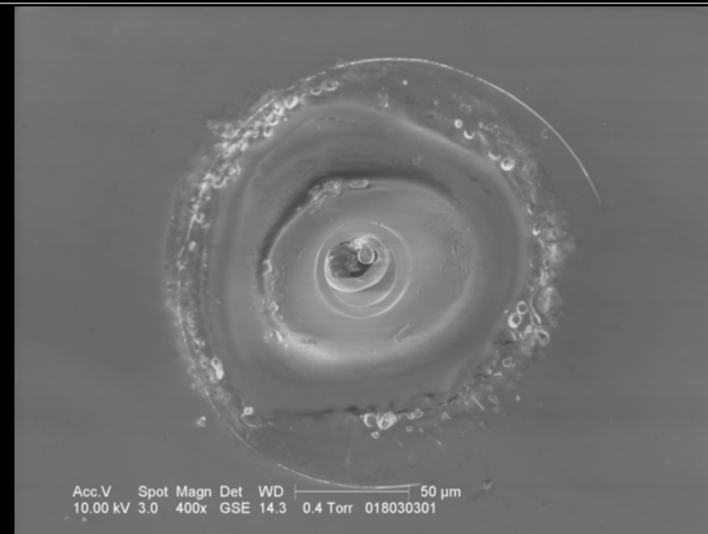

GLASS

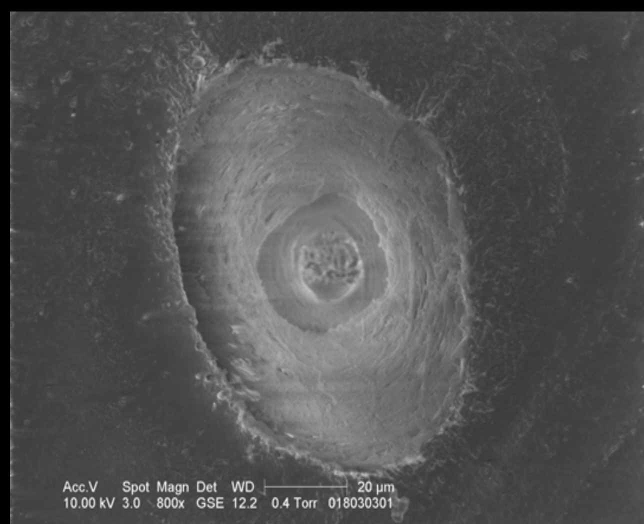

TEFLON

small scale cell-ECM experiments

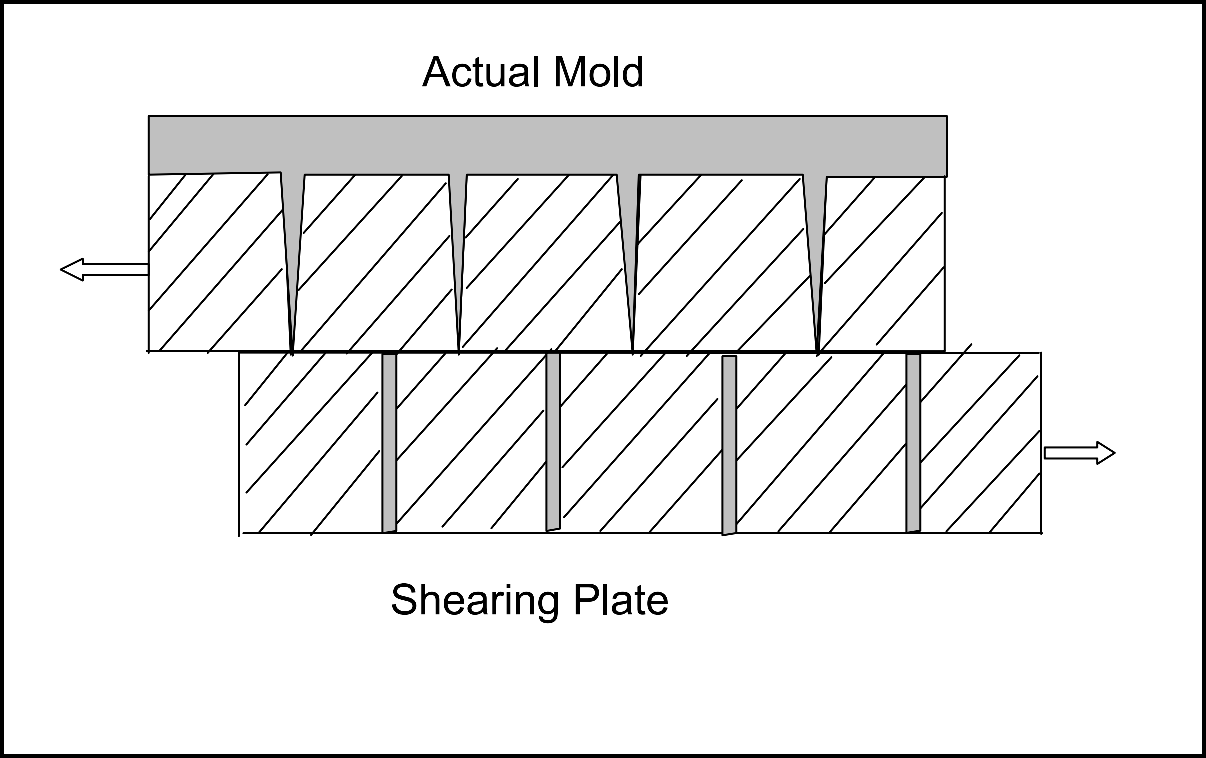

small scale cell-ECM experiments

The injection vessel.

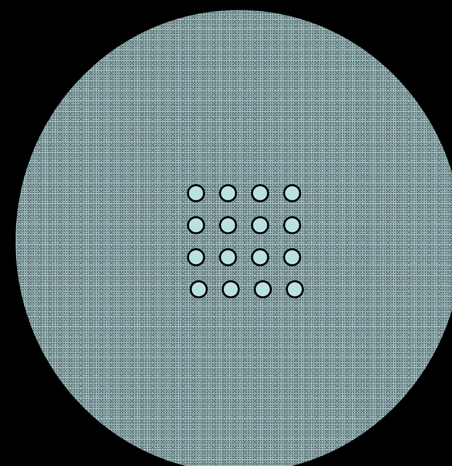

250 μm thick steel mold with 16 laser drilled holes of 10 μm at the top and 2μm at the bottom.

small scale cell-ECM experiments

1) Small Deflection Theory (Linear Approach)

- The stiffness of a microcone is derived from basic form of Euler equations.

$$\frac{d^2}{dx^2}\left[EI(x)\frac{d^2v(x)}{dx^2}\right]$$

- The stiffness of a single microcone is derived as:

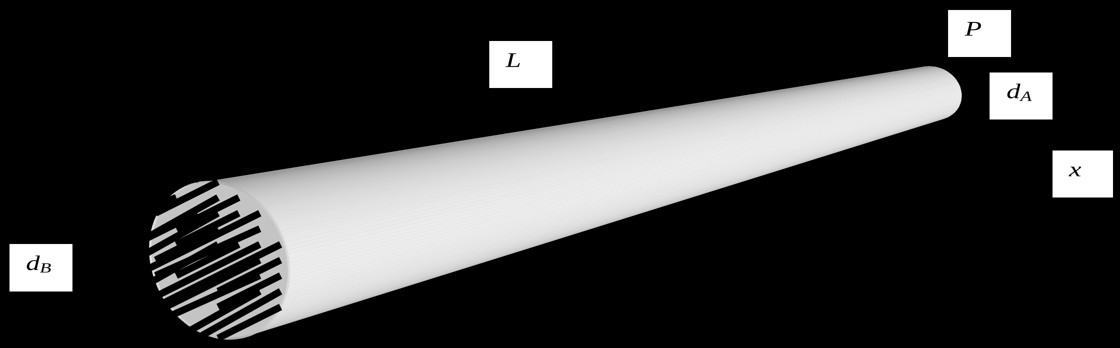

$$k = \frac{3E\pi r_A^4}{4L^3a^3}$$

THANKS TO:

NASA DDF05-553

DEPARTMENT OF HEALTH

NIST

THANKS TO:

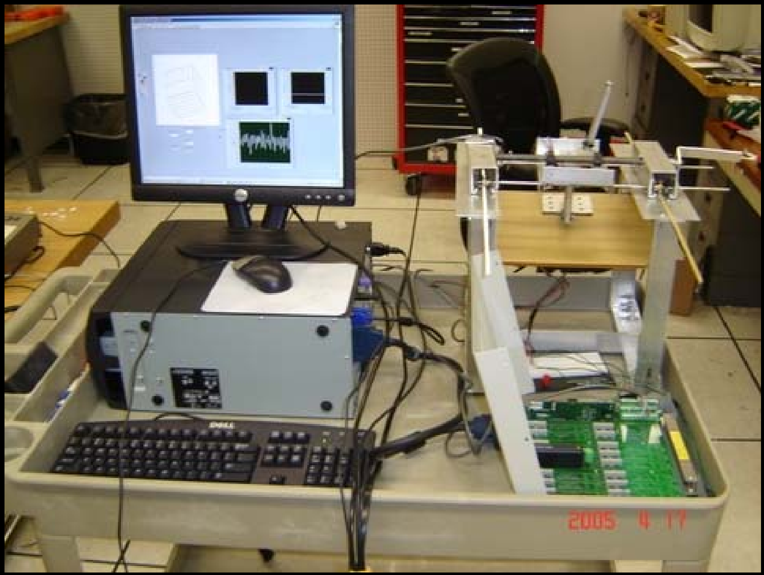

PATENT # 2

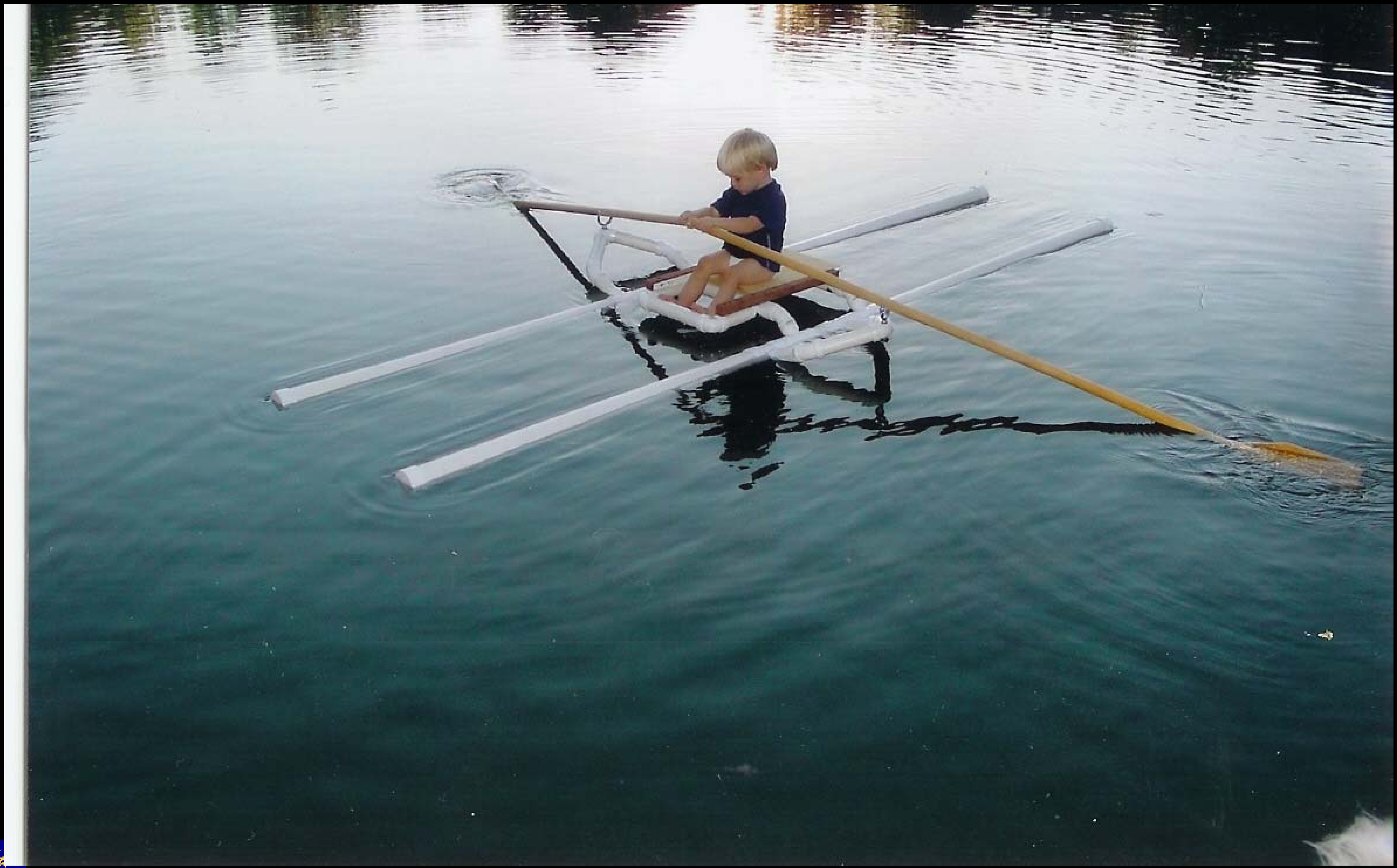

CURVATURE OF THE EARTH

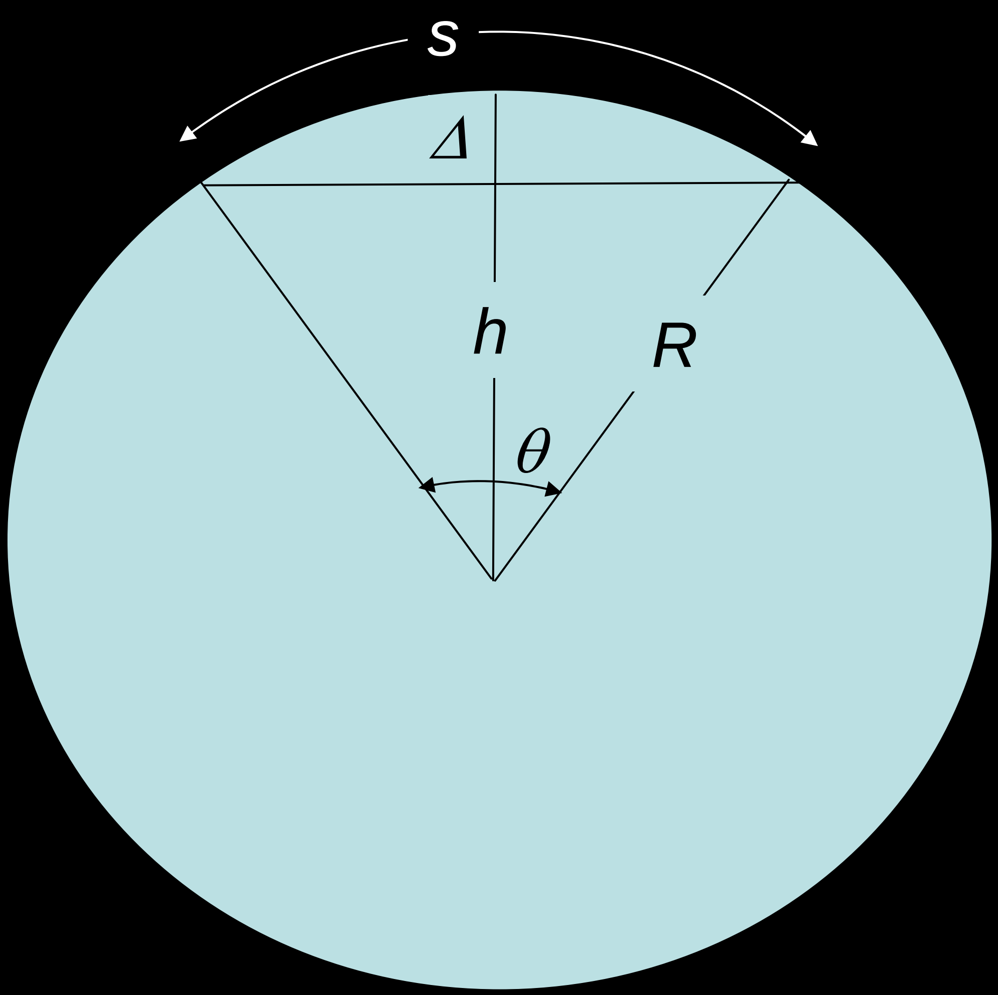

$$\Delta = R - h$$
$$= R - R\cos(\theta/2)$$
$$= R(1-\cos(s/2R))$$

CURVATURE OF THE EARTH

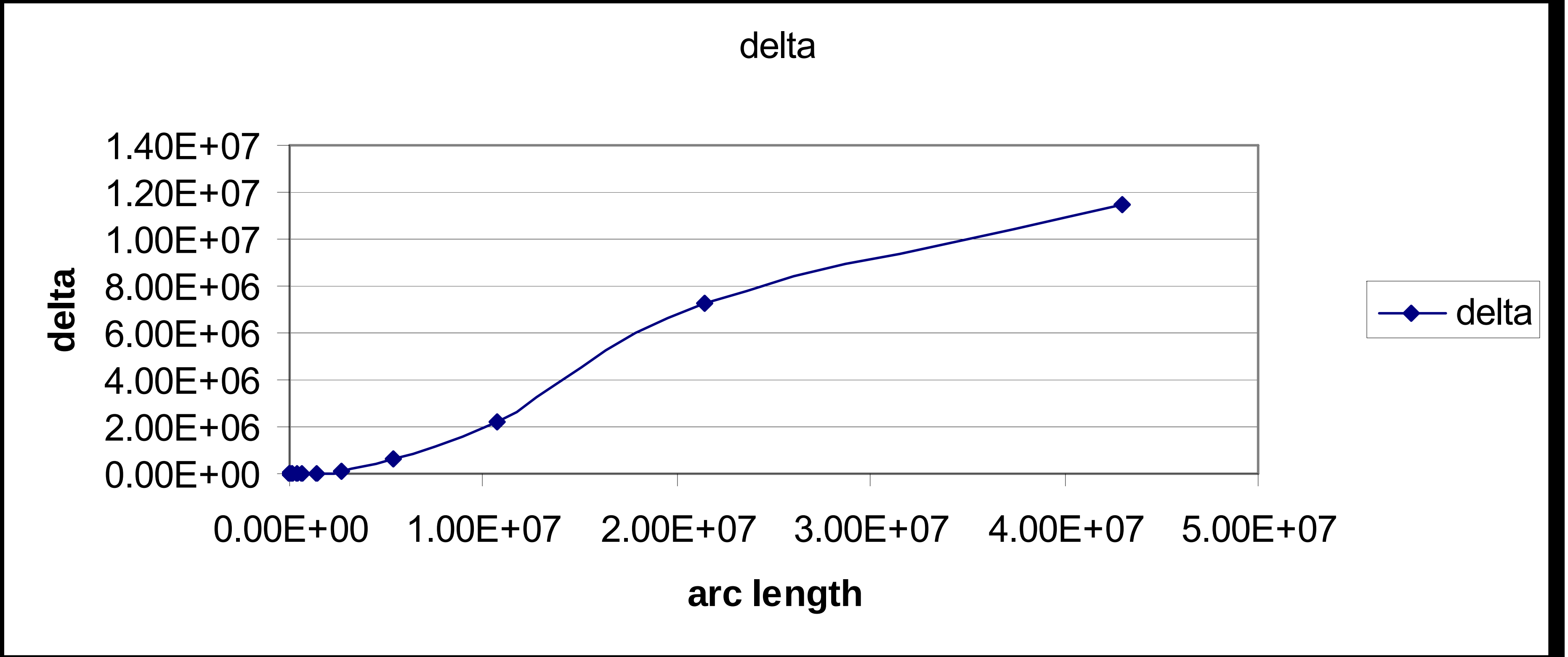

CURVATURE OF THE EARTH

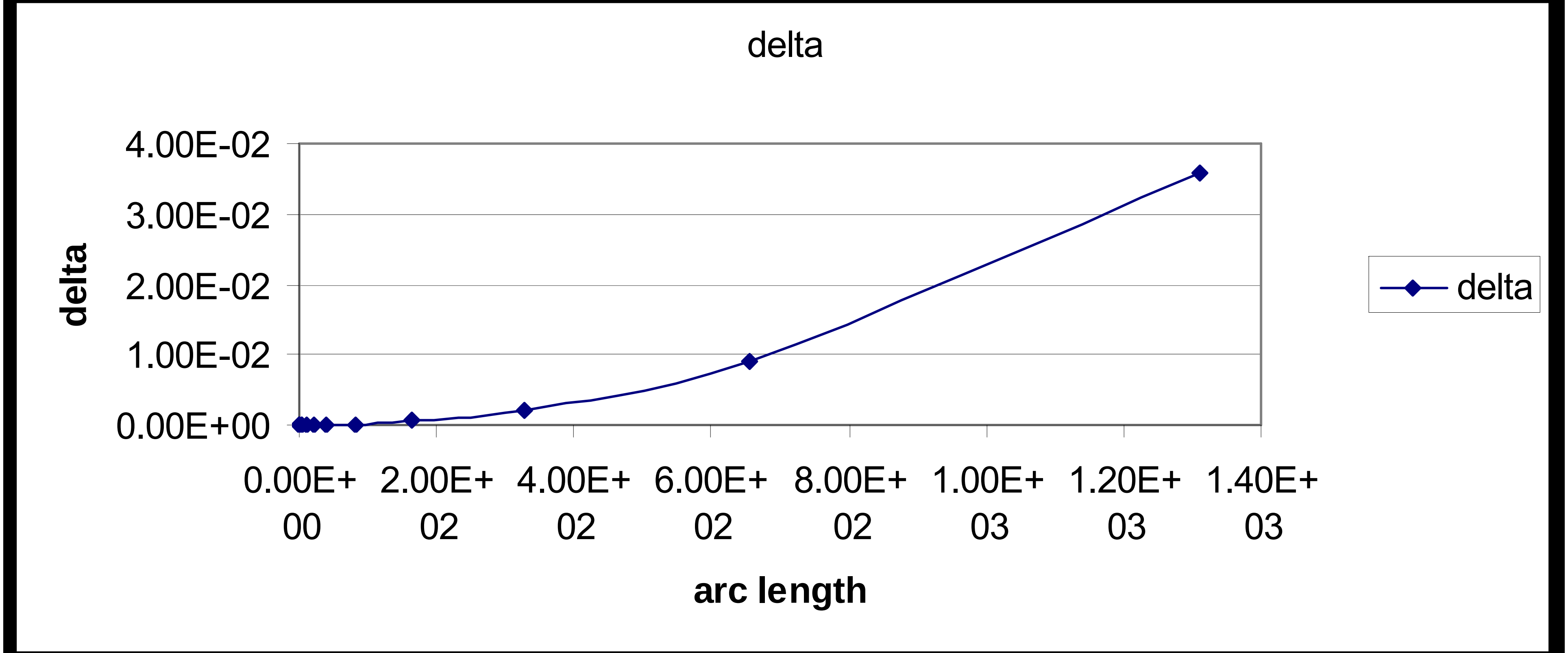

CURVATURE OF THE EARTH

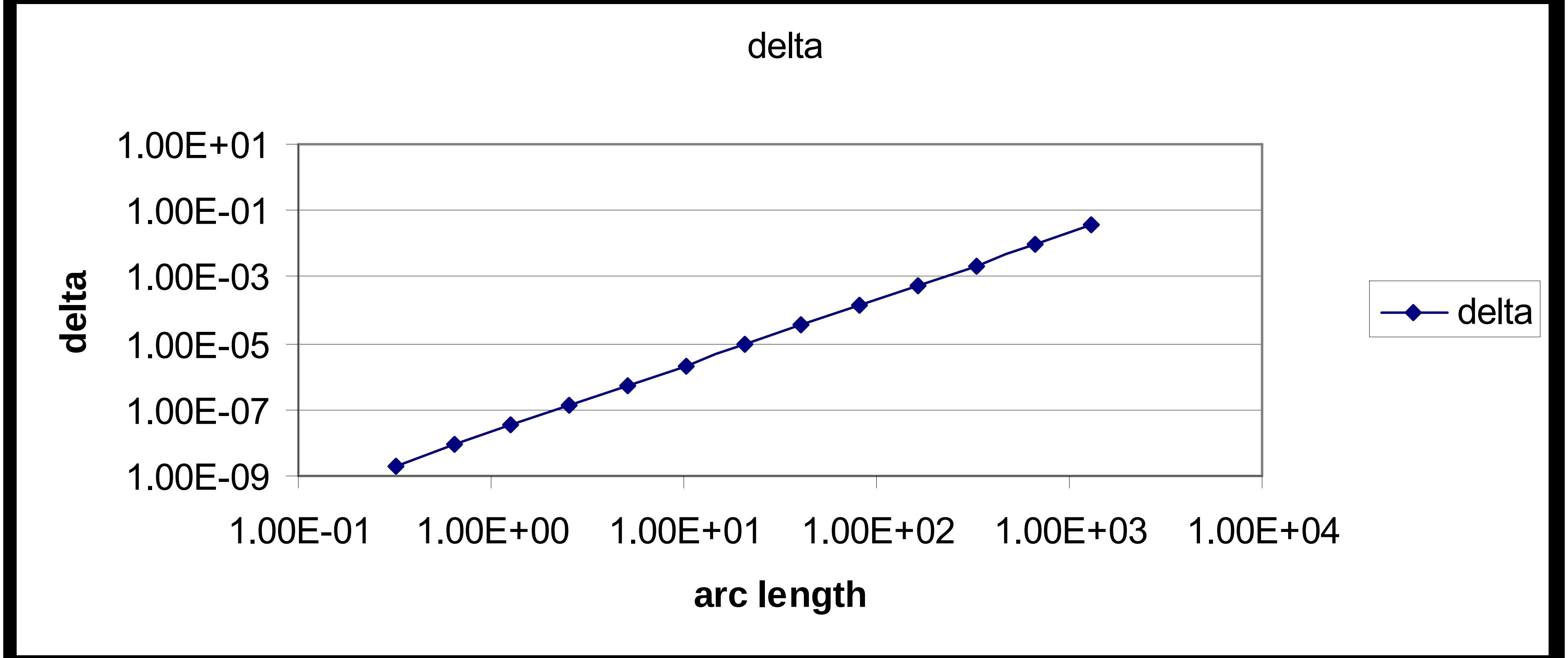

EXPERIMENTAL DETAILS

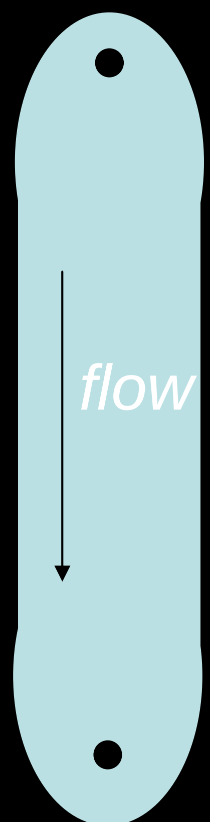

elliptical prebed and post bed regions to reduce turbulence

idea swiped from Lawrence Livermore talk in Session 16-1